THE TIMING OF LARAMIDE DEFORMATION IN THE NORTHERN ROCKY
MOUNTAINS

Laura Rose Neser

A dissertation submitted to the faculty at the University of North Carolina at Chapel Hill in
partial fulfillment of the requirements for the degree of Doctor of Philosophy in the Geological
Sciences in the College of Arts and Sciences.

Chapel Hill
2014

Approved by:

Kevin G. Stewart

Louis R. Bartek III

Jonathan M. Lees

Elana L. Leithold

Tamlin M. Pavelsky

ABSTRACT

Laura Rose Neser: The Timing of Laramide Deformation in the Northern Rocky Mountains
(Under the direction of Kevin G. Stewart)

Along the western edge of the Bighorn Basin in northwestern Wyoming, geologic
mapping of Late Cretaceous-Paleogene sediments has revealed a deep paleovalley that formed in
the latest Cretaceous. The paleovalley was a principal control for the timing and type of
Paleogene sediments deposited in the area. Tilting in the latest Cretaceous led to the erosion of
these Cretaceous rocks, and subsequent deformation occurred in the latest Paleocene-early
Eocene that steeply tilted them along with basal late Paleocene-early Eocene Willwood rocks to
their present-day orientations. The extent of the paleovalley included the Line Creek, Clarks
Fork Canyon, and Kimball Bench areas.

There have been varying interpretations regarding the direction(s) of shortening during
Laramide deformation of the Rocky Mountains. Our research has revealed a complex multi-stage
Laramide deformational history that resulted in the development of variously oriented structures
as well as differently aged angular unconformities within Cretaceous-Paleogene strata along the
western edge of the Bighorn Basin. In the northern Rocky Mountains, there were three stages of
deformation with differing shortening directions. The three stages of deformation occurred as a
result of (1) north-northeast-directed shortening in the latest Cretaceous-early Paleocene; (2)
east-northeast-directed shortening in the late Paleocene; and (3) east-directed shortening in the
early Eocene.

Deformed late Paleocene-early Eocene Willwood sediments are adjacent to a complex system of Laramide structures and in our study area, the absolute ages of these Willwood sediments are not well constrained. We calculated the age of the youngest deformed Willwood sediments based on chronostratigraphy tied to climate cycles. Our analyses also revealed a significant spectral peak corresponding to a cycle thickness of 13.1 meters, which correlates with a 21-ky climatic precession cycle. This indicates that precession-scale climate variations likely affected paleosol development within the Willwood Formation by way of cyclic changes from mostly overbank mudstone deposition to channel-avulsion deposition. Our study has revealed that deformation began in the early Eocene in the Kimball Bench area along the western edge of the Bighorn Basin. It is apparent that during Paleogene deposition, there was a complex deformational history along the western edge of the Bighorn Basin.

ACKNOWLEDGEMENTS

TABLE OF CONTENTS

LIST OF FIGURES

CHAPTER 1 FIGURES

CHAPTER 3 FIGURES

LIST OF TABLES

Table

xiii

LIST OF ABBREVIATIONS

‰	per mil
$\delta^{13}C$	delta 13C
a*	redness
CIE	carbon isotope excursion
cm	centimeter
FFT	fast Fourier transform
km	kilometer
ky	thousand years
LPTM	late(st) Paleocene thermal maximum
m	meter
Ma	million years before present
my	million years
P-E	Paleocene-Eocene
PETM	Paleocene-Eocene Thermal Maximum

CHAPTER 1: A LATE CRETACEOUS PALEOVALLEY IN THE VICINITY OF CLARKS FORK CANYON AND RESULTING PALEOGENE FACIES DEVELOPMENT, NORTHWESTERN WYOMING

Introduction

Foreland basins contain a record of the tectonic history of their adjacent mountain belts, and the strata within a foreland basin can be used to accurately interpret the manner in which that basin was filled (Flemings and Jordan, 1989). Syntectonic deposits in foreland basins also contain subtle indicators of tectonic activity, including changes in clast composition that record uplift and erosion of the source areas (Colombo, 1994). The progressive erosion of rock units and deposition of the eroded material can record the rates and timing of deformation in the source area (DeCelles et al., 1987; DeCelles and Hertel, 1989). It is important, however, to understand the paleotopography of such an area, because paleotopography exerts significant control on the distribution of siliciclastics sediments within the depocenter (Oplustil, 2005).

The topography of the earth's surface is crucially important in both climatic and tectonic studies. Various methods have been used to constrain paleotopography including paleobotany, cosmogenic nuclides, isotopic composition of authigenic minerals, sedimentologic provenance studies, and apatite fission-track evidence (DeCelles et al., 1991b; Omar et al., 1994; Brook et al., 1995; Forest et al., 1999; Chamberlain and Poage, 2000; Mulch et al., 2006). Paleovalleys are part of regional unconformities that give important constraints on the development of foreland systems (Sears and Ryan, 2003). In this paper, we focus on structural and sedimentologic

information to estimate the paleotopography along the western edge of the Bighorn Basin in northwestern Wyoming.

Our research revealed a deep paleovalley along the western edge of the Bighorn Basin which was the result of differential erosion of the Late Cretaceous rocks east of the nascent uplift of the Beartooth Mountains. Topographic features such as valleys can have an important control on the distribution of sediments in an area (Oplustil, 2005), and the paleovalley in the vicinity of the Clarks Fork Canyon played a central role in the evolution of the basin. Structural-topographic highs often serve as intrabasinal sources of sediment (Meyers et al., 1992), and the Beartooth uplift provided the source sediment for Paleogene deposits within the paleovalley and surrounding areas along the western edge of the Bighorn Basin. DeCelles et al. (1991a,b) used lithologic provenance modeling to describe the nature of deposition during uplift of the Beartooth Mountains. They attributed the changes in source sediment composition to changes in source-area relief of the Beartooth block throughout time. Source-area relief played a fundamental role in determining the type of sediment that was deposited in the basin (DeCelles et al., 1991b); however, paleotopography must equally be considered as it also governed the location and type of sediment.

During the late Paleocene, the Clarks Fork Canyon area subsided and filled with detritus sourced from the Beartooth uplift (Hickey, 1980; Gingerich, 1983). However, there is a compositional difference in deposits which are considered contemporaneous (Dutcher et al., 1986; DeCelles et al., 1991a,b) at varying locations along the western edge of the Bighorn Basin. Our research indicates that the Late Cretaceous paleovalley was a principal control for the timing and type of Paleogene deposits in these areas, with deposition occurring first in the deepest part of the paleovalley and becoming more widespread as the valley was filled. Well-exposed

Paleogene sediments along the western edge of the Bighorn Basin were ideal for this study, as ancient topographic features can be recognized where post-depositional controls are favorable to their preservation (Corcoran, 2008), for instance in the vicinity of Clarks Fork Canyon. Our field mapping of Paleogene facies along the western edge of the Bighorn Basin reveals the existence of a relict Late Cretaceous paleovalley that resulted from removal of over 4,000 feet of Late Cretaceous strata prior to Paleogene deposition.

Geological Setting

Synkinematic late Paleocene and Eocene sediments rest on top of Cretaceous rocks along at least a 30 kilometer-long segment of the western edge of the Bighorn Basin of northwestern Wyoming (Fig. 1). The Laramide Beartooth Mountains are a 130-by-60-kilometer uplifted block of Precambrian crystalline rocks located in the northern Rocky Mountains of northwestern Wyoming and south-central Montana (Fig. 1). The crystalline core of the range is roughly rectangular, with its long axis oriented northwest-southeast (Dutcher et al., 1986). The east flank of the Beartooth uplift is oriented roughly north-south (Fig. 1). Along the east and northeast, folded and faulted Paleozoic and Mesozoic strata border the mountains. During the Late Cretaceous, andesites and dacites were intruded into the range. All of these rock types can be found as clasts in the Paleocene Beartooth Conglomerate, which was deposited during uplift of the Beartooth Mountains (DeCelles et al., 1991b).

The Absaroka volcanic field was active in from the early middle Eocene to the late Eocene, extending from northwestern Wyoming into southwestern Montana. The volcanic field contains andesite, basalt, and related intrusive rocks which constitute part of the present-day Beartooth Mountains and are also present north of the range (Smedes and Prostka, 1972). At the southern end of the Beartooth Mountains, the hanging wall of the Beartooth Arch is folded into

3
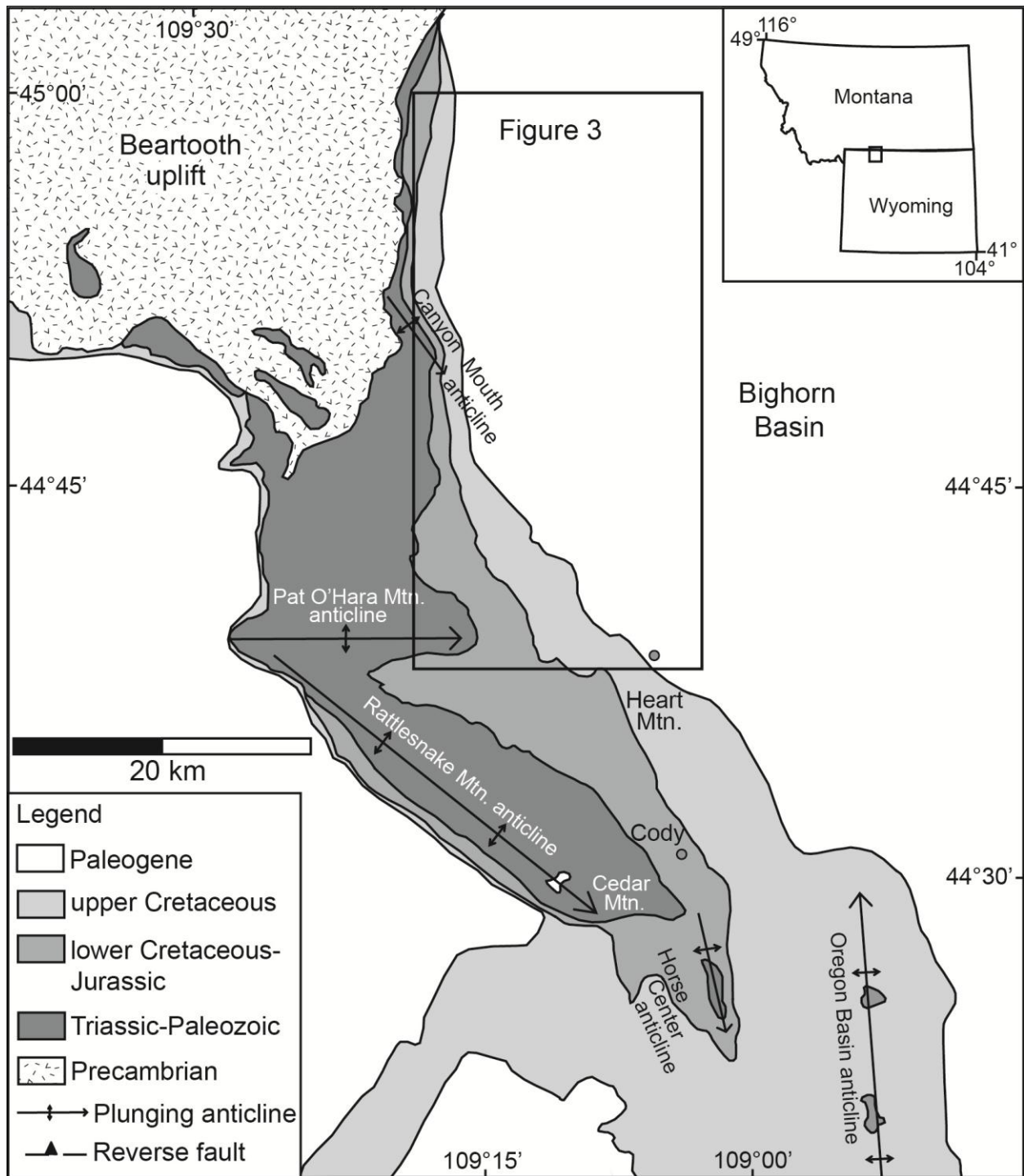
Figure 1. Simplified geologic map of the western Bighorn Basin and adjacent Laramide structures, modified from Neely and Erslev, 2009. Black box outlines study area (Figure 3).

4

the E-W trending Pat O'Hara Mountain, an anomalously east-plunging, south-facing anticline (Neely and Erslev, 2009). The western terminus of the Pat O'Hara Mountain anticline reveals the Mississippian Madison Limestone gently folded into the crest of the NW-trending Rattlesnake Mountain anticline (Fig. 1; Neely and Erslev, 2009). Here, the Rattlesnake Mountain anticline terminates at Pat O'Hara Mountain (Neely, 2006).

Late Cretaceous Formations

In northwestern Wyoming, the Cretaceous Cody Shale ranges in thickness from 500 to 1000 meters thick, composed dominantly of marine shale, siltstone, and sandstone (Kauffman, 1977). The lower part consists of predominantly interbedded shale and siltstone which coarsens upward into interbedded shale, siltstone, and sandstone (Kauffman, 1977). The upper part consists of buff sandy shale and thinly laminated buff sandstone (Pierce, 1965, 1966, 1968, 1997; Lillegraven, 2004).

Above the Cody Shale, the Cretaceous Mesaverde Formation is comprised of interbedded sandstone and shale in its upper part, and massive light-buff, ledge-forming sandstones with thin coal beds in the lower part (Pierce, 1965, 1966, 1997; Lillegraven, 2004). The thickness of this unit in our study area is about 330 meters (Pierce, 1966).

The Mesaverde Formation is beneath the Cretaceous Meeteetse Formation, which includes gray to white clayey sand, drab sandstone, gray-brown shale, and bentonitic clay (Pierce, 1965, 1966, 1997). The remains of fossil plants are abundant within the formation, and locally it may contain thin lignite beds. The Meeteetse Formation is poorly indurated, valley forming, and markedly bentonitic. This unit has a thickness of about 360 meters (Pierce, 1965, 1966, 1997; Lillegraven, 2004).

The uppermost Cretaceous Formation is the Lance, which is 100 to 500 meters thick and comprises a sequence of thick-bedded, buff-colored fluvial sandstones interbedded with drab to green shales (Pierce, 1966, 1997). It contains medium- to very fine-grained sandstones, silty-sandstones, siltstones, and mudstones (Webb and Steel, 2001).

Paleocene-Eocene Formations

Above the Cretaceous Lance Formation, the late Paleocene Fort Union Formation preserves internal angular unconformities that record synkinematic uplift and sedimentation. In northwestern Wyoming, the Fort Union Formation is comprised of synkinematic alluvial fan deposits and fluvial deposits (Hickey, 1980; Johnson and Middleton, 1990).

DeCelles et al. (1991b) defines the Paleocene Beartooth Conglomerate as the coarse conglomerate interbedded with minor sandstones and siltstones that crops out on the northeastern and eastern border of the Beartooth Mountains, extending from the north side of the Clarks Fork of the Yellowstone River (WY) to the west side of West Red Lodge Creek (MT) (Fig. 2). Due to similarities in lithology and stratigraphic position, Lopez (2005) classified the Beartooth Conglomerate along with the Laramide synorogenic deposits of Flueckinger (1970) as part of the Linley Conglomerate Member of the Fort Union Formation. For the same reason, we use the term Linley Conglomerate to describe the late Paleocene sediments that occur along the northern and eastern mountain front of the Beartooth Mountains, considered to be Laramide synorogenic deposits (Lopez, 2005).

In the late Paleocene Epoch, bedload-dominated streams coming off alluvial fans during uplift of the Beartooth Mountains deposited coarse sediments of the Linley Conglomerate (DeCelles et al., 1991a). The Linley Conglomerate consists of mainly red-brown to gray-brown interbedded conglomerate, coarse-grained sandstone, siltstone, and mudstone, with the coarser

6
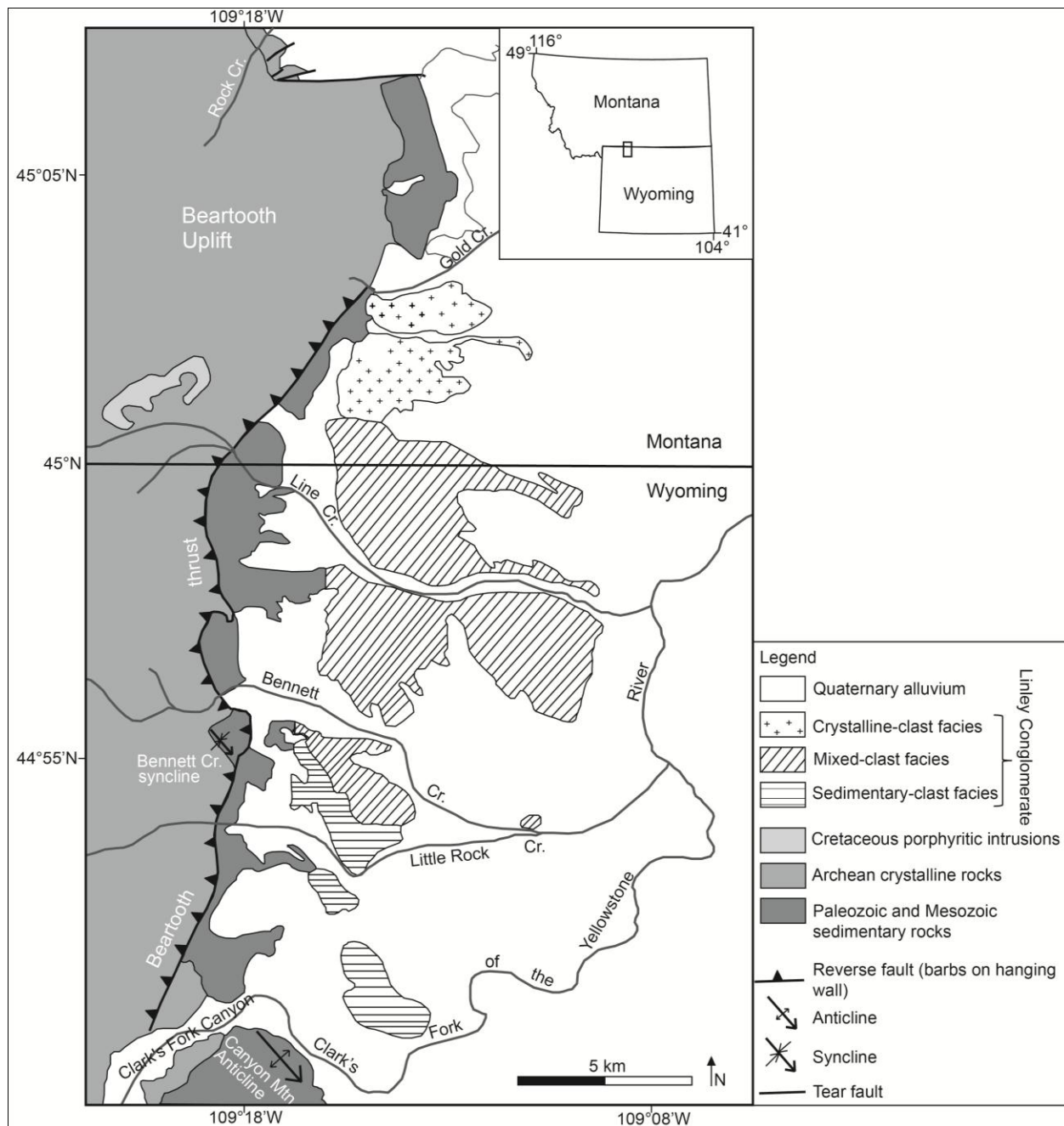
Figure 2. Geologic map of the northwestern Bighorn Basin and adjacent Laramide structures, after DeCelles et al., 1991. Map shows locations of Linley Conglomerate facies based on clast type. DeCelles et al. (1991) referred to the Linley Conglomerate member of the Fort Union Formation as the "Beartooth Conglomerate" and defined it as the coarse conglomerate interbedded with minor sandstones and siltstones that outcrops on the northeastern and eastern border of the Beartooth Mountains.

7

facies generally found near the mountain front (Lopez, 2005). The Linley Conglomerate is the uppermost member of the Paleocene Fort Union Formation and contains intraformational folds, faults, and unconformities that DeCelles et al. (1991a,b) used to infer that the uplift of the Beartooth Mountains occurred in the late Paleocene (DeCelles et al., 1991a,b). The Linley Conglomerate contains metamorphic, igneous, and sedimentary clasts derived from the Precambrian-through-Cretaceous rocks that constitute the Beartooth Mountains.

Jobling (1974) proposed a lithofacies of this member of the Fort Union Formation which existed adjacent to and parallel to the eastern perimeter of the Beartooth Mountains, called the "Proximal facies". The lower part of the Proximal facies consists of pebble conglomerates, coarse sandstones, and siltstones. In the lower part, conglomerate clasts are mostly Paleozoic limestone and black chert, with rare metamorphic and igneous rock fragments. The upper part of the Proximal facies includes pebble to boulder conglomerates interstratified with fine-to -coarse sandstones, siltstones, and minor shales. In the upper part of the Proximal facies, conglomerate clasts are mostly metamorphic and igneous rock fragments with some Paleozoic limestone clasts (Jobling, 1974). The changes in composition of the conglomerate clasts in Jobling's Proximal facies reflect the unroofing of the Beartooth Mountains, where clasts from the sedimentary cover are found near the base and clasts from the Precambrian basement occur higher in the section (Lopez, 2005). Six to eight kilometers east of the range front, the Linley Conglomerate grades laterally into lacustrine deposits, overbank mudstones, and fluvial sandstones of the Fort Union Formation (DeCelles, 1991b).

The late Paleocene-Eocene Willwood Formation consists of fluvial and alluvial pebbly-to-fine-grained sandstones, variegated mudstones, and locally abundant carbonaceous shales. The maximum thickness of the formation is 1200 meters near Heart Mountain. The presence of

red beds has commonly been used to differentiate it from the Paleocene Fort Union Formation (Gingerich, 1983).

In northwestern Wyoming and south-central Montana, the same strata have been mapped as both the late Paleocene-Eocene Willwood Formation and upper members of the Paleocene Fort Union Formation. Pierce (1965a, 1965b, 1966, 1968) appears to have mapped post-Cretaceous rocks containing red beds along the mountain front as the Willwood Formation. Just north of Line Creek in Montana, Lopez (2001) mapped the same rocks as the Fort Union Formation. In this paper, all late Paleocene-Eocene rocks in contact with Cretaceous sediments are referred to as "Willwood Formation" with the exception of the area near Heart Mountain where the Fort Union Formation is easily distinguished from the overlying Willwood Formation.

Geologic Mapping and Interpretation

We focused our field study in four specific areas along a 30 kilometer-long segment of the western edge of the Bighorn Basin in Park County, Wyoming (Fig. 1). These areas include (1) Line Creek; (2) Clarks Fork Canyon; (3) Kimball Bench; and (4) Heart Mountain (Fig. 3). We chose these locations because the Paleogene-Cretaceous contacts are exposed at the surface. For Paleogene Willwood conglomerates, we used clast-types to determine their stratigraphic level (and therefore relative age) within the Willwood Formation. Crystalline-clast conglomerates correspond to younger Willwood sediments, as they were deposited during the final unroofing stages of the crystalline-cored Beartooth uplift. Sedimentary-clast conglomerates are older Willwood deposits, as they formed during early Beartooth unroofing stages during the removal of the sedimentary cover (Jobling, 1974; Dutcher et al., 1986; Hickey et al., 1986; DeCelles et al., 1991b.; Lopez, 2005).

9
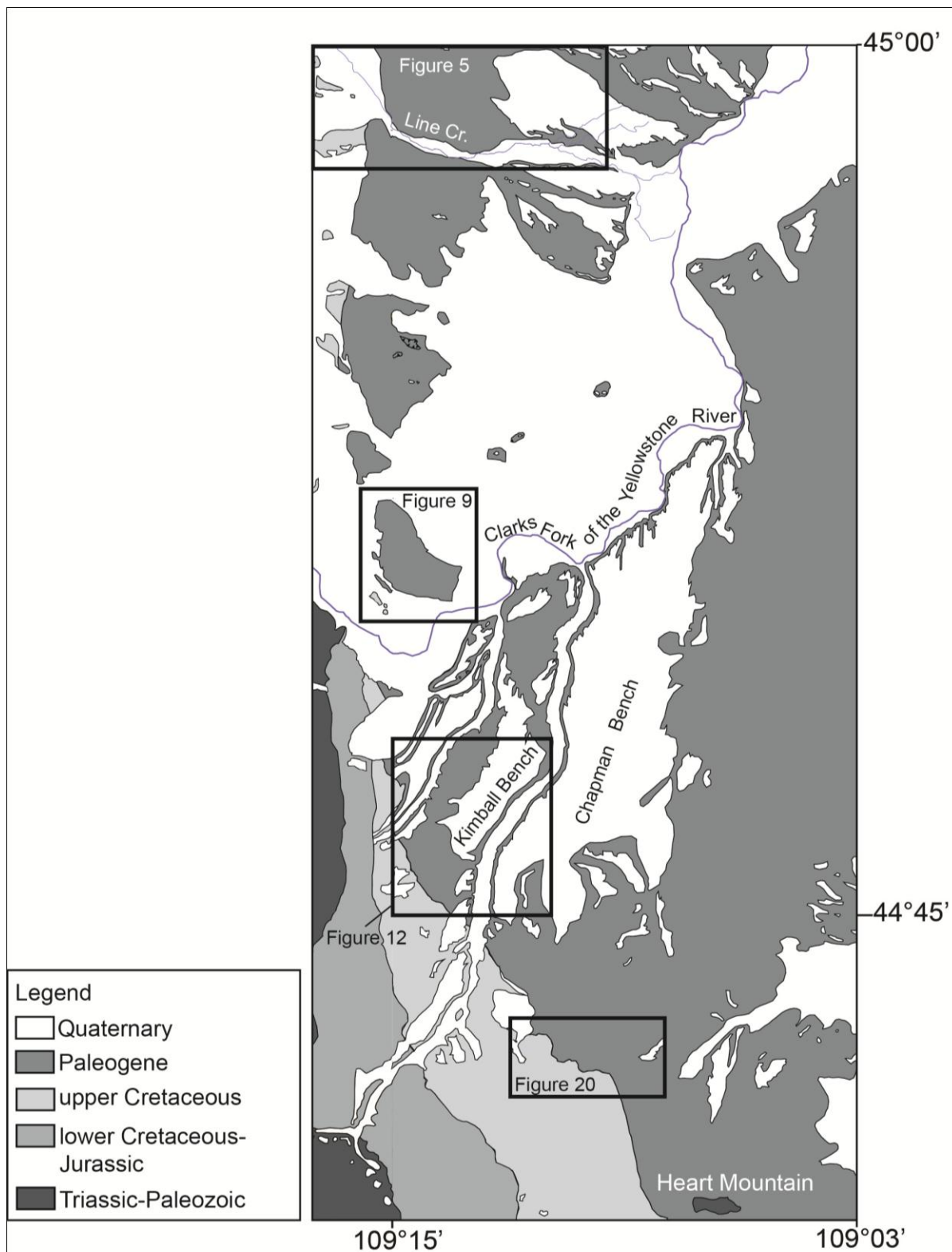
Figure 3. Generalized geologic map, modified from Pierce (1965). Boxes show locations of areas of interest based on exposure of Paleogene-Cretaceous contacts. North to south: Line Creek area; Clarks Fork Canyon area; Kimball Bench area; Heart Mountain area.

<u>Line Creek</u>

In the Line Creek area (Fig. 3), Meeteetse Formation rocks are in contact with the overlying Paleogene Willwood Formation. Well data in the northwestern Bighorn Basin show that near the Beartooth mountain front, the Lance Formation has an average thickness of 420 meters and the underlying Meeteetse Formation has a thickness of 280 meters (Fig. 4; Finn et al., 2010). Our map of the Line Creek area shows that the Willwood-Meeteetse contact is located 200 meters east of the Meeteetse-Mesaverde contact (Fig. 5). Using the mapped width of the formation and the dip of the layers, the preserved thickness of the Meeteetse Formation is 140 meters, as shown in our cross section through the Line Creek area (Fig. 6). The uppermost Cretaceous Lance Formation is completely absent in this area. In addition, the upper 140 meters of the Meeteetse Formation are missing, indicating that at least 560 meters of Cretaceous sediments were eroded away before Paleogene deposition began. The basal Willwood sediments here are characterized by interbedded red and tan siltstones, fine-to-coarse-grained sandstones, and pebble- to cobble-sized conglomerates (Fig. 7). The conglomerates are approximately 80% crystalline-clast and 20% sedimentary clast. The long axes of the crystalline clasts are 5-20 centimeters and the long axes of the sedimentary clasts are 2-5 centimeters. The matrix within the conglomerates consists of gray and red sand-sized grains. The presence of predominately crystalline clasts in the Willwood indicates that at the time of deposition, unroofing of the Beartooth Mountains to the west had progressed from erosion of the Upper Paleozoic-Mesozoic sedimentary cover to the point where the Middle and Lower Paleozoic crystalline core of the Beartooth block had been exposed. The red beds in the Willwood suggest that the sediments were subaerially exposed, interpreted to reflect a relatively dry environment of deposition (Bown and Kraus, 1987).
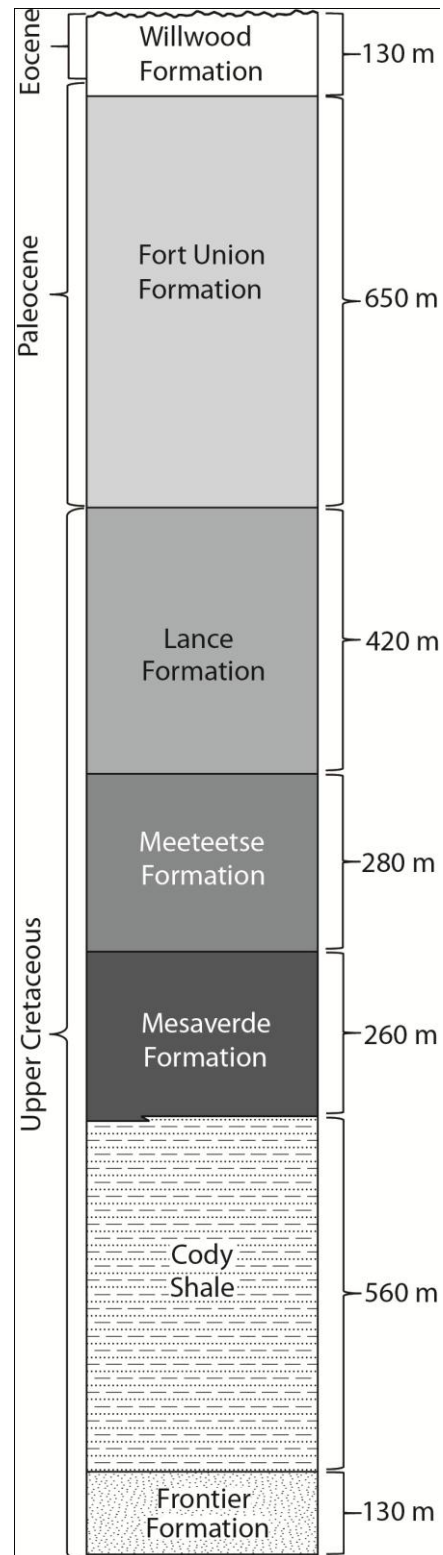
Figure 4. Stratigraphic column of Late Cretaceous-Paleogene formations. Approximate thicknesses along the northwestern margin of the Bighorn Basin from Impel Corp. O'Hara Federal 5-24 well, presented in Finn et al., 2010.
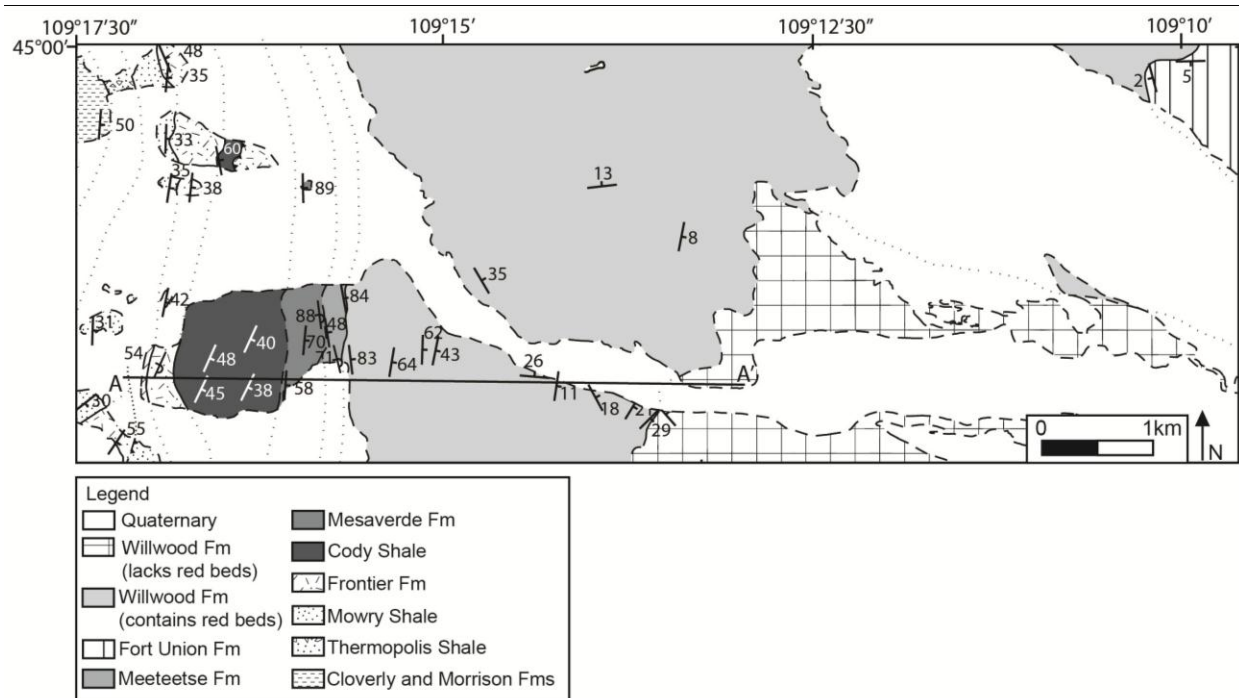
Figure 5. Geologic map of the Line Creek area. The Paleogene Willwood Formation transitions from gently dipping basinward to steeply tilted near the mountain front where it is in contact with the steeply tilted Cretaceous Meeteetse Formation in this area (Cretaceous Lance Formation is absent). A-A' is line of section in Figure 6.
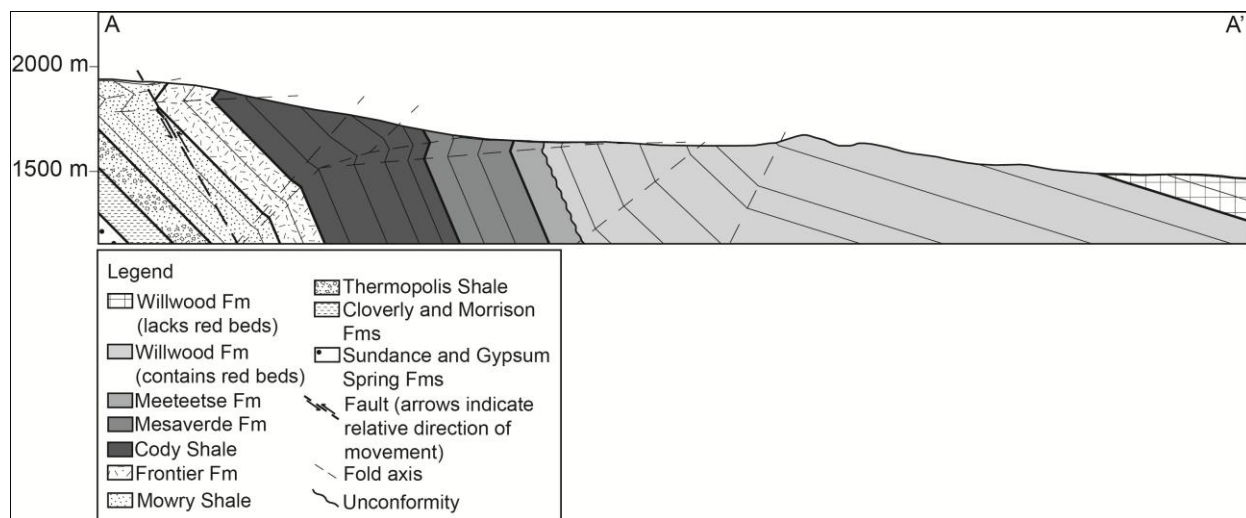
Figure 6. West-east cross section in the Line Creek area. The Cretaceous Lance Formation is absent and the Cretaceous Meeteetse Formation is 140 meters thick, indicating that approximately 560 meters of Cretaceous sediments were eroded away prior to Willwood deposition. In this area, the Paleogene Willwood Formation is steeply tilted along with the Late Cretaceous formations.

13

Figure 7. Pebble- to cobble-sized crystalline-clast conglomerates of the basal Willwood Formation, Line Creek area (clasts range 5-20 cm). Clasts are approximately 80% crystalline and 20% sedimentary, indicating that at the time of deposition, unroofing of the Beartooth Mountains had progressed to the point where the Middle and Lower Paleozoic crystalline core of the Beartooth block had been exposed.

In and around our study areas, Lillegraven (2009) proposed the existence of large-scale thrust faulting at the base of the Willwood. His proposed west-vergent thrust faults created approximately 30 kilometers of displacement along the western edge of the Bighorn Basin. A problem exists with this interpretation, however, as the siltstones and shales of the Willwood Formation are easily deformed. In the Kimball Bench area, we did find evidence of faulting within the Willwood, indicated by offset bedding and a shatter zone at the fault where bedding has been destroyed. This fault created approximately 15 meters of offset and resulted in a 4-meter-wide shatter zone. Thus, thrust faulting on the scale of multiple kilometers would necessitate a fault zone tens of meters wide in the Willwood Formation.

In the Line Creek area, Lillegraven (2009) described basal Willwood as containing "semi-chaotic bedding of mudstone rip-ups and pebbles in [the] thrust zone." However, we found that bedding is well-preserved in the basal Willwood and upper Meeteetse layers with no distinct shatter zone near the contact. Another common feature of faulting is slickensided surfaces, of which we found none after excavating around the contact. In the Line Creek area, Mowry Shale rocks are faulted with a few meters of offset; however there was no evidence of offset or a shatter zone near the base of the Willwood Formation (Fig. 8). It is probable that the "pebbles in [the] thrust zone" described by Lillegraven (2009) are in fact lag deposits, which are numerous throughout the Willwood Formation.

Structurally, the basal late Paleocene-Eocene Willwood Formation is steeply tilted to overturned and in depositional contact with underlying tilted Cretaceous Meeteetse sediments in the Line Creek area (Fig. 5, 6). Approximately 28 kilometers northeast of the Line Creek area, Lopez (2001) mapped gently-dipping Cretaceous Lance Formation in the Bighorn Basin. In the Line Creek area, Lance rocks are completely absent, indicating that they were eroded away at the

Figure 8. Preserved bedding at base of Willwood Formation, Line Creek area. In this area, Lillegraven (2009) described basal Willwood as containing "semi-chaotic bedding of mudstone rip-ups and pebbles in [the] thrust zone"; however, bedding is well-preserved with no evidence of offset or a shatter zone near the base of the Willwood. Compass points north, pencil is parallel to bedding.

mountain front but preserved in the basin. Regarding the timing of deformation, the presence of

the Lance Formation in the basin suggests that Late Cretaceous rocks including the Lance were

deposited together and then slightly tilted, eroding away the uppermost Cretaceous rocks, the

Lance Formation. After the removal of Lance strata near the mountain front, deposition of the

Willwood Formation began. Continued deformation tilted Late Cretaceous and Paleogene rocks

together, resulting in the present-day orientations of these rocks near the mountain front (Fig. 5).

Basinward of the Paleogene-Cretaceous contact, upper Willwood Formation sediments transition

to gently-dipping. The dominance of crystalline clasts in basal Willwood conglomerates

indicates deposition post-dating that of basal Willwood in the Clarks Fork Canyon area, Kimball

Bench area, and area west of Heart Mountain. Here, the paleovalley did not receive Paleogene

sediments until the deeper parts of the valley were filled.

Clarks Fork Canyon

      South of the Line Creek area is the Clarks Fork Canyon area (Fig. 3). Here, Mesaverde

Formation is the youngest Cretaceous unit in contact with the overlying Paleogene Willwood

Formation. The entire Late Cretaceous Lance and Meeteetse Formations, along with a part of the

upper Mesaverde Formation, are absent in this area. Well data show the approximate thicknesses

of these formations as follows: Lance Formation, 400 meters; Meeteetse Formation, 280 meters;

and Mesaverde Formation, 250 meters (Fig. 4; Finn et al., 2010). Our map of the Clarks Fork

Canyon area shows that the Willwood-Mesaverde contact is located 210 meters east of the

Mesaverde-Cody contact (Fig. 9). Using our measured attitudes of the strata, we calculated the

true thickness of the Mesaverde Formation in this area to be 190 meters, seen in our cross section

through the Clarks Fork Canyon area (Fig. 10). In addition, the upper 90 meters of the
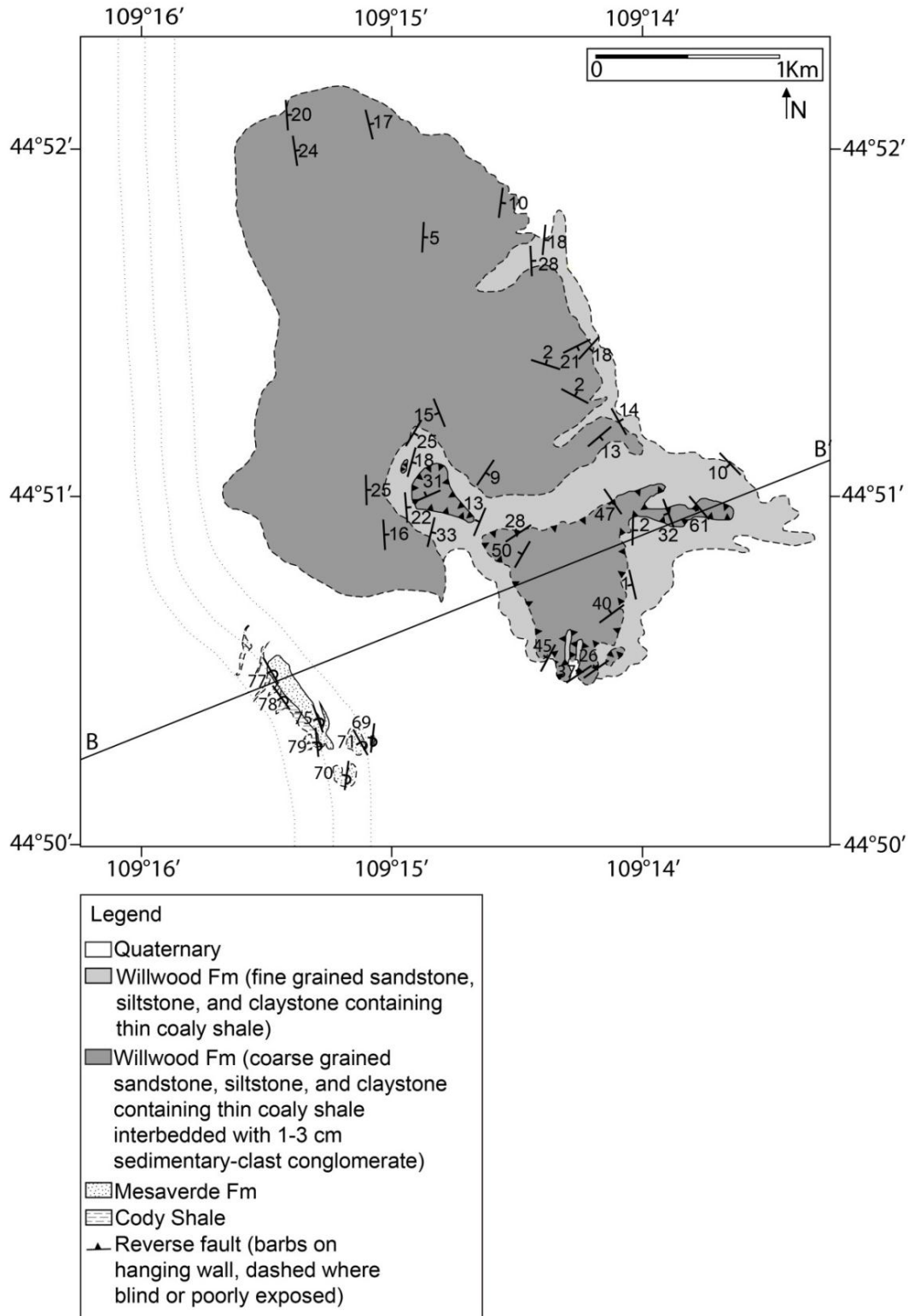
Figure 9. Geologic map of the Clarks Fork Canyon area. The Paleogene Willwood Formation is steeply tilted to overturned and in conformable contact with underlying tilted Mesaverde sediments (Cretaceous Meeteetse and Lance formations are absent). B-B' is line of section in Figure 10.

18
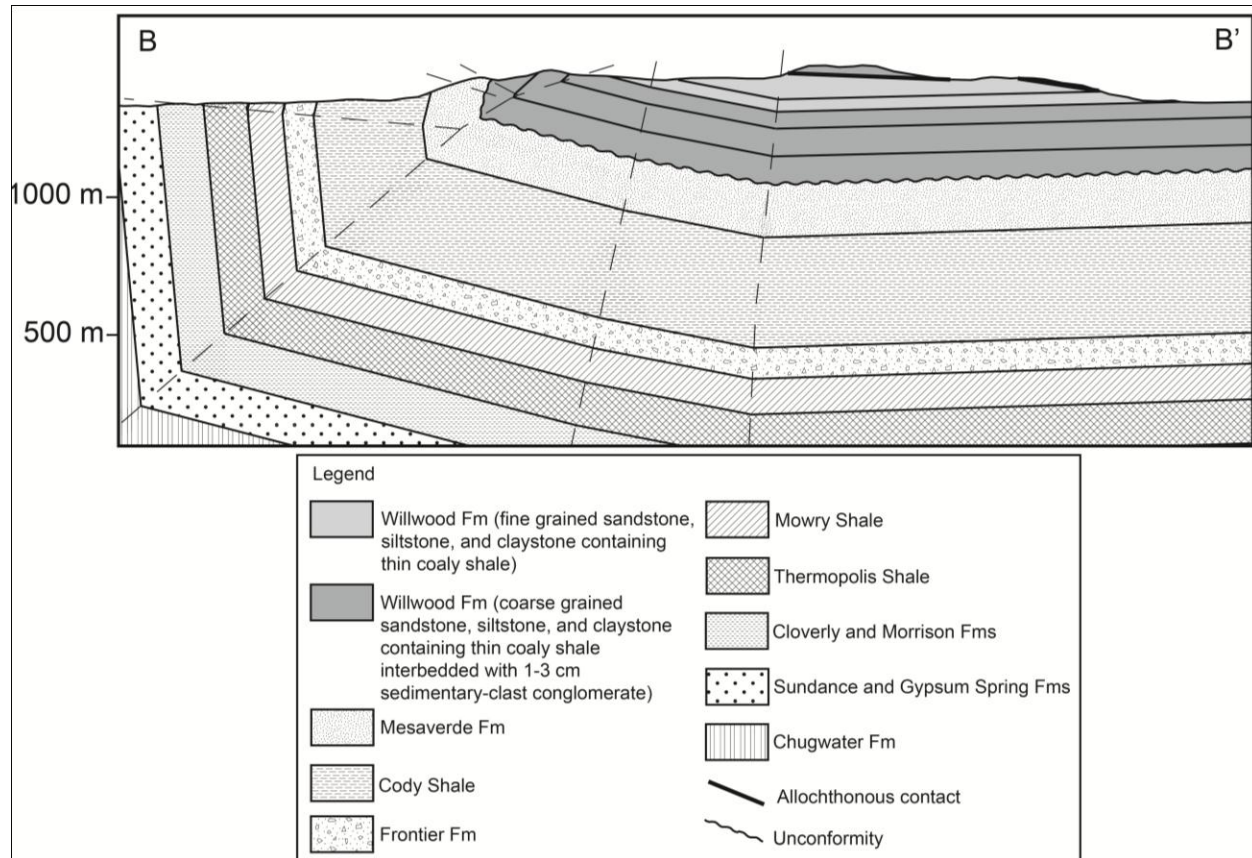
Figure 10. West-east cross section in the Clarks Fork Canyon area. The Cretaceous Meeteetse and Lance formations are absent and the Cretaceous Mesaverde Formation is 190 meters thick, indicating that approximately 790 meters of Cretaceous sediments were eroded away prior to Willwood deposition. In this area, the Paleogene Willwood Formation is steeply tilted to overturned along with the Late Cretaceous formations.

Mesaverde Formation are missing, indicating that approximately 790 meters of Cretaceous sediments were eroded away.

It is difficult to determine if basal Willwood was eroded away along with Late Cretaceous rocks in the Clarks Fork Canyon area. The oldest preserved Willwood sediments in the area consist of tan and brown medium-to-coarse-grained sandstones containing thin coal seams interbedded with sedimentary-clast conglomerates, predominantly limestone cobbles (Fig. 11). The conglomerates in the Willwood contain poorly sorted, rounded sedimentary clasts measuring less than 1 centimeter to 15 centimeters in length. The clasts include limestone, chert, and sandstone. Higher in the section, the Willwood Formation transitions to mostly brown and beige fine-grained siltstones and shales, interbedded with coal seams and conglomeratic pebble lags. The presence of sedimentary-clast conglomerate in the Willwood here indicates that deposition occurred during early unroofing stages of the Beartooth Mountains to the west, during removal of the sedimentary cover of the Beartooths.

In the Kimball Bench area, fine-grained basal Willwood sediments sourced from the nascent Beartooth Mountains were deposited prior to deposition of sedimentary-clast conglomeratic Willwood. There is a lack of fine-grained basal Willwood in the Clarks Fork Canyon area and it is likely that this area is near the mouth of the paleovalley. This would cause the fine-grained lower Willwood sediments to bypass the Clarks Fork Canyon area during the erosion of the nascent Beartooth Mountains. In the Clarks Fork Canyon area, basal Willwood is conglomeratic. As the fine-grained sediments filled the more distal parts of the paleovalley, erosion to the west progressed past the point where the Mesozoic and Upper Paleozoic sedimentary cover of the Beartooths was exposed, leading to deposition of sedimentary-clast conglomerates of the Willwood Formation in the Clarks Fork Canyon area and above the fine-grained deposits in the Kimball Bench area.

Figure 11. Pebble- to cobble-sized sedimentary-clast Willwood Formation conglomerates in the Clarks Fork Canyon area (hammer length 30 cm). Clasts are predominately limestone with some chert and sandstone. The presence of sedimentary-clast conglomerate in the Willwood here indicates that deposition occurred during early unroofing stages of the Beartooth Mountains to the west, during removal of the sedimentary cover of the Beartooths.

In the Clarks Fork Canyon area, basal Willwood sediments are steeply tilted to overturned and in depositional contact with underlying tilted Mesaverde sediments (Fig. 9, 10). The depositional contact between Mesaverde and Willwood strata suggests that major deformation of these formations occurred after deposition of at least lower Willwood rocks. In this area, the lack of red beds in the Willwood Formation and the presence of coal seams are interpreted to reflect a relatively wet environment of deposition (Bown and Kraus, 1987).

Kimball Bench

In the Kimball Bench area to the south of the Clarks Fork Canyon area (Fig. 3), basal Paleogene Willwood sediments are in contact with Cretaceous formations of varying ages including the Meeteetse, Mesaverde, and Cody Shale (Fig. 12). Near the mountain front, well data show the approximate thicknesses of these formations as follows: Lance Formation, 400 meters; Meeteetse Formation, 280 meters; Mesaverde Formation, 250 meters; and Cody Shale, 570 meters (Fig. 4; Finn et al., 2010). The deepest section of the paleovalley is where the Willwood rocks are in contact with the Cody Shale. Our map of the Kimball Bench area shows a distance of 580 meters between the Willwood-Cody contact and the Cody-Frontier contact (Fig. 12). Using our measured orientations of the beds, the thickness of the Cody Shale is calculated to be 530 meters thick here. In addition to 50 meters of the upper part of the Cody Shale missing, the Mesaverde, Meeteetse, and Lance Formations are also absent. This means that where Willwood rocks are in contact with the Cody Shale, nearly 1000 meters of Cretaceous rocks were eroded away. It is possible that basal Willwood strata were deposited and eroded along with Cretaceous rocks; however, due to the preserved fine-grained basal Willwood below conglomeratic Willwood at Kimball Bench, it is likely that little to no Willwood was eroded away before deformation began.

Figure 12. Geologic map of the Kimball Bench area. The Paleogene Willwood Formation transitions from gently dipping basinward to steeply tilted near the mountain front where it is in contact with Cretaceous formations of varying ages including the Meeteetse, Mesaverde, and Cody Shale (Cretaceous Lance Formation is absent). C-C' is line of section in Figure 17.

23

Lillegraven (2009) described the Willwood-Mesaverde contact in the Kimball Bench area as a "thrust zone…of chaotically deformed black mudstone abundantly admixed with rip-up pebbles of siltstone and sandstone within base of Willwood Formation hanging wall." We mapped the Mesaverde-Willwood contact throughout the Kimball Bench area and found well-preserved bedding at the base of the Willwood. It is probable that the "rip-up pebbles of siltstone and sandstones" are lag deposits which are commonly found throughout both the Willwood and Mesaverde Formations (Fig. 13). "Chaotically deformed black mudstone" may refer to fine-grained organic-rich shaly Willwood which is commonly found in the formation, although we did not find evidence of chaotic deformation. It is possible Lillegraven (2009) was referring to soft-sediment deformation, also common in the Willwood Formation (Fig. 14).

Where basal Willwood is in contact with the Mesaverde, the lowest Willwood sediments consist of variegated shales, claystones, and siltstones, transitioning up-section into pebble-to-cobble-sized sedimentary-clast conglomerates interbedded with sandstones, siltstones, and shales (Fig. 15). We interpreted these sediments to reflect deposition in a relatively dry environment due to the presence of red beds. Recall that in the Clarks Fork Canyon area, basal Willwood is also in contact with the Mesaverde; however, these sediments consist of conglomeratic Willwood rather than the fine-grained basal Willwood in the Kimball Bench area. Regarding the history of deformation, it is likely that the fine-grained sediments of the basal Willwood in the Kimball Bench area were sourced from sediments eroded off the nascent Beartooth Mountains to the west. Because these lower Willwood deposits were eroded from the Clarks Fork Canyon area but preserved in the Kimball Bench area, it is likely that the Clarks Fork Canyon area was closer to the mouth of the paleovalley, resulting in the bypass and/or erosion of the earliest Willwood deposits during early deformation. The sedimentary-clast conglomerates were then sourced from

Figure 13. Typical lag deposits in the Paleogene Willwood Formation, Kimball Bench area.

Figure 14. Soft-sediment deformation in the Paleogene Willwood Formation, Kimball Bench area.

Figure 15. Willwood Formation sediments in the Kimball Bench area. (A) Fine grained basal Willwood strata near the Willwood-Cody contact, sourced from sediments eroded off the nascent Beartooth Mountains to the west. (B) Limestone-clast conglomeratic Willwood up-section from fine-grained sediments, sourced from the Mesozoic and Upper Paleozoic sedimentary cover during the unroofing of the Beartooth Mountains, prior to exposure of the crystalline core of the mountains

the Mesozoic and Upper Paleozoic sedimentary cover during the unroofing of the Beartooth Mountains, prior to exposure of the crystalline core of the mountains.

In the Kimball Bench area south of the Cody-Willwood contact, the lower Willwood contact cuts into the Cretaceous Mesaverde Formation. The thickness of Mesaverde strata visibly decreases to the north, indicating that the paleovalley cut deeper into the Cretaceous section, ultimately cutting out the entire Mesaverde Formation and the top of the Cody Shale (Fig. 16, Fig. 12). Where Willwood sediments are in contact with Cody Shale, the deepest part of the paleovalley had formed. After the paleovalley formed, Willwood sediments were deposited on Late Cretaceous rocks. There was continued deformation which tilted Willwood strata along with Late Cretaceous rocks of varying ages (Fig. 12, 17, 18).

West of Heart Mountain

In the southernmost part of the study area, the area west of Heart Mountain (Fig. 3), Willwood Formation strata consist of brown-to-tan sandstones and variegated siltstones interbedded with pebble-sized sedimentary-clast conglomerates (Fig. 19). The long axes of the conglomerate clasts are less than 6 centimeters and are predominately made up of black chert and quartz. The clasts are well-rounded and poorly sorted. The sedimentary-clast conglomerates in the Willwood Formation in this area suggest that the source sediments came from the Mesozoic and Upper Paleozoic sedimentary cover on the Beartooths, after the fine-grained sediments of the nascent Beartooths bypassed the Clarks Fork Canyon area and deposited in the Kimball Bench area.

The presence of red beds indicates that the basal Willwood in this area were likely deposited in a relatively dry environment of deposition (Bown and Kraus, 1987). In this location, basal Willwood is in contact with Late Cretaceous and late Paleocene formations of varying

27
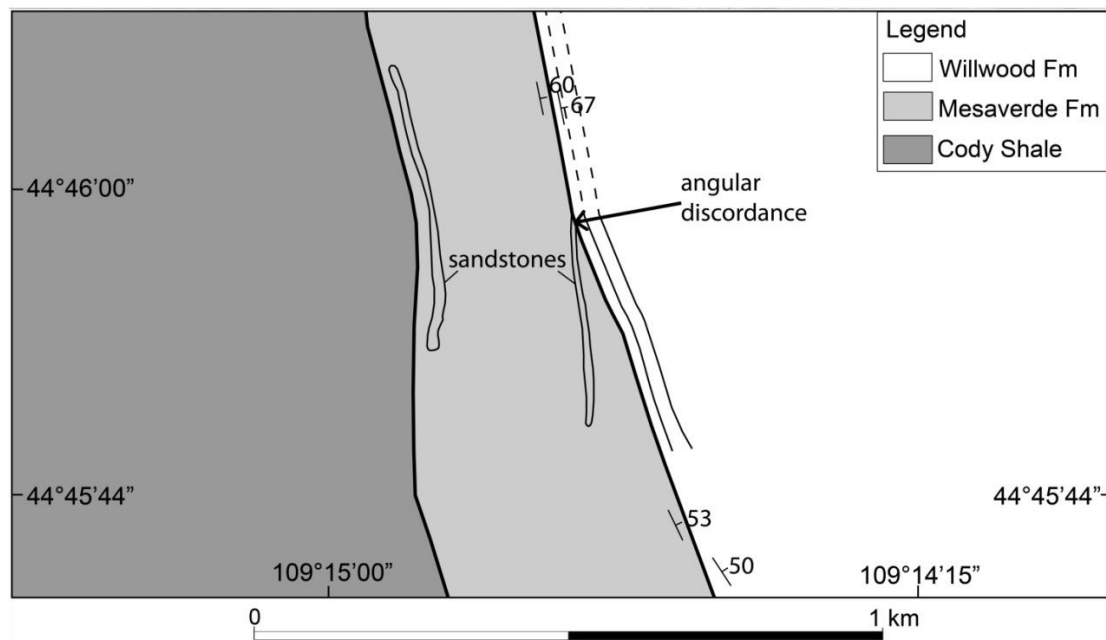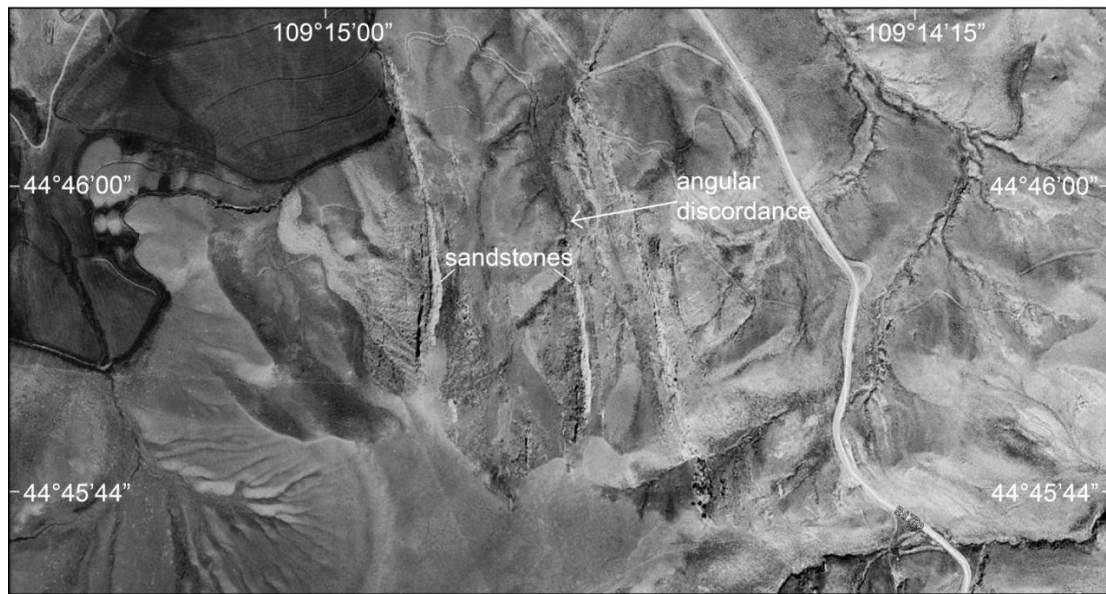
Figure 16. Top: aerial photo from Google Earth in Kimball Bench area. Bottom: line drawing of aerial photo in Kimball Bench area. Here, the Paleogene Willwood Formation cuts into the Cretaceous Mesaverde Formation (Cretaceous Meeteetse and Lance formations are absent). The thickness of Mesaverde strata visibly decreases to the north, indicating that the paleovalley cut deeper into the Cretaceous section, ultimately cutting out the entire Mesaverde Formation and the top of the Cody Shale.
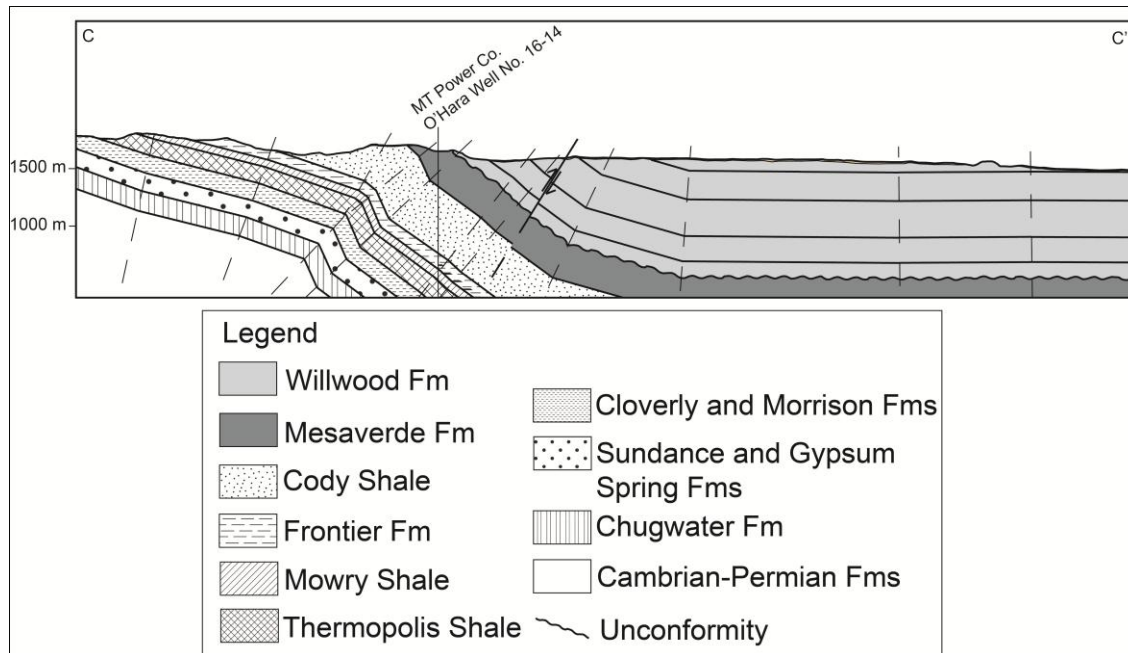
Figure 17. Southwest- northeast cross section in the Kimball Bench area. The Cretaceous Meeteetse and Lance formations are absent, indicating that approximately 700 meters of Cretaceous sediments were eroded away prior to Willwood deposition. In this area, the Paleogene Willwood Formation is steeply tilted to overturned along with the Late Cretaceous formations.
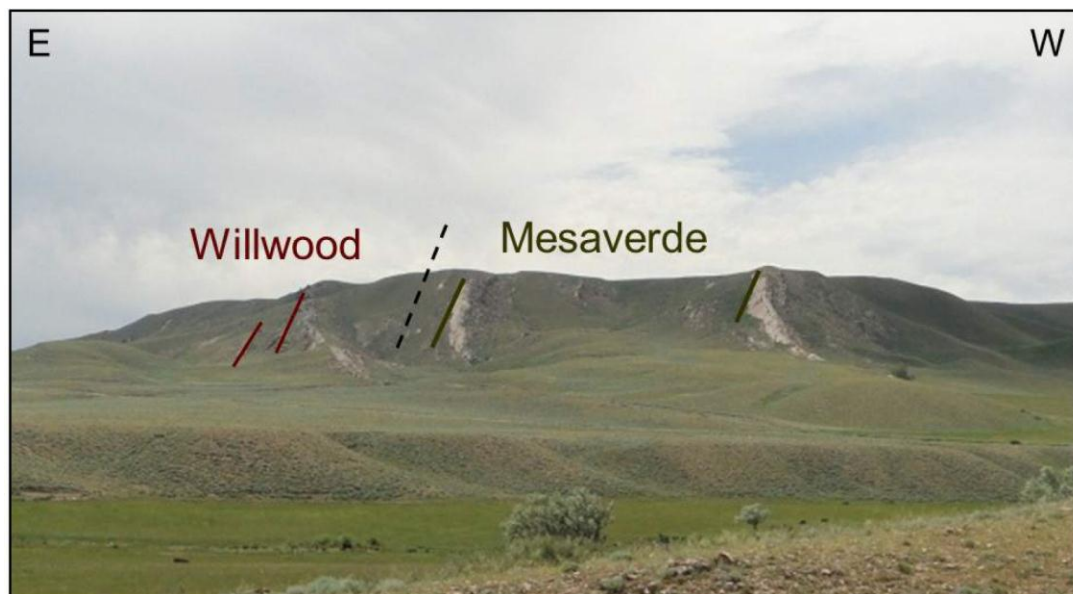
Figure 18. Willwood Formation sediments tilted with Cretaceous Mesaverde Formation sediments in the Kimball Bench area (Cretaceous Lance and Meeteetse formations are absent). In this area, differential erosion removed Late Cretaceous rocks during formation of the paleovalley, followed by Paleogene Willwood deposition and then major deformation which tilted the rocks together.

Figure 19. Sedimentary-clast Willwood Formation conglomerates in the area west of Heart Mountain (clasts < 6 cm). Clasts are predominately black chert and quartz, indicating that at the time of deposition, conglomerate clasts were sourced from the Mesozoic and Upper Paleozoic sedimentary cover during the unroofing of the Beartooth Mountains, prior to exposure of the crystalline core of the mountains.

ages, including the Cretaceous Meeteetse Formation, the Cretaceous Lance Formation, and the late Paleocene Fort Union Formation (Fig. 20). The uppermost Cretaceous Lance Formation is 420 meters thick in this area, similar to the thickness shown in a well log a few kilometers south of the area (Finn et al., 2010). This indicates that little to no erosion occurred prior to Paleogene deposition. Basal Willwood sediments are in angular discordance with underlying formations, as Willwood layers are gently dipping and the underlying Cretaceous and late Paleocene layers are tilted (Fig. 21, 22). The nature of this angular unconformity indicates that a majority of deformation in this area occurred prior to Willwood deposition and therefore earlier than a majority of deformation in the other study areas where we see Paleogene and Late Cretaceous rocks tilted together. It is possible that punctuated deformation events occurred, first in the area west of Heart Mountain, followed by further deformation northward after deposition of lower Willwood sediments. This could suggest that deformation in the area west of Heart Mountain was occurring during the development of the Pat O'Hara anticline to the west, and that the Kimball Bench, Clarks Fork Canyon, and Line Creek areas were later deformed during the unroofing of the Beartooth Mountains.

Lillegraven (2009) suggested that a thrust fault exists at the Willwood-Fort Union contact southwest of Heart Mountain. He described the thrust fault as an "unweathered, strongly slickensided, abrupt contact between well-indurated and apparently little-deformed sandstone units occurring in opposed hanging wall and footwall." We excavated the Willwood-Fort Union contact near Lillegraven's site and did find abundant slickensides in Willwood sediments. However, these slickensides are randomly oriented, indicating that they formed from shrink-swell rather than faulting (Fig. 23; Kraus and Aslan, 1993). At the Willwood-Lance contact northwest of Heart Mountain, Lillegraven (2009) described a thrust zone as a "chaotic mélange
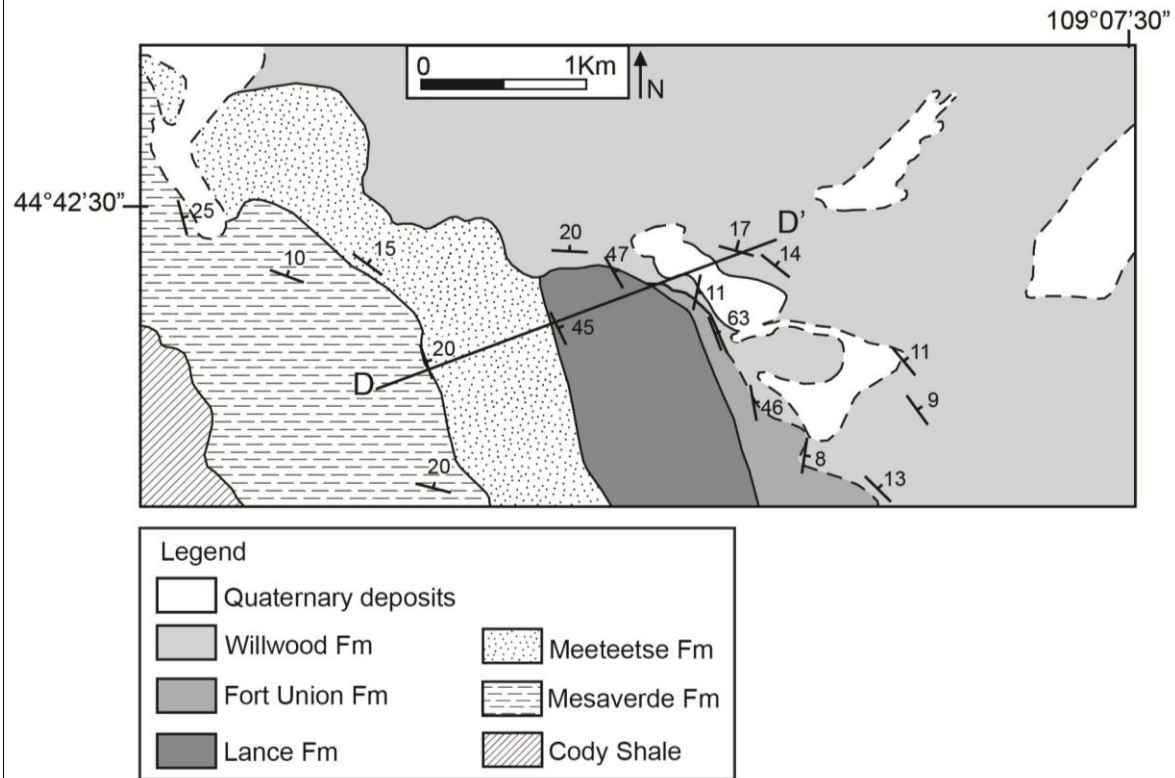
Figure 20. Geologic map of the area west of Heart Mountain. The Paleogene Willwood
Formation is gently-dipping and rests at angular discordance on top of tilted Late Cretaceous and
late Paleocene formations of varying ages including the Cretaceous Meeteetse, Cretaceous
Lance, and Paleocene Fort Union formations. D-D' is line of section in Figure 21.
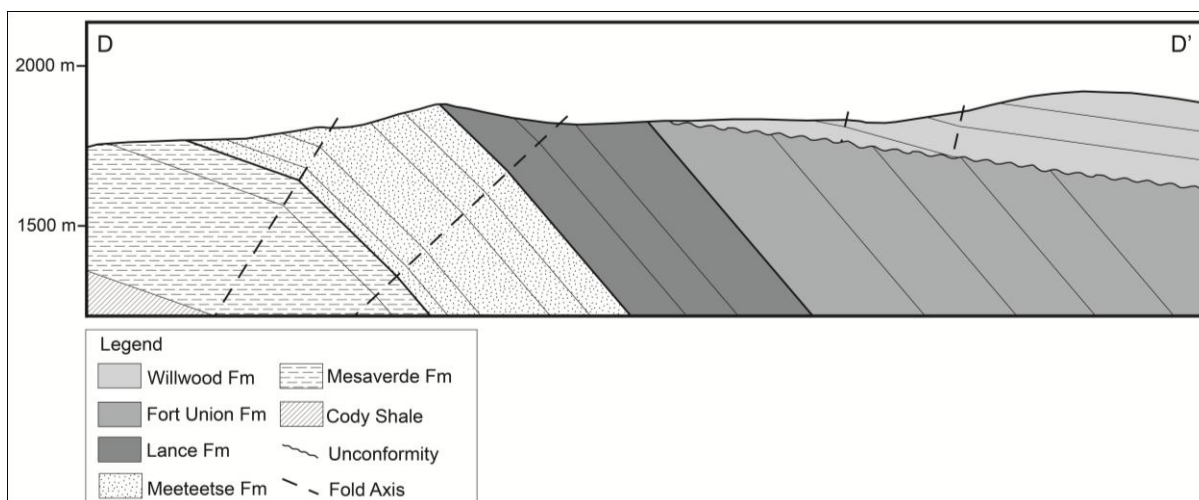
Figure 21. West-east cross section in the area west of Heart Mountain. In this area, the Paleogene
Willwood Formation is gently dipping on top of tilted Late Cretaceous-Paleocene formations.
This indicates that a majority of deformation in this area occurred prior to Willwood deposition
and therefore earlier than a majority of deformation in the other study areas.
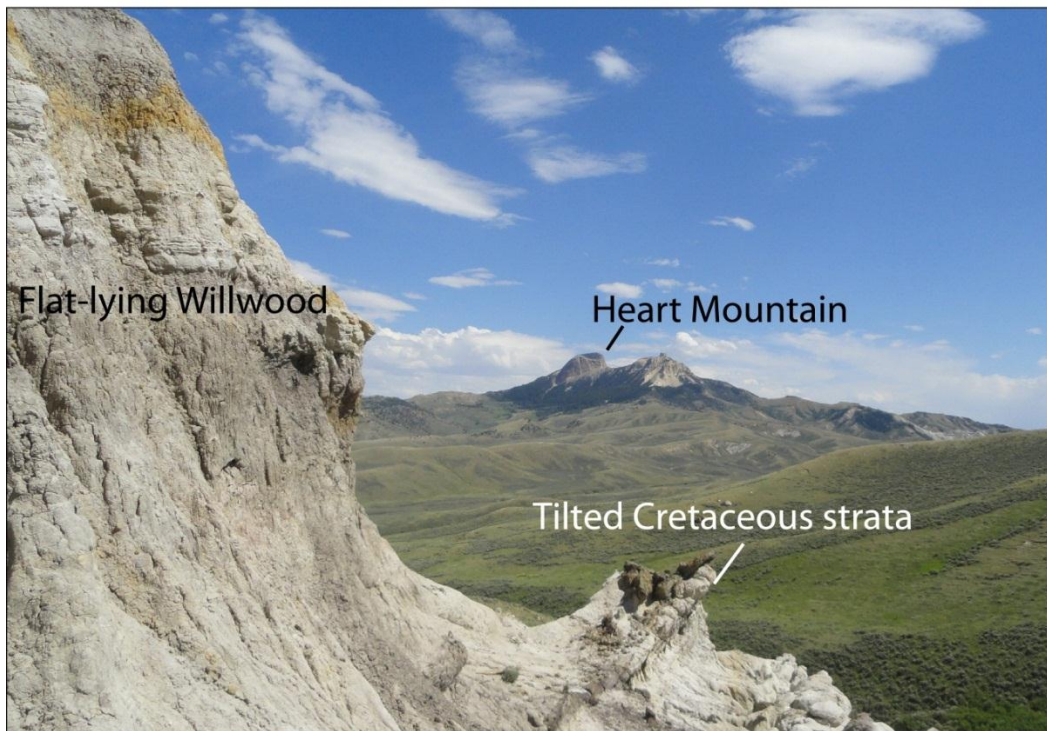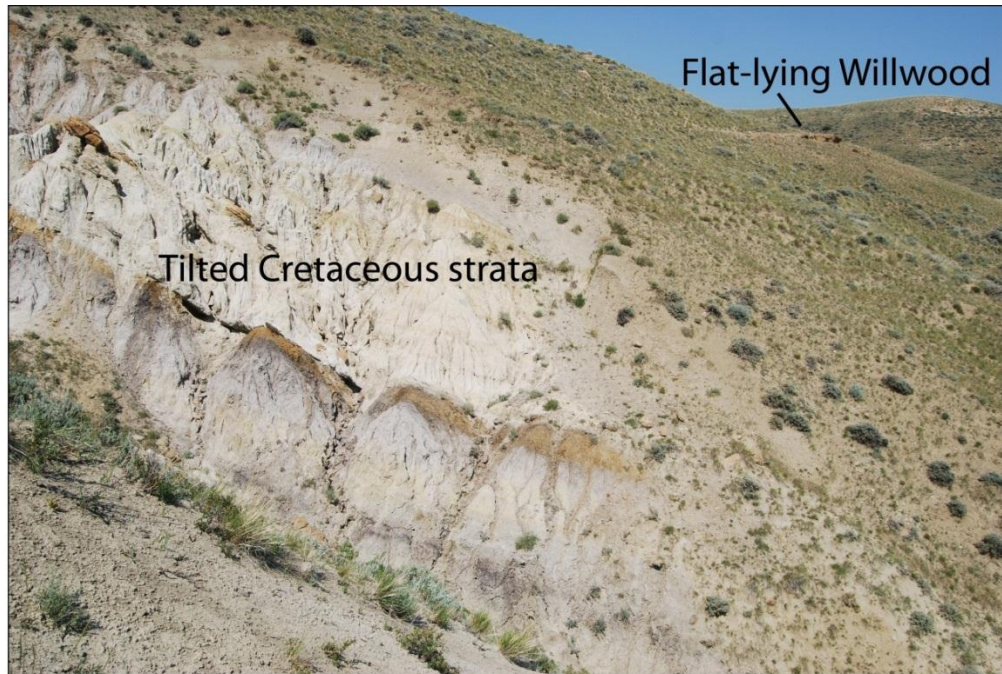
Figure 22. Gently-dipping Paleogene Willwood on top of tilted Cretaceous rocks west of Heart Mountain. The nature of this angular unconformity indicates that a majority of deformation in this area occurred prior to Willwood deposition and therefore earlier than a majority of deformation in the other study areas where we see Paleogene and Late Cretaceous rocks tilted together.

Figure 23. Multi-directional slickensided shale in the Willwood Formation, southwest of Heart Mountain. Black lines highlight various directions of slickensides, indicating that they formed from shrink-swell cycles rather than faulting.

of strongly slickensided mudstone and sandstone rip-up clasts." Once again, we did find slickensides in this area but they were randomly oriented as a result of shrink-swell. We also found rip-up clasts near the Willwood-Lance contact, but determined that they were depositional rip-up clasts within lag deposits, as bedding was preserved at the contact where they were found (Fig. 24).

Geometry of Pre-Paleogene Cretaceous Strata

The varying ages of the Cretaceous rocks in contact with Paleogene strata along the western edge of the Bighorn Basin could be the result of a deep paleovalley eroded into Cretaceous rocks, down to the Cody Shale in the deepest part of the valley. Another possibility is that there was a broad, east-west trending anticline prior to Paleogene deposition that was subsequently eroded, exposing Cody Shale in the core and progressively younger Cretaceous rocks along its flanks.

In order to determine whether an anticline was present prior to Paleogene deposition, we rotated lowermost Willwood strata to horizontal and rotated the adjacent Cretaceous units the same amount. This should show the orientation of the Cretaceous rocks immediately prior to Willwood deposition. If there was an anticline present, the rotated Cretaceous strata should be north-dipping in the north, south-dipping in the south, and nearly horizontal at the fold hinge of the anticline.

We restored the Paleogene rocks to horizontal at ten locations in our field area. Table 1 lists the present-day strikes and dips of Cretaceous and Paleogene rocks at each location as well as the restored strikes and dips of Cretaceous rocks prior to Paleogene deposition. At localities 2, 3, 5, 6, and 8 (Table 1; Fig. 25), restored Cretaceous beds have a nearly horizontal dip in similar orientation with Willwood strata. At all other localities, restored Cretaceous orientations dip

Figure 24. Depositional rip-up clasts in the basal Willwood Formation, northwest of Heart Mountain. In this area, Lillegraven (2009) described a "chaotic mélange of strongly slickensided mudstone and sandstone rip-up clasts in [the] thrust zone within base of shallowly dipping Willwood formation"; however, we only found depositional rip-up clasts in this area.

Location Number	Present-day Cretaceous strike and dip	Present-day Paleogene strike and dip	Restored Cretaceous strike and dip	Number of Cretaceous Measurements	Number of Paleogene measurements
1	169°, 79° W	356°, 86° E	331°, 17° E	5	4
2	002°, 71° E	007°, 75° E	231°, 06° N	2	4
3	190°, 76° W	185°, 69° W	223°, 08° W	6	1
4	171°, 58° W	343°, 88° E	355°, 34° E	1	3
5	346°, 60° E	345°, 60° E	084°, 01° S	7	8
6	333°, 45° E	333°, 40° E	336°, 05° E	6	7
7	333°, 44° E	324°, 28° E	347°, 17° E	8	5
8	319°, 33° E	317°, 25° E	325°, 08° E	1	1
9	330°, 20° E	301°, 11° E	356°, 12° E	1	2
10	332°, 57° E	329°, 46° E	340°, 10° E	3	18

Table 1. Paleogene-Cretaceous orientations in ten locations along the western edge of the Bighorn Basin (see Figure 25 for map locations).

Figure 25. North-south cross section of paleovalley before major tilting. Geologic map inset shows location of A-A' line, restored Cretaceous bedding orientations labeled by locality, and locations of fossil data from Hickey (1980), Rose (1981), Gingerich (1990), and Johnson and Middleton (1990). In the cross section: brackets are labeled with the range of ages for each fossil locality. Dashed lines represent approximated isochrones at 56-54 Ma. Location and type of Willwood conglomerates were determined from our mapping data along with Flueckinger (1970) and Dutcher et al. (1986) Paleogene conglomerate clast count data. Restored Cretaceous bedding orientations (labeled on inset) were found by rotating present-day Paleogene bedding orientations to horizontal and recording the resulting restored Cretaceous bedding orientations.

eastward in angular discordance with the overlying Willwood Formation (Table 1; Fig. 25). We used the restored bedding data in Table 1 to create a cross section through the western edge of the Bighorn Basin (Fig. 25). Our cross section indicates that the orientations of the restored Cretaceous strata in contact with the Willwood Formation do not support the existence of a broad anticline along the entire eastern flank of the Wyoming Beartooth Mountains and east of Pat O'Hara Mountain (Fig. 25).

Discussion of Cretaceous-Paleogene Relationships within the Paleovalley

Based on our field mapping, we found that the basal Willwood sediments in contact with the oldest Cretaceous rocks are located in the Kimball Bench area, where basal Willwood is seen tilted similarly to Cretaceous Cody Shale. Along the western edge of the Bighorn Basin, basal Willwood sediments in contact with underlying Cretaceous rocks of varying ages indicate that a deep paleovalley existed in this area prior to Paleogene Willwood deposition (Fig. 25). Conglomerate clast count data from Flueckinger (1970) and lithological data from Dutcher et al. (1986) along with our own mapping data was used to determine the stratigraphic position and lithologies of Paleogene infill in various parts of the paleovalley (Fig. 25). The deepest parts of this paleovalley were in the Kimball Bench area which filled first with fine-grained sediments sourced from the nascent Beartooth Mountains to the west. The mouth of the paleovalley was likely at present-day Clarks Fork Canyon which allowed for bypass of the earliest Willwood sediments through the Clarks Fork Canyon area into the Kimball Bench area. As the deeper sections of the paleovalley were filled, sediment deposition became more widespread with sedimentary-clast conglomeratic Willwood being deposited across the Clarks Fork Canyon and Kimball Bench areas. Finally, the Line Creek area was filled with crystalline-clast conglomeratic Willwood, reflecting the later stages of unroofing of the Beartooth Mountains (Fig. 25). Based

on the angular discordance of gently-dipping sedimentary-clast conglomeratic Willwood with underlying tilted Paleocene-Cretaceous strata, the area west of Heart Mountain has a different deformation history than the other study areas. This reflects an earlier period of deformation prior to deposition of sedimentary-clast conglomeratic Willwood, which can be explained by slightly earlier uplift of the Pat O'Hara anticline prior to the unroofing of the Beartooth Mountains.

We attempted to constrain absolute ages of Paleogene infill of the paleovalley through the use of late Paleocene-Eocene fossil ages. Previous studies by Hickey (1980), Rose (1981), Gingerich (1990), and Johnson and Middleton (1990) describe fossil locations with given age ranges along the western edge of the Bighorn Basin. We were able to calculate the true stratigraphic thickness of the Willwood at each fossil locality, which we superimposed onto our paleovalley cross section (Fig. 25). We projected the fossil age ranges onto the paleovalley as age brackets; however, we found that a complication in using these fossil localities is that they are basinward of the Cretaceous-Paleogene geologic map contacts. In some places, the fossil localities are 6- 7 km east of the Cretaceous-Paleogene geologic map contacts (Fig. 25). Because sediment accumulation rates vary with geographical location, the specific stratigraphic position of each fossil locality may not be correlative with the same stratigraphic position directly above the exposed Cretaceous-Paleogene contact westward.

Discussion

In this study, we used structural and sedimentologic information to estimate paleotopography along the western edge of the Bighorn Basin. The nature of Cretaceous-Paleogene contacts and the thicknesses of sediments have revealed a deep paleovalley carved into Late Cretaceous layers (Fig. 25). The Cretaceous rocks in contact with the basal Paleogene

Willwood Formation vary in age along the basin edge, and these varying ages indicate that there was differential erosion of the Late Cretaceous layers which resulted in a paleovalley that was filled in by Paleogene sediments.

<u>Removal of Late Cretaceous Sediments, Paleogene Facies Development</u>

In the deepest part of the paleovalley around the Kimball Bench area (Fig. 12), the Cretaceous Cody Shale is in contact with basal Willwood sediments. In this area, at least 1200 meters of Cretaceous sediments (Mesaverde, Meeteetse, and Lance Formations) were eroded away before Paleogene deposition began. In the Clarks Fork Canyon area (Fig. 9), basal Willwood sediments rest on top of sediments of the lower Mesaverde Formation. Here, at least 1100 meters of Cretaceous sediments were removed before deposition of Willwood. In the Line Creek area (Fig. 5), basal Willwood is in contact with the Cretaceous Meeteetse Formation. In this area, about 400 meters of Cretaceous sediments were eroded away before Willwood deposition. In the area west of Heart Mountain (Fig. 20), gently-dipping Willwood strata rest on top of steeply tilted Late Cretaceous-Paleocene rocks. Where Willwood sits atop Paleocene Fort Union sediments, little to no erosion occurred prior to Willwood deposition.

Various facies of the Willwood Formation were deposited at varying depths of the paleovalley, with earliest deposition in the deepest areas first. The facies reflect the unroofing of the Beartooth block, with fine-grained facies deposition occurring first in the deepest areas, followed by deposition of limestone-clast conglomerates and finally crystalline-clast conglomerates. These facies correlate with their stratigraphic position and therefore allow for an interpretation of the topography of the paleovalley at their time of deposition.

In the Line Creek study area, basal Willwood sediments are characterized by fine grained red and tan siltstones and sandstones interbedded with cobble-sized crystalline-clast

40

conglomerates (Fig. 7). The dominance of crystalline clasts indicates that these Willwood sediments were deposited during late stages of unroofing, past the point where the crystalline core of the Beartooth block had been exposed. South of the Line Creek area in the Clarks Fork Canyon area, basal Willwood is dominated by sedimentary-clast conglomerates, mostly limestone cobbles (Fig. 11). Here, the Willwood represents earlier deposition than the crystalline-clast conglomeratic Willwood from the Line Creek study area. The Willwood present in the Clarks Fork Canyon area was deposited during earlier unroofing stages of the Beartooth Mountains. In this area, the Willwood Formation grades into brown and beige shales, siltstones, and sandstones containing some conglomeratic lags, seen up-section from the conglomerate-dominated Willwood.

In the Kimball Bench area, basal Willwood consists of a thick section (~50 visible meters) of variegated fine-grained material (Fig. 15). Up-section from this, the Willwood Formation grades into pebble to cobble-sized sedimentary-clast conglomeratic sediments. Here, the fine-grained basal sediments correlate with earliest Willwood deposition as a result of the earliest erosion of the nascent Beartooth Mountains to the west. In the area west of Heart Mountain, the Willwood Formation is comprised of tan to brown shales, siltstones, and sandstones interbedded with pebble to cobble-sized sedimentary-clast conglomerates (Fig.19). The sedimentary-clast conglomerates were deposited during removal of the Upper Paleozoic-Mesozoic sedimentary cover of the Beartooths to the west.

Another notable feature of the Willwood Formation is the presence or lack of red beds in certain areas. The presence of red beds indicates subaerial exposure of sediments after deposition, suggesting a relatively dry terrestrial environment of deposition. The lack of red beds in the Willwood Formation correlates with wetter environments of deposition. In the deepest part

41

of the paleovalley around the Kimball Bench area, basal Willwood contains variegated red, tan, and brown beds, indicating a relatively dry setting. In the Clarks Fork Canyon area, sediments of the Willwood Formation are at a higher stratigraphic position than those in the Kimball Bench area. These Willwood sediments contain coal seams and lack the presence of red beds, indicative of a wetter environment at the time of deposition. Up-section of these deposits, particularly in the Line Creek area, Willwood sediments consist of interbedded tan to red rocks. Here, the environment once again became drier at the time of deposition.

Slight angular unconformities between Cretaceous and Paleogene rocks in some areas suggest that the Cretaceous layers had been somewhat tilted before Paleogene deposition. However, present-day orientations among these formations in most areas are still very similar and this suggests that deposition of Willwood occurred during the earliest stages of tilting, before major uplift that resulted in the steep tilting of the Cretaceous and Paleogene layers together.

Development of a Late Cretaceous Paleovalley

Our research has allowed for an understanding of events that led to the present-day orientation of Late Cretaceous and Paleogene sediments along the western edge of the Bighorn Basin in northwestern Wyoming (Fig. 26). Before unroofing of the Beartooth Mountains began, there was deposition of original flat-lying Cretaceous layers (Fig. 26A). After their deposition, slight tilting and differential erosion occurred as a result of tectonism beginning to the west, resulting in a large drainage area centered near the present day mouth of the Clarks Fork Canyon. This reflected the first stages of uplift of the Beartooth Mountains (Fig. 26B). This was how the paleovalley formed, with the deepest part located in the Kimball Bench area. After the erosion of Cretaceous layers, deposition of the Willwood Formation began. Fine-grained Willwood was deposited on top of the Cretaceous Cody Shale early on in the deepest part of the paleovalley in

the Kimball Bench area (Fig. 26C). Sedimentary-clast conglomerates within the Willwood were then deposited in the Kimball Bench and Clarks Fork Canyon areas, reflecting early unroofing stages of the Beartooth block to the west (Fig. 26D). As deposition continued, Willwood sediments changed from being dominated by limestone-clast conglomerate to crystalline-clast conglomerate which reflected later stages of the Beartooth uplift as the crystalline core was unroofed (Fig. 26E). Lastly, major tilting occurred, resulting in the present-day orientations of the Paleogene and Cretaceous rocks in the area.

Conclusions

Historically, Late Cretaceous and Paleogene sediments have been used to explain the timing of uplift and deposition correlating with the unroofing of the Beartooth Mountains in this part of northwestern Wyoming (Jobling, 1974; Dutcher et al., 1986; Hickey et al., 1986; Parker and Jones, 1986; DeCelles et al., 1991b.). Our study of Cretaceous-Paleogene geology in northwestern Wyoming represents the first to use structural and sedimentologic data along the western edge of the Bighorn Basin in order to reconstruct the paleotopography that existed along the western edge of the Bighorn Basin prior to and during the unroofing of the Beartooth Mountains. Our data have revealed a deep paleovalley carved into Cretaceous sediments prior to Paleogene deposition, which explains most of the unconformities present within these layers. This has also led to an interpretation that links the nature and ages of the Cretaceous-Paleogene contacts to the deformation and depositional history along the western edge of the Bighorn Basin in a way that hasn't been suggested before.

43
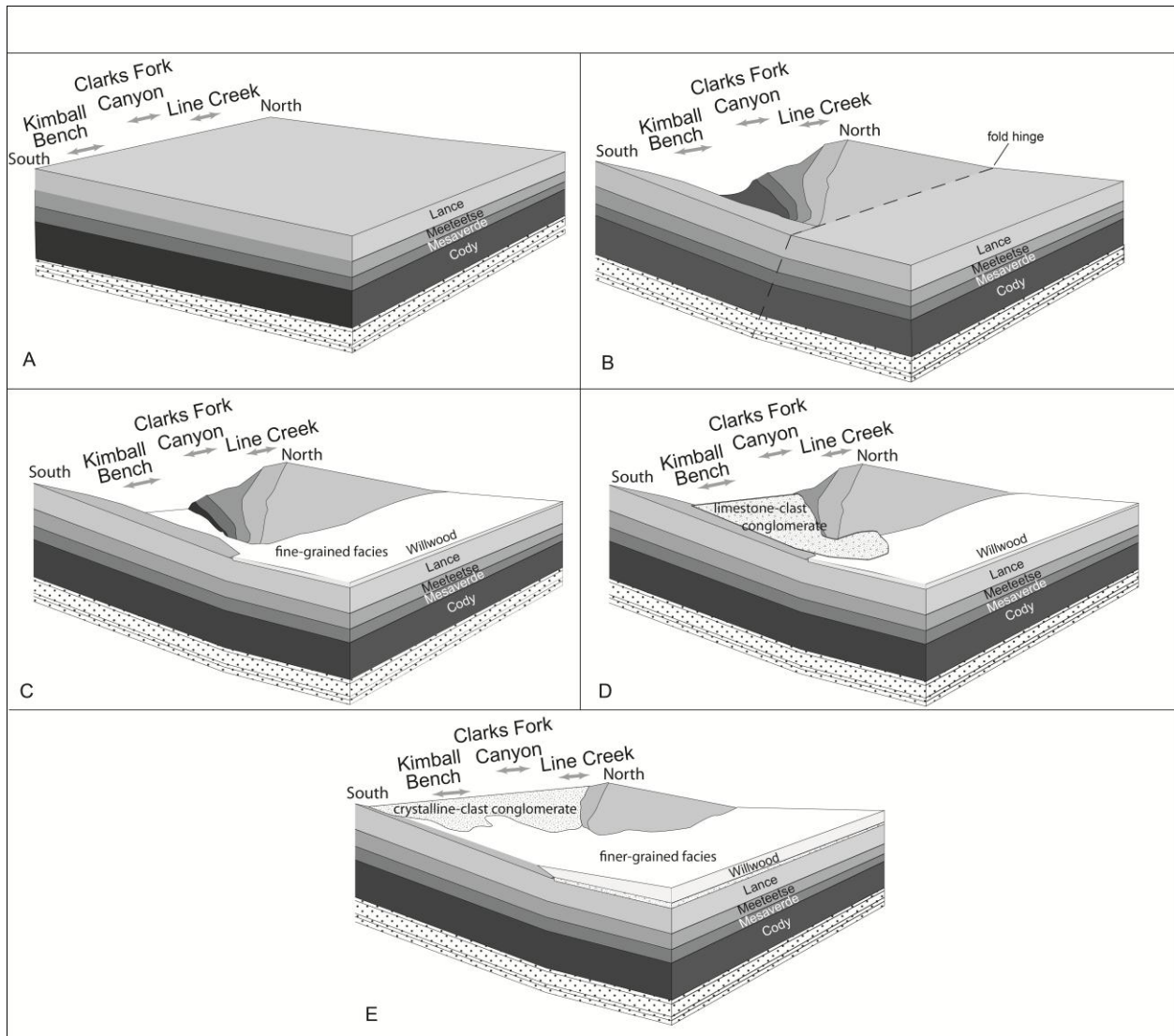
Figure 26. Block diagrams showing formation of paleovalley and subsequent Willwood deposition along the western edge of the Bighorn Basin. A. Deposition of original flat-lying Cretaceous layers. B. Slight tilting and differential erosion of Late Cretaceous layers. C. Beginning of fine-grained Willwood deposition. D. Sedimentary-clast conglomeratic Willwood deposition. E. Crystalline-clast conglomeratic Willwood deposition. After the carving and subsequent infill of the paleovalley, major tilting occurred, resulting in the present-day orientations of the Paleogene and Cretaceous rocks in the area.

REFERENCES

Bown, Thomas M., and Kraus, Mary J., 1987, Integration of channel and floodplain suites, I. Developmental sequence and lateral relations of alluvial paleosols: Journal of Sedimentary Petrology, v. 57, No. 4, p. 587-601.

Brook, E.J., Brown, E.T., Kurz, M.D., Ackert, R.P., Jr., Raisbeck, G.M., and Yiou, F., 1995, Constraints on age, erosion, and uplift of Neogene glacial deposits in the Transantarctic Mountains determined from in situ cosmogenic ^{10}Be and ^{26}Al: Geology, v. 23, p. 1063-1066.

Chamberlain, C.P., and Poage, M.A., 2000, Reconstructing the paleotopography of mountain belts from the isotopic composition of authigenic minerals: Geology, v. 28, no. 2, p. 115-118.

Colombo, F., 1994, Normal and reverse unroofing sequences in syntectonic conglomerates as evidence of progressive basinward deformation: Geology, v. 22, p. 235-238.

Corcoran, P.L., 2008, Ordovician paleotopography as evidenced from original dips and differential compaction of dolostone and shale unconformably overlying Precambrian basement on Manitoulin Island, Canada: Sedimentary Geology, v. 207, p. 22-33, doi: 10.1016/j.sedgeo.2008.04.003.

DeCelles, P.G., Tolson, R.B., Graham, S.A., Smith, G.A., Ingersoll, R.V., White, J., Schmidt, C.J., Rice, R., Moxon, I., Lemke, L., Handschy, J.W., Follo, M.F., Edwards, D.P., Cavazza, W., Caldwell, M., and Bargar, E., 1987, Laramide thrust-generated alluvial-fan sedimentation, Sphinx Conglomerate, southwestern Montana: The American Association of Petroleum Geologists Bulletin, v. 71, No. 2, p. 135-155.

DeCelles, P.G., and Hertel, F., 1989, Petrology of fluvial sands from the Amazonian foreland basin, Peru and Bolivia: Geological Society of America Bulletin, v. 101, p. 1552-1562.

DeCelles, P.G., Gray, M.B., Ridgway, K.D., Cole, R.B., Pivnik, D.A., Pequera, N., and Srivastava, P., 1991a, Controls on synorogenic alluvial-fan architecture, Beartooth Conglomerate (Palaeocene), Wyoming and Montana: Sedimentology, v. 38, p. 567-590.

DeCelles, P.G., Gray, M.B., Ridgway, K.D., Cole, R.B., Srivastava, P., Pequera, N., and Pivnik, D.A., 1991b, Kinematic history of a foreland uplift from Paleocene synorogenic conglomerate, Beartooth Range, Wyoming and Montana: Geological Society of America Bulletin, v. 103, p. 1458-1475.

Dutcher, L.A.F., Jobling, J.L., and Dutcher, R.R., 1986, Stratigraphy, sedimentology and structural geology of Laramide synorogenic sediments marginal to the Beartooth Mountains, Montana and Wyoming, *in* Montana Geological Society and Yellowstone Bighorn Research Association joint field conference and symposium; geology of the Beartooth Uplift and adjacent basins: Yellowstone Bighorn Research Association, p. 33-52.

Finn, T.M., Kirschbaum, M.A., Roberts, S.B., Condon, S.M., Roberts, L.N.R., and Johnson, R.C., 2010, Cretaceous-Tertiary Composite Total Petroleum System (503402), Bighorn Basin, Wyoming and Montana: U.S. Geological Survey Digital Data Series, 156 p.

Flemings, P.B., and Jordan, T.E., 1989, A synthetic stratigraphic model of foreland basin development: Journal of Geophysical Research, v. 94, p. 3851-3866.

Flueckinger, L.A., 1970, Stratigraphy, petrography and origin of Tertiary sediments off the front of the Beartooth Mountains, Montana-Wyoming [Ph.D. thesis]: Pennsylvania State University, 382 p.

Forest, C.E., Wolfe, J.A., Molnar, P., and Emanuel, K.A., 1999, Paleoaltimetry incorporating atmospheric physics and botanical estimates of paleoclimate: Geological Society of America Bulletin, v. 111, p. 497-511.

Gingerich, P.D., 1983, Paleocene-Eocene faunal zones and a preliminary analysis of Laramide structural deformation in the Clark's Fork Basin, Wyoming, *in* Wyoming Geological Association Guidebook, v. 34, p. 185-195.

Hickey, L.J., 1980, Paleocene stratigraphy and flora of the Clark's Fork Basin: Papers on Paleontology, issue 24, p. 33-50.

Hickey, L.J., Johnson, K.R., and Yuretich, R.F., 1986, Road log—Red Lodge, Montana to Clark, Wyoming via Elk Basin & Powell, Wyoming: Field trip through the facies of the Fort Union Formation *in* Montana Geological Society and Yellowstone Bighorn Research Association joint field conference and symposium; geology of the Beartooth Uplift and adjacent basins: Yellowstone Bighorn Research Association, p. 279-290.

Jobling, J.L., 1974, Stratigraphy, petrography, and structure of the Laramide (Paleocene) sediments marginal to the Beartooth Mountains, Montana [Ph.D. Thesis]: The Pennsylvania State University, 102 p.

Johnson, S.J., and Middleton, L.T., 1990, Tectonic significance of Paleocene alluvial sequence, Clark's Fork Basin, Wyoming-Montana, *in* Specht, R.W., ed., Wyoming sedimentation and tectonics: Wyoming Geological Association 41st Field Conference Guidebook, p. 69-87.

Kauffman, E.G., 1977, Geological and biological overview—Western Interior Cretaceous Basin,
in Kauffman, E.G., ed., Cretaceous facies, faunas, and paleoenvironments across the
Western Interior Basin: The Mountain Geologist, v. 14, nos. 3 and 4, p. 75-99.

Kraus, M.J., and Aslan, A., 1993, Eocene hydromorphic paleosols: significance for interpreting
ancient floodplain processes: Journal of Sedimentary Petrology, v. 63, no. 3, p. 453-463.

Lillegraven, J.A., 2004, Revisions to upper Cretaceous stratigraphy near Hell's Half Acre,
eastern Wind River Basin, central Wyoming: Bulletin of Carnegie Museum of Natural
History, v. 36, p. 137-158.

Lillegraven, J.A., 2009, Where was the western margin of northwestern Wyoming's Bighorn
Basin late in the Early Eocene?: Papers on Geology, Vertebrate Paleontology, and
Biostratigraphy in Honor of Michael O. Woodburne, Museum of Northern Arizona
Bulletin, v. 65, p. 37-82.

Lopez, D.A., 2001, Preliminary Geologic map of the Red Lodge 30' x 60' quadrangle, south-
central Montana: Montana Bureau of Mines and Geology, Open-File Report MBMG
423, scale 1:100 000, 1 sheet.

Lopez, D.A., 2005, Geologic map of the Red Lodge area, Carbon County, Montana: Montana
Bureau of Mines and Geology, Open-File Report MBMG 524, scale 1:100 000, 1 sheet.

Meyers, J.H., Suttner, L.J., Furer, L.C., May, M.T., and Soreghan, M.J., 1992, Intrabasinal
tectonic control on fluvial sandstone bodies in the Cloverly Formation (Early
Cretaceous), west-central Wyoming, USA: Basin Research, v. 4, p. 315-333, doi:
10.1111/j.1365-2117.1992.tb00051.x.

Mulch, A., Graham, S.A., and Chamberlain, C.P., 2006, Hydrogen isotopes in Eocene river
gravels and paleoelevation of the Sierra Nevada: Science, v. 313, p. 87-89.

Neely, T.G., 2006, Three-dimensional strain at foreland arch transitions: structural modeling of
the southern Beartooth Arch transition zone, northwest Wyoming [M.S. thesis]:
Colorado State University, 113 p.

Neely, T.G., and Erslev, E.A., 2009, The interplay of fold mechanisms and basement weaknesses
at the transition between Laramide basement-involved arches, north-central Wyoming,
USA: Journal of Structural Geology, v. 31, p. 1012-1027.

Omar, G.I., Lutz, T.M., and Giegengack, R., 1994, Apatite fission-track evidence for Laramide
and post-Laramide uplift and anomalous thermal regime at the Beartooth overthrust,
Montana-Wyoming: Geological Society of America Bulletin, v. 106, p. 74-85.

Oplustil, S., 2005, The effect of paleotopography, tectonics and sediment supply on quality of
coal seams in continental basins of central and western Bohemia (Westphalian), Czech
Republic: International Journal of Coal Geology, v. 64, p. 173-203.

Parker, S.E., and Jones, R.W., 1986, Influence of faulting on upper Cretaceous-lower Tertiary deposition, Bighorn Basin, Wyoming, *in* Montana Geological Society and Yellowstone Bighorn Research Association joint field conference and symposium; geology of the Beartooth Uplift and adjacent basins: Yellowstone Bighorn Research Association, p. 137-144.

Pierce, W.G., 1965a, Geologic map of the Clark Quadrangle, Park County, Wyoming: U.S. Geological Survey, scale 1:62 500, 1 sheet.

Pierce, W.G., 1965b, Geologic map of the Deep Lake Quadrangle, Park County, Wyoming: U.S. Geological Survey, scale 1:62 500, 1 sheet.

Pierce, W.G., 1966, Geologic map of the Cody Quadrangle, Park County, Wyoming: U.S. Geological Survey, scale 1:62 500, 1 sheet.

Pierce, W.G., 1968, Geologic map of the Pat O'Hara Quadrangle, Park County, Wyoming: U.S. Geological Survey, scale 1:62 500, 1 sheet.

Sears, J.W., and Ryan, P.C., 2003, Cenozoic Evolution of the Montana Cordillera: Evidence from Paleovalleys, *in* Raynolds, R., and Flores, J., eds., Cenozoic Paleogeography of western US: Denver, CO, Society of Exploration Paleontologists and Mineralogists, p. 289-301.

Smedes, H.W., and Prostka, H.J., 1972, Stratigraphic framework of the Absaroka Volcanic Supergroup in the Yellowstone National Park region: Geological Survey Professional Paper 729-C, p. C1-C33.

Webb, M.W., and Steel, R.J., 2001, Incised paleovalleys in the Lance Formation, southwestern Bighorn Basin, Wyoming: Annual Meeting Expanded Abstracts-American Association of Petroleum Geologists, v. 2001, p. 212.

CHAPTER 2: MULTI-STAGE LARAMIDE SHORTENING AS REVEALED BY CRETACEOUS-PALEOGENE UNCONFORMITIES IN THE VICINITY OF HEART MOUNTAIN, NORTHWESTERN WYOMING

Introduction

The Bighorn Basin is a topographic and structural basin bordered by Laramide structures (Fig.1; Bown, 1980). The Pryor, Bighorn, Bridger, Owl Creek, and Absaroka ranges border the north, east, south, southwest, and west edges of the basin, respectively (Bucher et al., 1933). The basin is bounded on the northwest by the Beartooth uplift. South of the Beartooth Mountains, the Pat O'Hara and Rattlesnake Mountain structures bound the basin (Fig. 2). In some areas along the western edge of the basin, the contact between the Cretaceous and Paleogene rocks is conformable; in other places the contact is either a disconformity or an angular unconformity (Pierce, 1965a, 1965b, 1966, 1968). Along the northwestern edge of the Bighorn Basin, Laramide structures have varying orientations. There have been multiple interpretations regarding their orientations: Wise (2000) suggested that different orientations reflect a change in shortening directions during the Laramide, while Neely and Erslev (2009) proposed that one dominant shortening direction reactivated pre-existing basement structures which resulted in varying orientations.

Heart Mountain is located near the western edge of the Bighorn Basin (Fig. 2). The Paleocene Fort Union Formation and late Paleocene-Eocene Willwood Formation in the vicinity of Heart Mountain were last mapped in detail by Lillegraven (2009) and previous to that by Pierce (1937 and 1938). Pierce's mapping revealed an angular unconformity between the
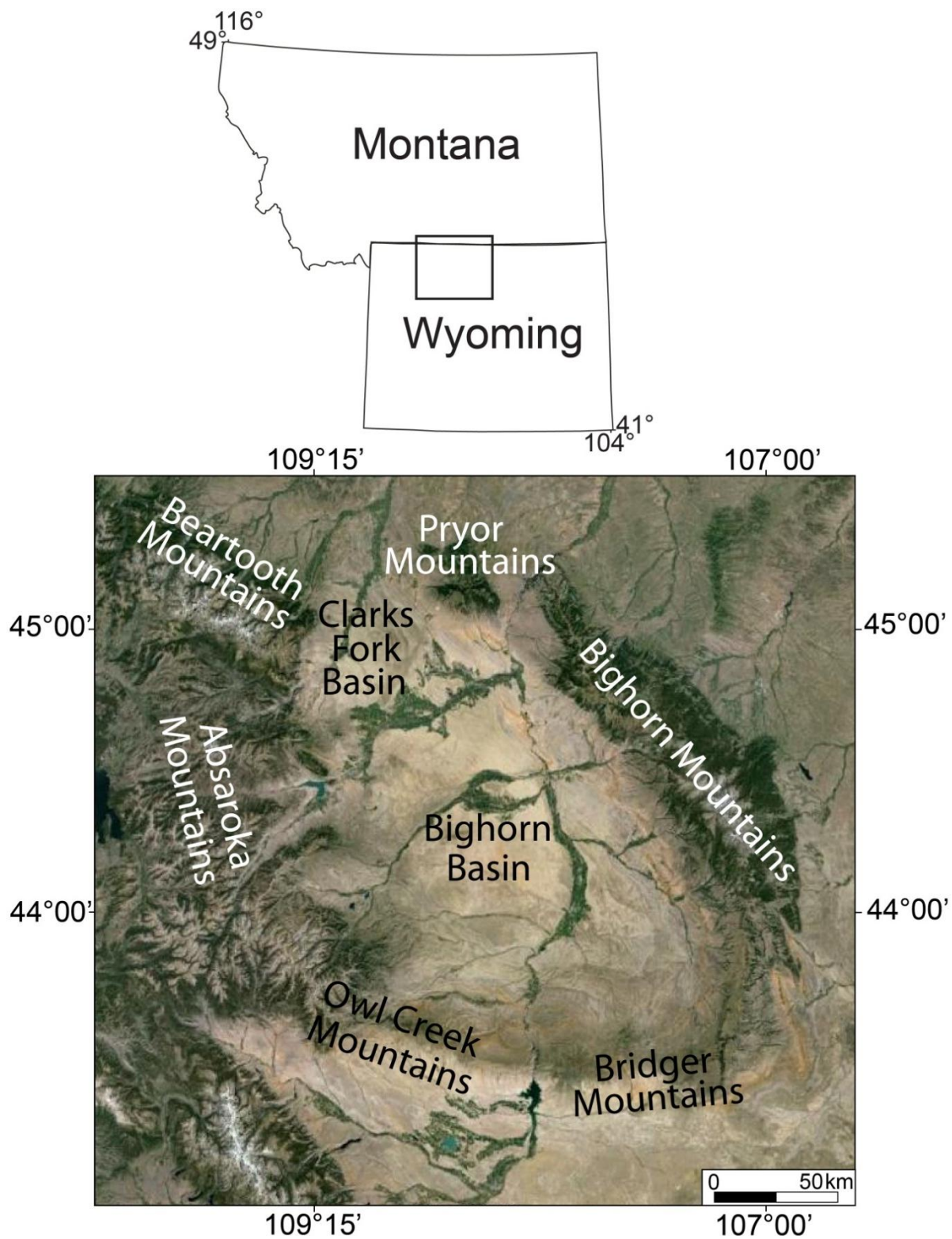
49

Figure 1. Location map of the Clarks Fork and Bighorn Basins and bounding Laramide ranges. Satellite image from Google Earth.
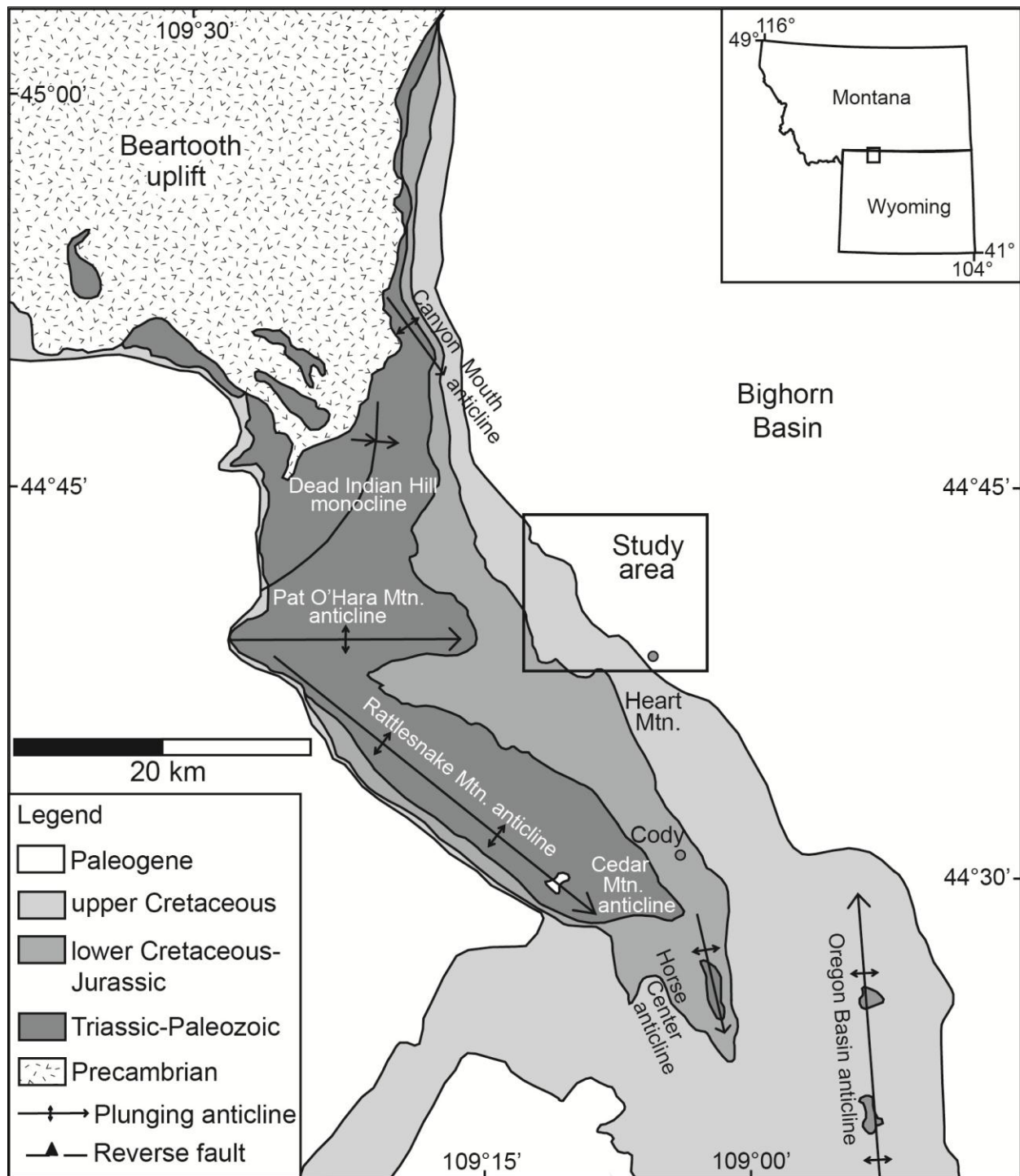
Figure 2. Simplified geologic map of the western Bighorn Basin and adjacent Laramide structures, modified from Neely and Erslev, 2009. Black box outlines study area (Figure 3).

Willwood Formation and underlying tilted Fort Union Formation and Late Cretaceous layers.

Lillegraven interpreted the contact at the base of the Willwood Formation as a west-vergent

thrust fault with tens of kilometers of slip. In this study, we utilized field-based mapping in order

to resolve the depositional and/or deformational nature of Cretaceous-Paleogene contacts in the

vicinity of Heart Mountain.

Regional Setting

Structural Geology

The Clarks Fork and Bighorn Basins of northwestern Wyoming developed during uplift

of the Rocky Mountains (Gingerich and Clyde, 2001). Mountainous areas including the Bighorn,

Owl Creek, Beartooth, and Pryor Mountains around the Bighorn Basin uplifted during the

middle-late Laramide orogeny (Fig. 1; Foose et al., 1961; Bown, 1980). The northern limit of the

basin does not have a bounding mountain mass; instead, the Nye-Bowler zone forms a structural

boundary where Precambrian basement has moved both vertically and horizontally (Foose et al.,

1961). South of the Beartooths, the Pat O'Hara and Rattlesnake Mountain structures bound the

basin. Our study area is focused in the northwestern Bighorn Basin in the vicinity of Heart

Mountain, located east of Pat O' Hara Mountain, southeast of the Beartooth uplift and northeast

of Rattlesnake Mountain (Fig. 2). The Rattlesnake Mountain anticline is northwest trending and

approximately 27 km long (Fig. 2; Neely, 2006). It is asymmetric, with its backlimb dipping 12-

15° NE and the forelimb overturned and dipping 45° SW. At its northwest end, the backlimb and

crest of the Rattlesnake Mountain structure terminates into the crest of the east-west trending Pat

O'Hara Mountain anticline (Fig. 2; Neely, 2006). North of the Pat O'Hara anticline, the

Beartooth Mountains are a 130 by 60 km block of Precambrian crystalline rocks. Major uplift of

the Beartooths occurred in the middle-late Paleocene, culminating during the early Eocene

(Foose et al., 1961; DeCelles et al., 1991). By the mid-Eocene, the Beartooths had reached their present structural relief with respect to adjacent crustal blocks; however, the Beartooths had not reached their present topographic relief until regional uplift of the Middle Rocky Mountains in the Miocene-Pliocene (Foose et al., 1961). The eastern edge of the Beartooth Mountains trends north-south in the vicinity of our study area (Fig. 2).

In northwestern Wyoming, there are differently-oriented Laramide structures bounding the western edge of the Bighorn Basin: the eastern edge of the Beartooth mountain front trends north-south, Rattlesnake Mountain anticline trends northwest, and the Pat O'Hara Mountain anticline trends east-west. In a study by Wise (2000), he used structural data near Red Lodge, Montana to constrain the kinematics of deformation and concluded that eastward escape tectonics caused a change in the thrust direction during Laramide compression of the Beartooth uplift, from a north-northeast direction to an east-directed compression. In a study by Neely and Erslev (2009), they collected data from 1581 slickensided minor faults which revealed a regional shortening direction of 065°. In their study, they suggested that differently-oriented Laramide structures in this area were in fact the result of fault-propagation and fault-bend folding combined with unidirectional compression that reactivated pre-existing basement weaknesses (Neely and Erslev, 2009). This paper addresses the nature of geologic contacts and the timing of deformation events in the vicinity of Heart Mountain in order to explain the present-day orientations of Cretaceous-Paleogene sediments and to relate these orientations to episodes of Laramide shortening.

Late Cretaceous-Paleogene Sedimentation in the Bighorn Basin

Continental sedimentation in the Bighorn Basin commenced in the latest Cretaceous, resulting in the accumulation of approximately 6400 meters of lacustrine and fluvial sediments in

the deepest parts of the basin by the end of the Eocene (Bown, 1980). The Cretaceous Mesaverde

Formation consists of massive sandstones with thin coal beds in the lower part, overlain by

interbedded sandstone and shale in the upper part. Above the Mesaverde is the Cretaceous

Meeteetse Formation, consisting of interbedded clayey sand, sandstone, and shale (Lillegraven,

2004). The Cretaceous Lance Formation overlies the Meeteetse Formation, comprised of fluvial

sandstones interbedded with siltstones, mudstones, and shales (Webb and Steel, 2001).

There was rapid accumulation of fluvial and paludal sediments in the basin during the

Paleocene, resulting in the development of the Fort Union Formation. Along the northwestern

margin of the basin, the upper part of the Paleocene Fort Union Formation consists of alluvial

fan and fluvial deposits which preserve internal angular unconformities that developed during

synkinematic uplift of the Beartooths and accompanying sedimentation (Gingerich, 1983). The

upper part of the formation contains interbedded conglomerates, sandstones, siltstones, and

mudstones. The late Paleocene-Eocene Willwood Formation was deposited mainly by

meandering streams on broad floodplains in the basin. Some carbonaceous shales and coal beds

formed in ponds, backswamps, and other low-lying areas on the floodplain (Bown, 1980).

Deposition was punctuated by intervals of nondeposition and ensuing soil formation, which

resulted in the present-day variegated paleosols seen throughout the Willwood Formation (Bown,

1979; Kraus, 1979). The thickness of the Paleocene and Eocene rocks varies greatly throughout

the basin, ranging from 400 m to over 2,430 m (Neasham and Vondra, 1972; Blackstone, 1986).

Mapping of Cretaceous-Paleogene Strata near Heart Mountain

Previous mapping by Pierce (1966) revealed an angular unconformity northwest of Heart

Mountain between the gently dipping late Paleocene-Eocene Willwood Formation and

underlying tilted Paleocene Fort Union Formation and Late Cretaceous layers. Southwest and

southeast of Heart Mountain, Pierce mapped approximate contacts at the base of the Willwood and took sparse bedding measurements near these contacts. We chose three study areas in the vicinity of Heart Mountain based on critical exposures of contacts between basal Paleogene Willwood strata and underlying Cretaceous-Paleocene rocks. These areas include northwest of Heart Mountain, southwest of Heart Mountain, and southeast of Heart Mountain (Fig. 3).

In the vicinity of Heart Mountain, Willwood sediments are in contact with Paleocene Fort Union and Late Cretaceous sediments. We focused mapping at the contacts, measuring bedding orientations and describing the sediments in detail. In the field, we mapped the late Paleocene-Eocene Willwood Formation based on the presence of variegated paleosols interbedded with tan-to-brown coarse-grained sandstones. Below the Willwood, the Paleocene Fort Union Formation is comprised of tan to brown sandstones, siltstones, and conglomerates. The formation contains coarse-grained sandstones with locally interbedded black chert conglomerate deposits. During geologic mapping, we used the presence of black chert-pebble conglomerates in the Fort Union Formation to distinguish it from the basal Willwood Formation. Sedimentary-clast Fort Union conglomerates near the base of the Willwood Formation were mapped northwest, southwest, and southeast of Heart Mountain. The deposits contain predominantly black chert clasts, and the conglomerates have a similar lithology: coarse sand matrix, clast supported with poorly sorted, well rounded, predominantly dark colored chert clasts. There are some limestone clasts present and the conglomerate clast composition is approximately 70% chert and 30% limestone, with clasts ranging from <1 to 8 cm in diameter. The conglomerates are commonly interbedded with tan, coarse-grained, cross-bedded sandstones of the Fort Union Formation. Based on their similar lithology and stratigraphic position in relation to the basal Willwood Formation, it is likely that the black-chert conglomerates and interbedded sandstones of the Fort Union Formation formed
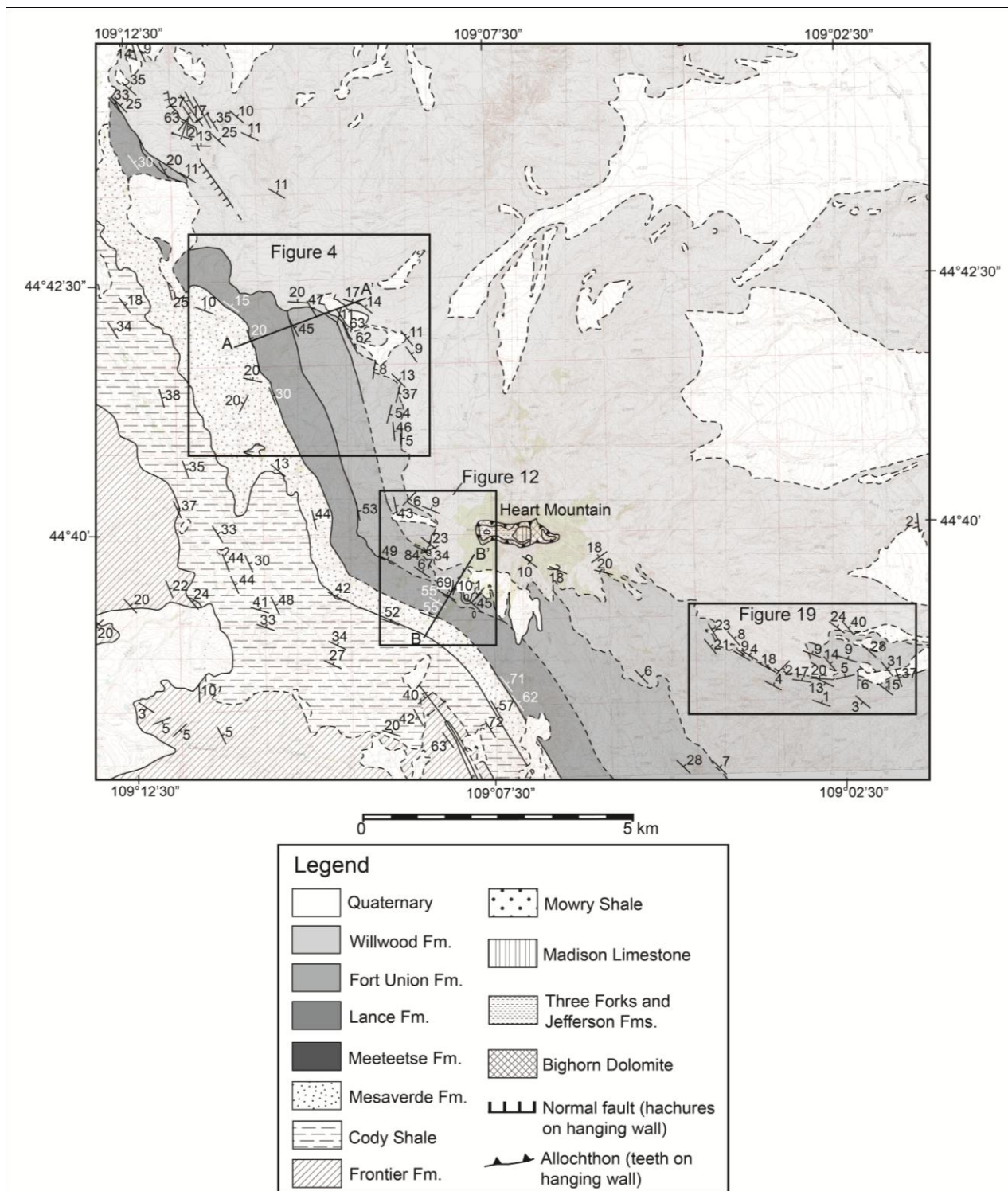
Figure 3. Geologic map in the vicinity of Heart Mountain. Black boxes outline study areas where basal contacts of the late Paleocene-Eocene Willwood Formation are well exposed.

in the same depositional setting; therefore, the black chert conglomerates mapped near Heart

Mountain represent synchronous deposits. This indicates that there was a complex deformational

history during Fort Union deposition, as the black chert conglomerate of the upper Fort Union

Formation is steeply folded northwest of Heart Mountain but gently-dipping southwest and

southeast of Heart Mountain. Along the western edge of the Bighorn Basin, Lillegraven (2009)

interpreted basal Willwood contacts as west-directed faults in multiple locations, including

locations in the vicinity of Heart Mountain. During field work, we excavated and described basal

Willwood sediments in order to determine whether the contacts were faulted or depositional.

Northwest of Heart Mountain

Northwest of Heart Mountain, Willwood rocks are in contact with Cretaceous Meeteetse,

Cretaceous Lance, and Paleocene Fort Union strata (Fig. 4). Willwood sediments here generally

contain coarse-grained sandstones and sedimentary-clast conglomerates. The sandstones are

coarse grained, poorly cemented, and gray, tan, and brown in color. Certain sandstones in the

Willwood are strongly cross bedded and contain limestone-clast pebble lags (Fig. 5). Where

Willwood is in contact with Lance Formation, Lillegraven (2009) described a "chaotic mélange

of strongly slickensided mudstone and sandstone rip-up clasts in [the] thrust zone within base of

shallowly dipping Willwood formation." We investigated this location and did find clasts in the

Willwood; however, these are sedimentary rip-up clasts and were not produced by faulting (Fig.

6). Instead of slickensides, we found carbonaceous segments of plant fossils within mudstone

pieces, commonly found in the Willwood Formation (Fig. 7).

Northwest of Heart Mountain, Paleocene Fort Union sediments are steeply dipping,

oriented similarly to underlying Cretaceous rocks (Fig. 8). Conglomerates in the Fort Union

Formation contain well-rounded, poorly sorted, less-than-1-to-8-centimeter sedimentary clasts

Figure 4. Geologic map of the study area northwest of Heart Mountain. The late Paleocene-Eocene Willwood Formation is gently-dipping and rests at angular discordance on top of tilted Late Cretaceous and late Paleocene formations of varying ages including the Cretaceous Meeteetse, Cretaceous Lance, and Paleocene Fort Union formations. A-A' is line of section in Figure 8.

Figure 5. Cross bedding in Willwood sandstone outcrops northwest of Heart Mountain. Hammer length 30 cm.

Figure 6. Depositional rip-up clasts in the basal Willwood Formation, northwest of Heart Mountain. In this area, Lillegraven (2009) described a "chaotic mélange of strongly slickensided mudstone and sandstone rip-up clasts in [the] thrust zone within base of shallowly dipping Willwood formation"; instead of a thrust zone within basal Willwood, only depositional rip-up clasts are present.
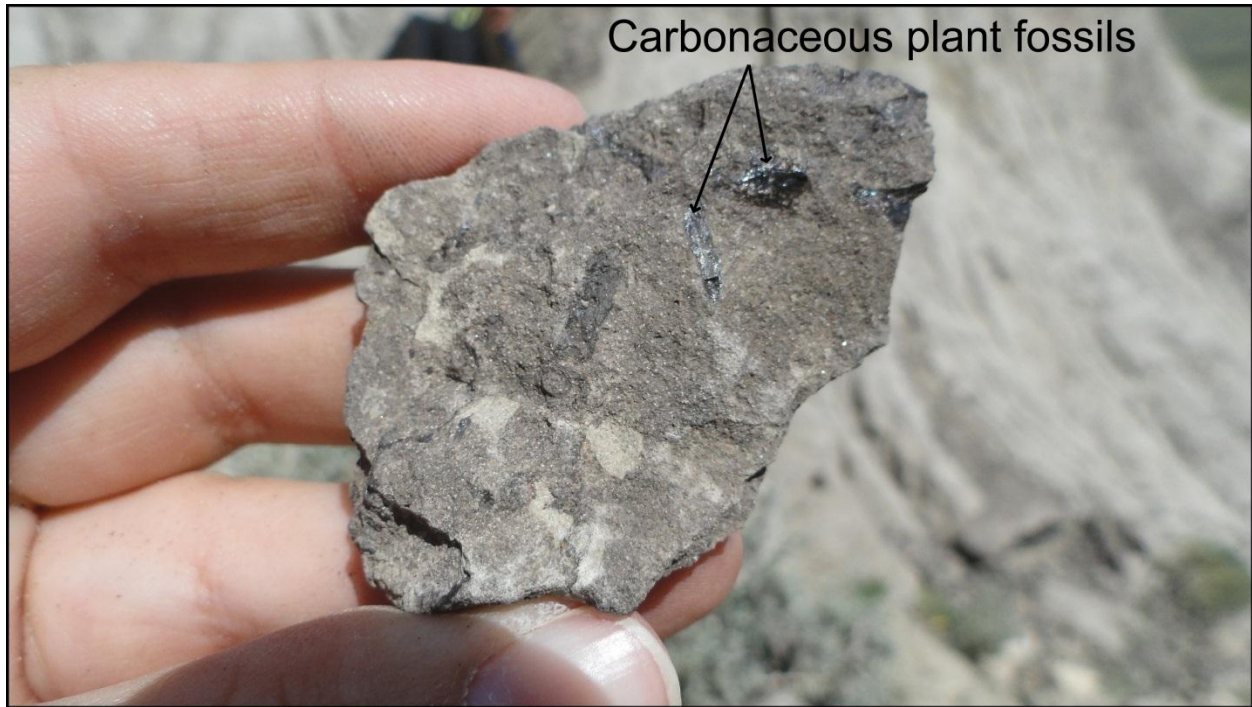
Figure 7. Carbonaceous plant fossils found in basal Willwood strata, northwest of Heart Mountain. Lillegraven (2009) described a "chaotic mélange of strongly slickensided mudstone and sandstone rip-up clasts in [the] thrust zone within base of shallowly dipping Willwood formation"; instead of slickensides, carbonaceous segments of plant fossils within mudstone pieces are present.
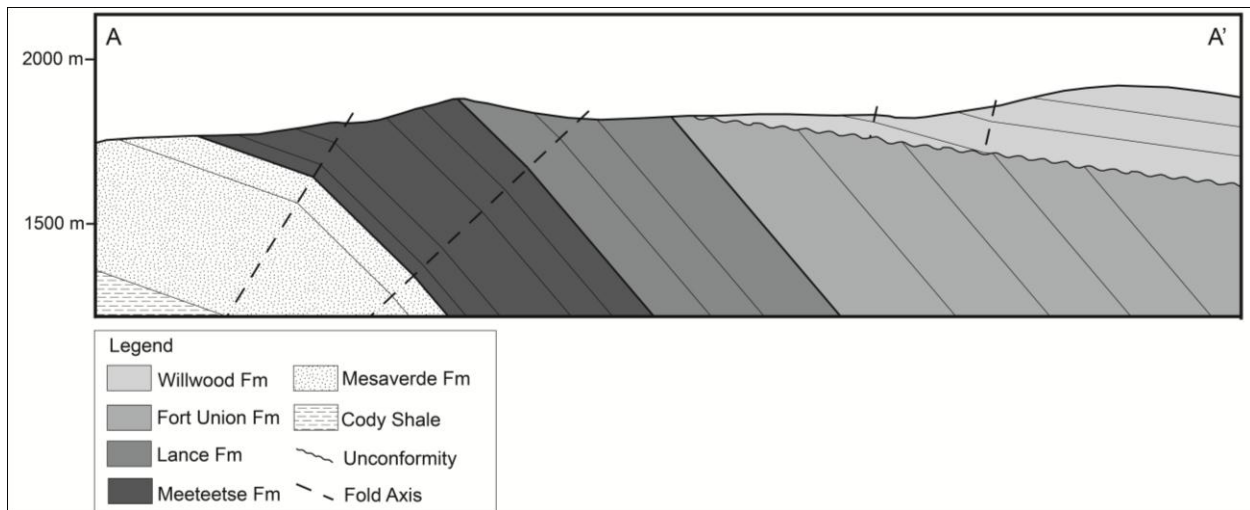
Figure 8. West-east cross section in the area northwest of Heart Mountain. The Paleogene Willwood Formation is gently dipping on top of tilted Late Cretaceous-Paleocene formations.

which include predominantly black chert (~70%), gray chert, some red chert, and some limestone clasts. The conglomerates have very coarse sandstone matrices and commonly incise into sandstones below (Fig. 9). late Paleocene-Eocene Willwood sediments are gently-dipping and lie in angular discordance with underlying tilted Paleocene Fort Union strata. Where Willwood is in contact with the Cretaceous Lance Formation, the Lance is steeply dipping in contact with flat-lying Willwood sediments (Fig. 10). Equal area projections showing density contours of poles to bedding clearly show an angular unconformity between the tilted Lance and Fort Union Formations and overlying gently-dipping Willwood (Fig. 11). Lance and Fort Union strata have mean strike and dip of 328°, 52° and 346°, 42°, respectively (following the right-hand rule), whereas Willwood layers have a mean strike and dip of 297°, 09°.

Southwest of Heart Mountain

In the area southwest of Heart Mountain (Fig. 12), the Willwood Formation is characterized by interbedded shale, sandstone, and conglomerate. The sandstones are generally tan to brown and coarse-grained, interbedded with finer grained shaly strata. Fine-grained layers in the Willwood here consist of mottled red and gray silty shale with some black shale layers. Lillegraven (2009) described thrust faulting at the Willwood-Fort Union contact, citing "abundant slickensides above [a] sharp contact." We investigated the Willwood-Fort Union contact southwest of Heart Mountain and found that some shaly layers in the Willwood display slickensides; however, the slickensides are oriented in multiple directions, indicating that they likely are a result of soil shrink-swell cycles rather than faulting (Fig. 13).

Southwest of Heart Mountain, conglomerates in the Willwood contain predominantly sedimentary clasts, greater than 85% chert, with some limestone and some crystalline clasts. The clasts are well-rounded and generally less than or equal to 15 cm in diameter (Fig. 14). Below

Figure 9. Conglomerate incising into sandstone in the Paleocene Fort Union Formation, northwest of Heart Mountain. Conglomerates in the Fort Union Formation contain well-rounded, poorly sorted, less-than-1- to 8-centimeter sedimentary clasts which include predominately black chert (~70%), gray chert, some red chert, and some limestone clasts.
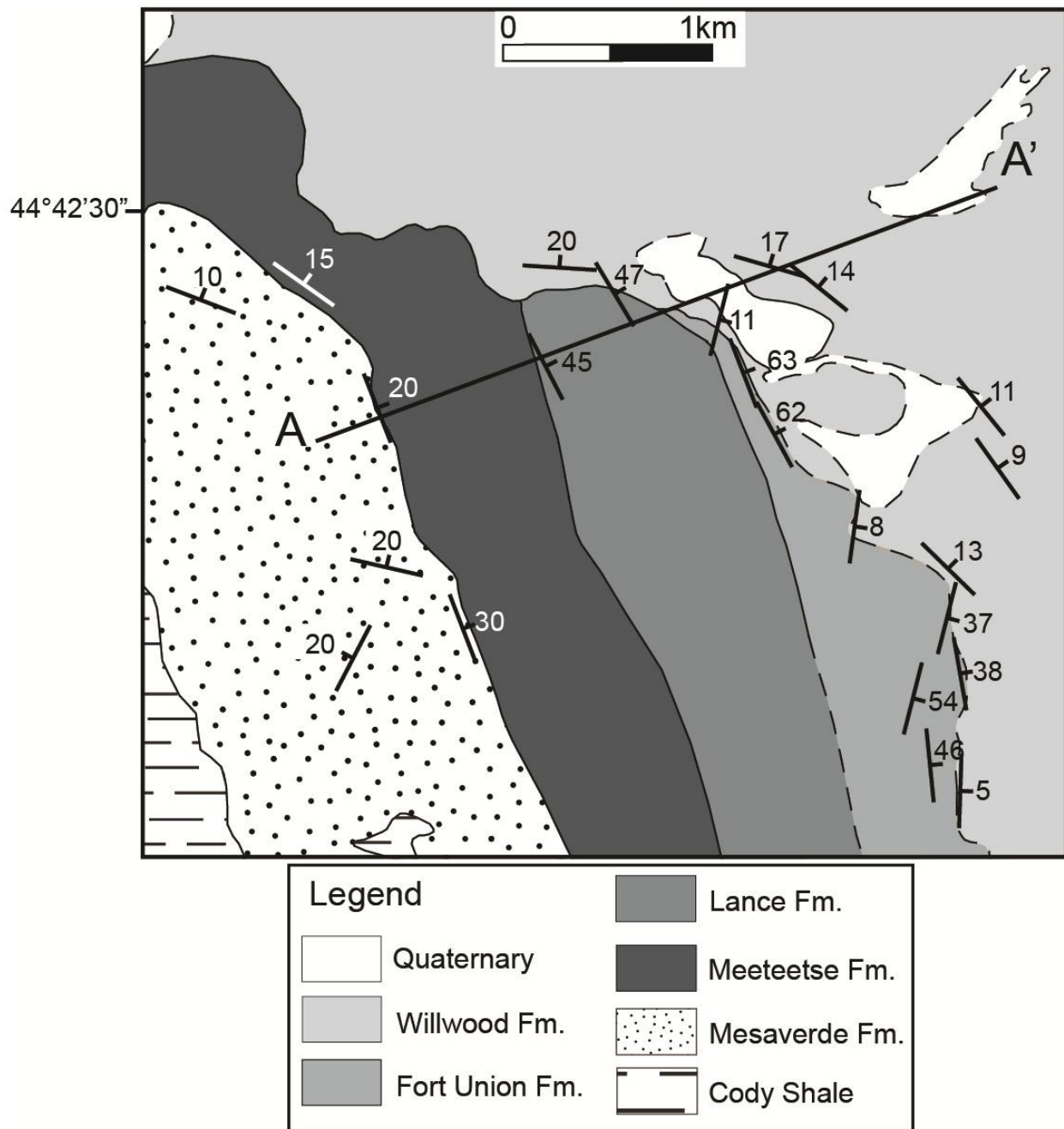

Figure 10. Angular discordance between tilted Cretaceous Lance Formation and gently-dipping late Paleocene-Eocene Willwood Formation northwest of Heart Mountain. View to the southeast.
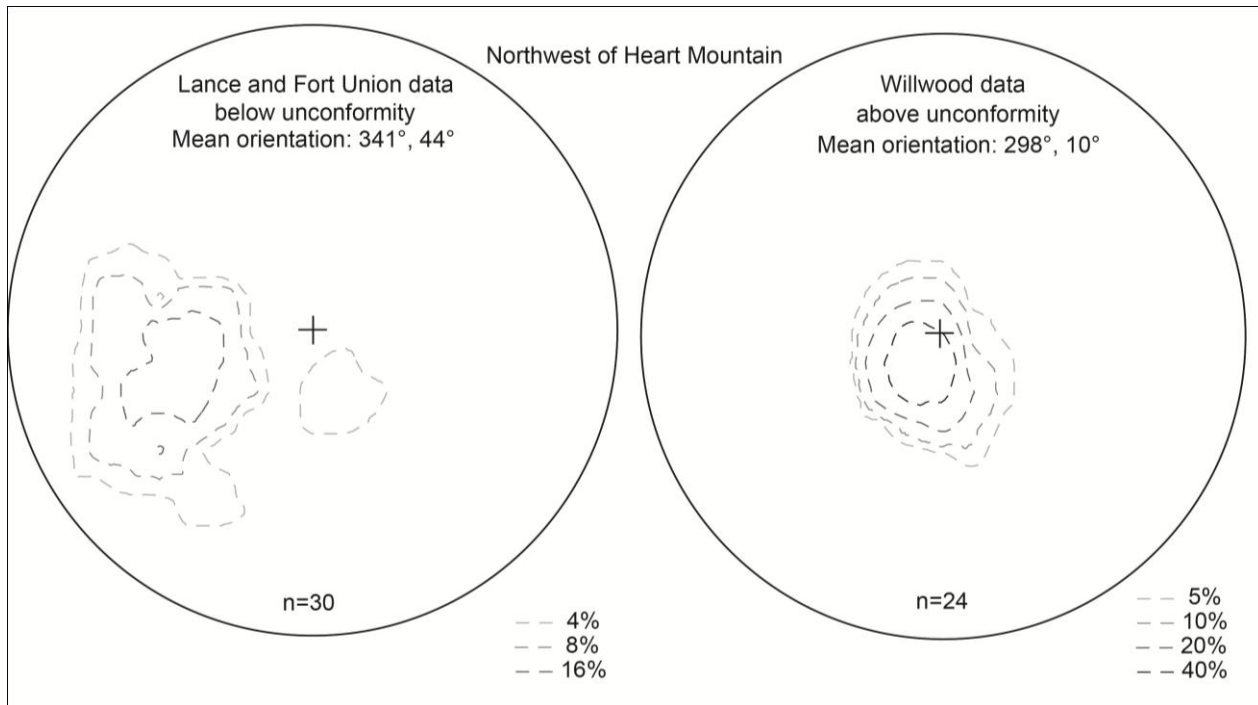
Figure 11. Equal area projections showing density contours of poles to bedding orientations of the tilted Cretaceous Lance, Paleocene Fort Union Formation and the gently-dipping late Paleocene-Eocene Willwood Formation, northwest of Heart Mountain. Mean strike and dip of Cretaceous-Paleocene bedding below Willwood Formation: strike 341°, dip 44°NE; mean strike and dip of late Paleocene-Eocene Willwood Formation: 298°, 10°N. Equal area projections created using GEOrient version 9.5.0.
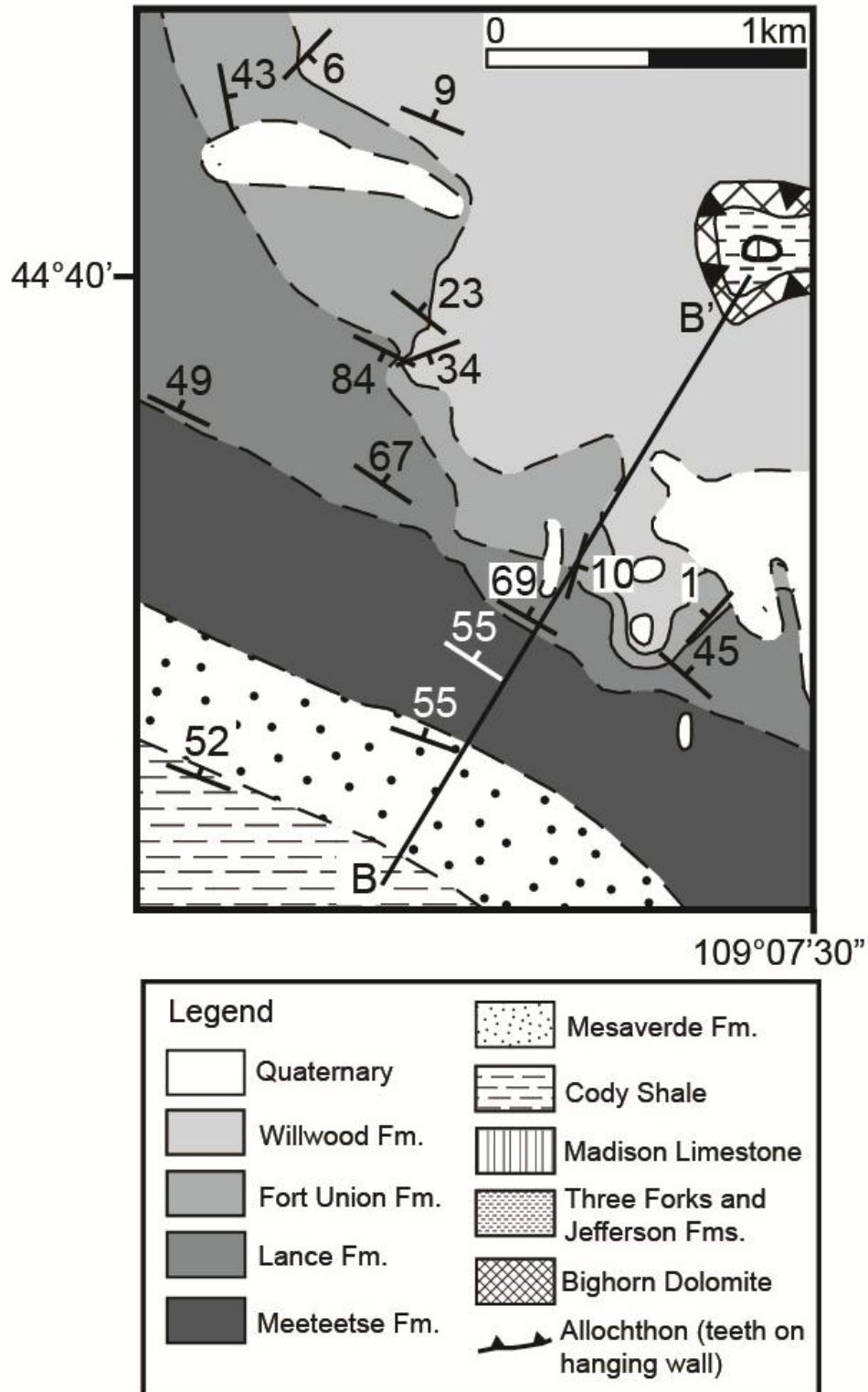
Figure 12. Geologic map of the area southwest of Heart Mountain. The late Paleocene-Eocene Willwood and Paleocene Fort Union formations are gently-dipping and rest at angular discordance on top of the tilted Cretaceous Lance Formation. B-B' is line of section in Figure 16.

Figure 13. Multi-directional slickensided shale in the Willwood Formation, southwest of Heart Mountain. Black lines highlight various directions of slickensides, indicating that they formed from shrink-swell cycles rather than faulting.

Figure 14. Gently-dipping sandstone overlying sedimentary-clast conglomerate of the Willwood Formation, southwest of Heart Mountain. Conglomerate clasts are >85% chert, <15% limestone and crystalline (clasts are ≤15 cm). Hammer length 30 cm.

the Willwood Formation, the Fort Union Formation contains interbedded sandstones, siltstones, and conglomerates. The conglomerates have tan, coarse-sand matrices and are clast supported, with poorly sorted, rounded, less than 1- to 20-cm predominately sedimentary clasts. Clasts in the Fort Union here include predominately black chert (>70%), limestone, and quartz (Fig. 15). The black chert conglomerate of the upper Fort Union is gently dipping southwest of Heart Mountain, differing in orientation from the coeval black-chert conglomerate layer that is tilted west and northwest of Heart Mountain. In this area, the Cretaceous Lance Formation is steeply dipping and lies in angular discordance beneath the gently-dipping Fort Union Formation, which is in conformable contact with the overlying gently-dipping Willwood Formation (Fig. 16). The Lance is characterized by thick, buff-colored sandstones interbedded with tan to gray shales. Equal area projections show differing bedding orientations between the tilted Cretaceous Lance Formation and overlying gently-dipping Fort Union and Willwood Formations (Fig. 17). In this area, Lance strata have a mean strike and dip of 301°, 55° (following the right-hand rule), whereas Fort Union and Willwood layers have mean strike and dips of 327°, 13° and 016°, 10°, respectively.

South of the area that we mapped, Pierce (1966) mapped an approximate location for the Lance-Fort Union contact. The contact geometry as drawn by Pierce implies that the Fort Union is steeply dipping in this area. However, the Fort Union strata near the basal contact dip gently. It is possible that there is an internal angular unconformity within the Fort Union Formation as the mapping by Pierce indicates; however, the mapped contacts in this area are approximate and due to the proximity of a shallowly-dipping Fort Union measurement to the contact, it is likely that this section was incorrectly mapped and requires revision. Using the topography of the area, we remapped this area with a more accurate Lance-Fort Union contact geometry (Fig. 18).

Figure 15. Interbedded sandstone and sedimentary-clast conglomerate in gently-dipping Fort Union Formation, southwest of Heart Mountain. Conglomerate clasts are >70% chert, <30% limestone and quartz. Clasts are <1-20 centimeters in diameter.
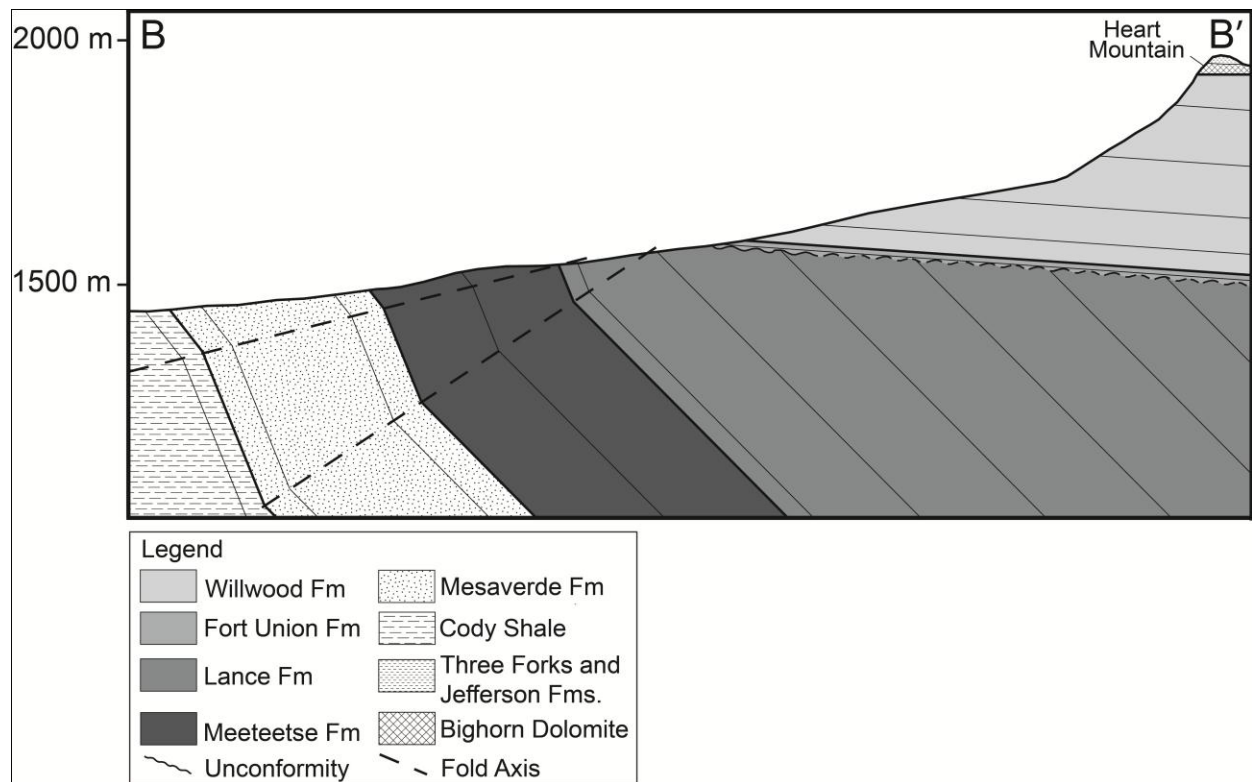
Figure 16. Southwest-northeast cross section southwest of Heart Mountain showing steeply dipping Cretaceous layers below the gently dipping Paleocene Fort Union and late Paleocene-Eocene Willwood Formations.

Figure 17. Equal area projections showing density contours of poles to bedding orientations of the tilted Late Cretaceous strata, gently-dipping Paleocene Fort Union Formation and the gently-dipping late Paleocene-Eocene Willwood Formation, southwest of Heart Mountain. Mean strike and dip of Late Cretaceous bedding below Paleogene Fort Union and Willwood Formations: strike 303°, dip 53°N; mean strike and dip of Paleogene Fort Union Willwood Formations: 348°, 11°N. Equal area projections created using GEOrient version 9.5.0.
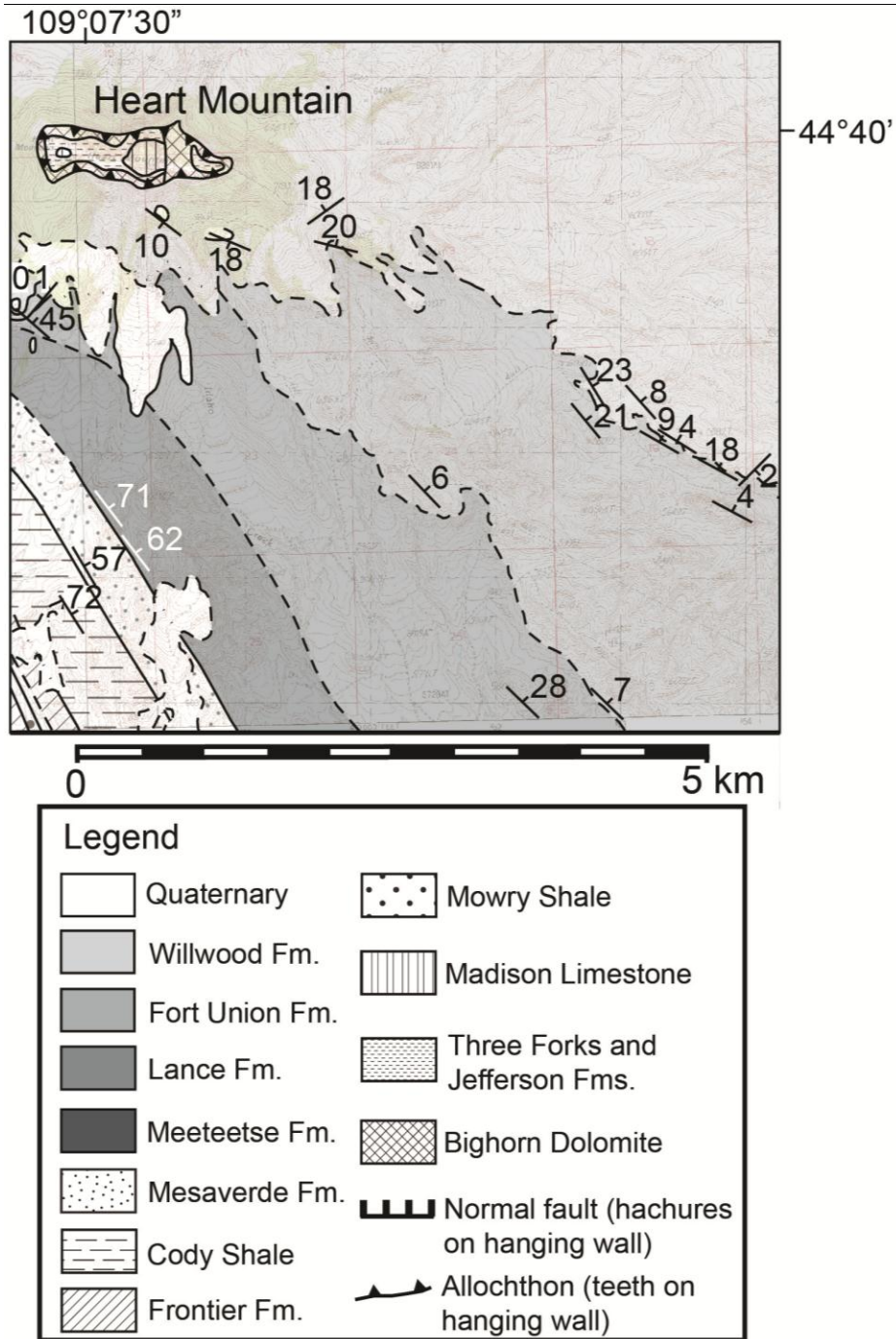
Figure 18. Geologic map of the area southeast of Heart Mountain. The Lance-Fort Union contact was remapped in order to resolve the incorrect contact geometry from previous mapping by Pierce (1966).

In the area southeast of Heart Mountain (Fig. 19), conglomerate clasts in the upper part of the Fort Union include predominantly chert (>70%) and limestone. The black chert conglomerate layer of the upper Fort Union is gently dipping southeast of Heart Mountain, similar in orientation with the synchronous black chert conglomerate layer that is gently-dipping southwest of Heart Mountain. At the Fort Union-Willwood contact at his Site 16, Lillegraven described a "strongly jointed, c. 18 m long, >3 m thick, allochthonous sandstone mass, severely shattered along base, wholly encased within c. 9 m-thick dark mudstone exhibiting fabric with many sharp bends." We visited this site and did not find evidence for faulting (Fig. 20). We were able to excavate into the mudstone and found that bedding was well-preserved and lacked fault indicators, such as slickensides or fault breccia. In this area, the Paleocene Fort Union Formation and late Paleocene-Eocene Willwood Formation are in conformable contact. Equal area projections showing density contours of poles to bedding show similar orientations of the gently-dipping Fort Union and Willwood Formations southeast of Heart Mountain (Fig. 21). Here, the mean orientation of Fort Union strata is 311°, 12°NE and the mean orientation of Willwood strata is 310°, 09°NE. Combined, the Fort Union and Willwood have a mean bedding orientation of 311°, 11°NE (Fig. 21).

Southeast of Heart Mountain, Lillegraven (2009) described an "almost horizontal bed of Quaternary cobble-bearing sandstone set with angular unconformity atop northeast-dipping Fort Union Formation." We mapped the outcrop during field research and then used Google Earth to trace the rocks to a known outcrop of Fort Union sediments (Fig. 22). We also traveled to this site during field work and determined that the "Quaternary cobble-bearing sandstone" does not match the description of known Quaternary conglomeratic deposits in the vicinity of Heart
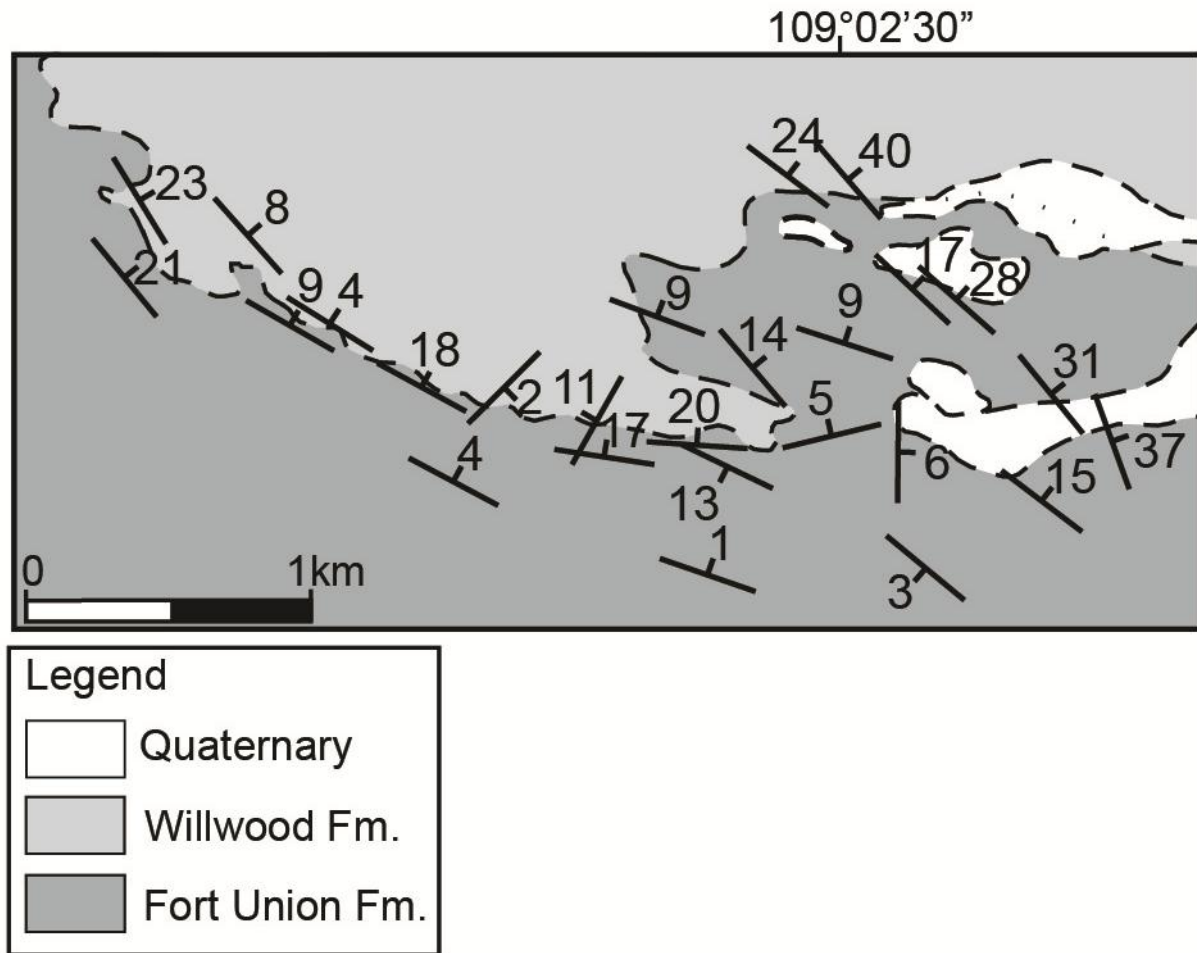
Figure 19. Geologic map of the area southeast of Heart Mountain. The late Paleocene-Eocene Willwood Formation is in conformable contact with the Paleocene Fort Union Formation in this area.
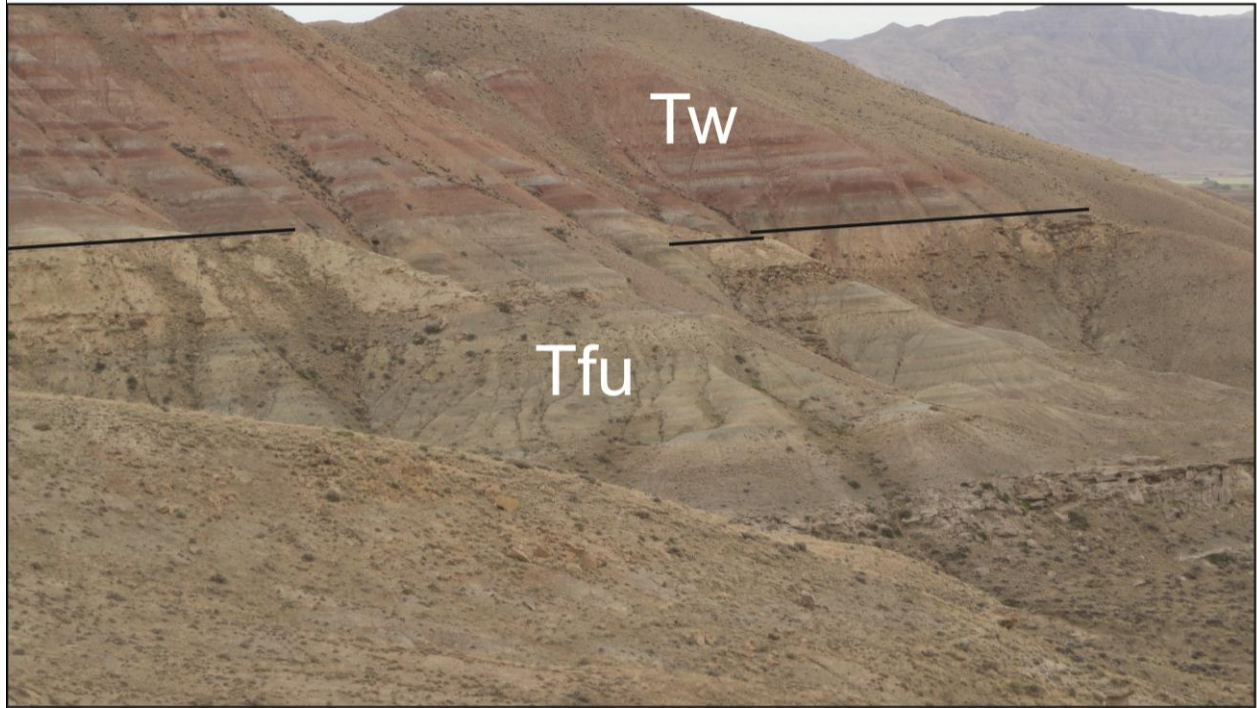
Figure 20. Photo taken by the authors showing site Lillegraven (2009) described as "view to southeast, with two arrows pointing to correlative stratigraphic levels within a broad and complex fault zone (heavily deformed strata between dashed lines) near base of Willwood Formation." In this photo, undeformed well-preserved layers of the Willwood (Tw) and Fort Union (Tfu) formations are visible. In this area, we excavated into fine grained strata and found that the sediments lacked fault indicators, such as slickensides or fault breccia.
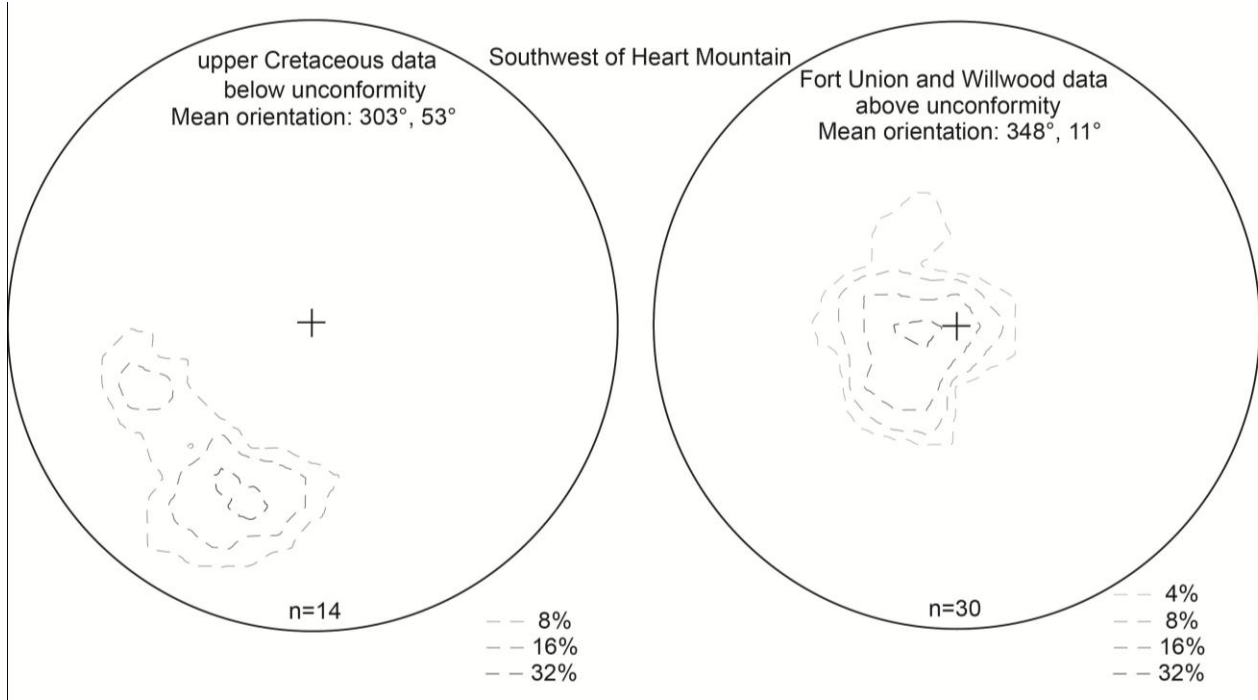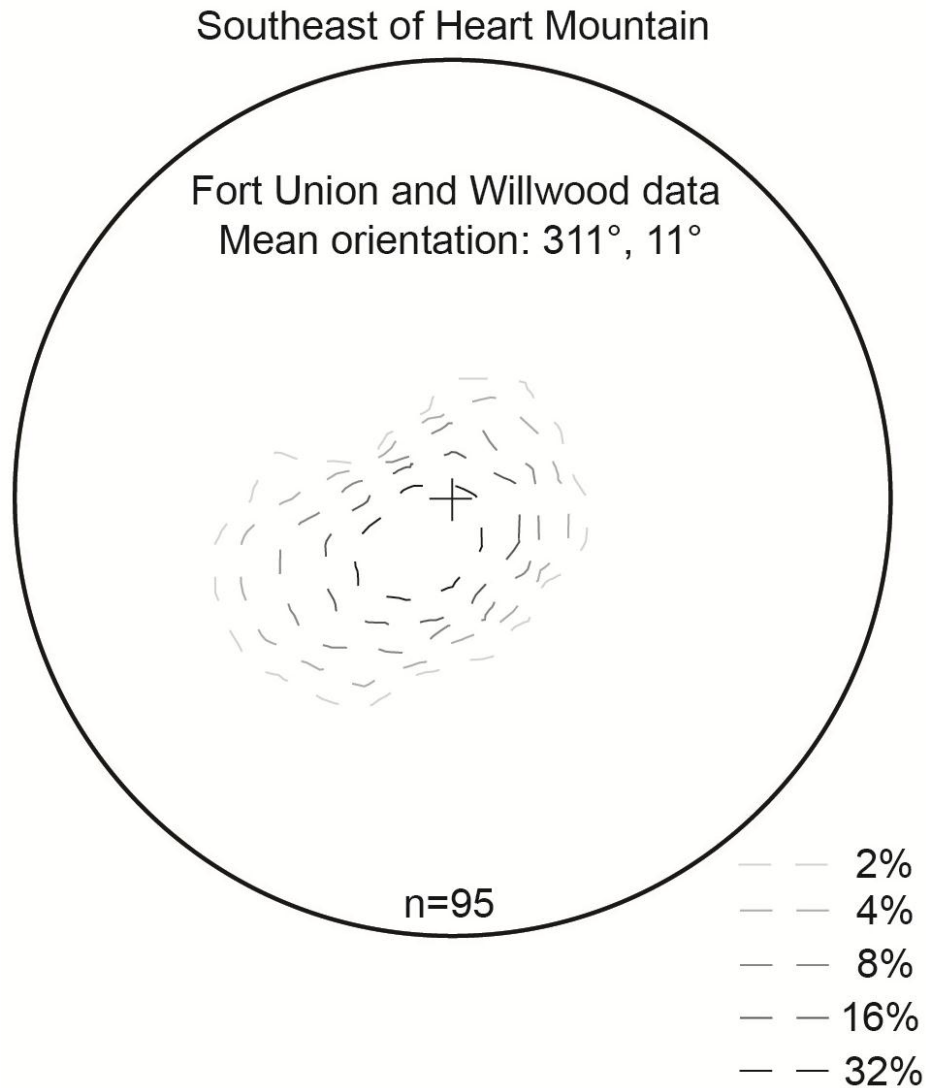
Figure 21. Equal area projections showing density contours of poles to bedding orientations of the gently-dipping Paleocene Fort Union and late Paleocene-Eocene Willwood Formations, southeast of Heart Mountain. Mean strike and dip of Paleogene Fort Union and Willwood Formations: strike 311°, dip 11°N. Equal area projections created using GEOrient version 9.5.0.
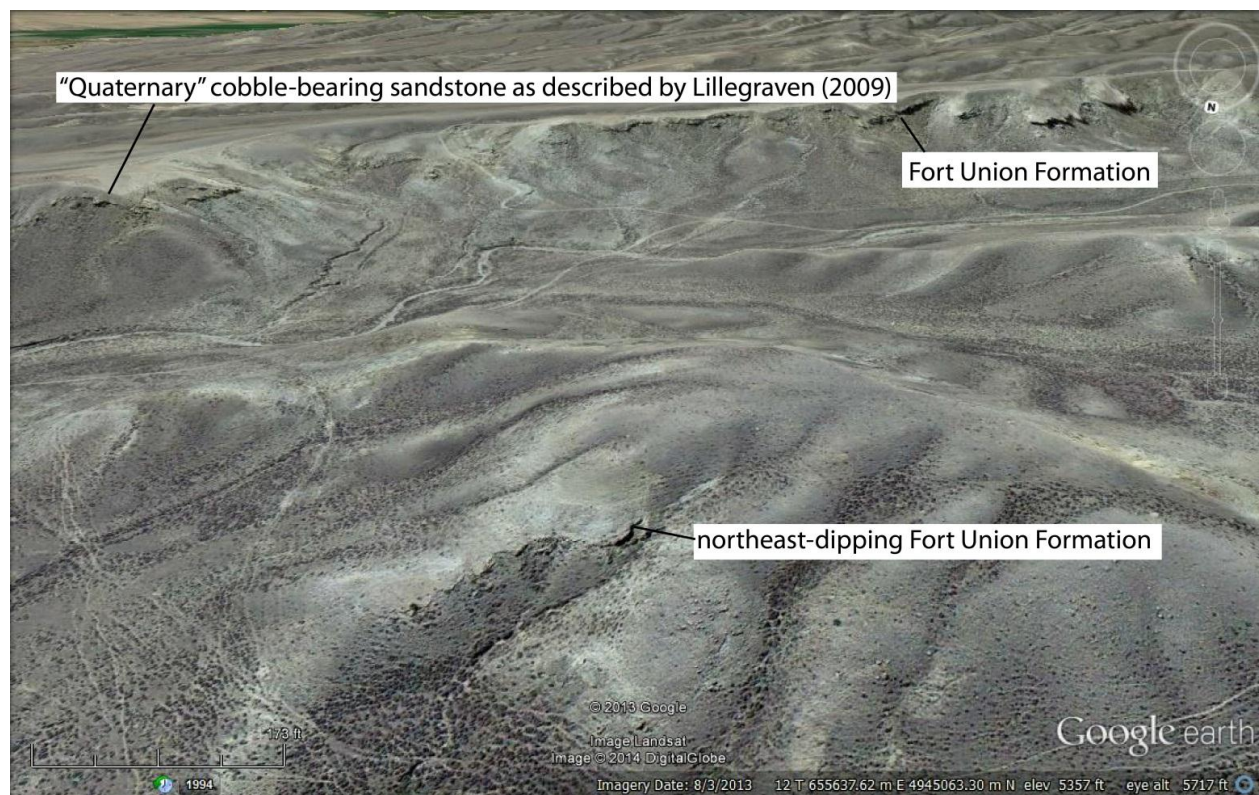
Figure 22. Google Earth image showing horizontal bedding, described by Lillegraven (2009) as "Quaternary cobble-bearing sandstone." Northeast-dipping Fort Union Formation is seen in the foreground. Known Fort Union sediments outcrop along strike from "Quaternary cobble-bearing sandstone" from Lillegraven (2009), indicating that the "Quaternary cobble-bearing sandstone" is part of the Paleocene Fort Union Formation.

Mountain. Quaternary conglomeratic deposits around Heart Mountain are generally very poorly cemented and flat-lying; the "Quaternary cobble-bearing sandstone" from Lillegraven (2009) is well-cemented and tilted in some places, indicating that it is indeed part of the Fort Union Formation. Northeast of Lillegraven's "almost horizontal bed of Quaternary cobble-bearing sandstone," the Fort Union Formation is seen tilted, dipping to the northeast (Fig. 23). Where it is tilted, the Fort Union is in similar orientation to the "northeast-dipping Fort Union Formation" from Lillegraven (2009). Using this information, we mapped the near-horizontal bed of cobble-bearing sandstone as the Fort Union Formation and determined that there is a fold within the Fort Union Formation southeast of Heart Mountain. Proximal to the location of northeast- dipping Fort Union strata, basal Willwood strata near the Willwood-Fort Union contact are also northeast- dipping in similar orientation (Fig. 24). This suggests that upper Fort Union and lower Willwood rocks were folded together during a stage of deformation in the latest Paleocene-early Eocene.

Joints in Cretaceous Strata Northwest of Heart Mountain

Joints are fractures that form without significant displacement parallel to the fracture and that display only slight movement normal to the fracture plane. Joint systems can be used to reveal the sequence and timing of tectonic events, and orientations of systematic fractures reflect the orientation of the principal stress directions involved in deformation (Fossen, 2010). North-striking tilted Cretaceous strata in the vicinity of Hogan Reservoir are indicative of an episode of east-directed shortening. The Cretaceous strata also display systematic joints that we used to find shortening directions in this area (Fig. 25). We measured 69 joints in the Cretaceous Frontier Formation on the northern shore of Hogan Reservoir. After rotating bedding to horizontal, the mean strike of the joints is 020°, indicating that there is strong evidence for north-northeast to

Figure 23. Unit described by Lillegraven (2009) as "Quaternary cobble-bearing sandstone." Photo shows unit dipping to the northeast and flat-lying to the southwest, indicating that it is part of the Paleocene Fort Union Formation. View to the southeast.
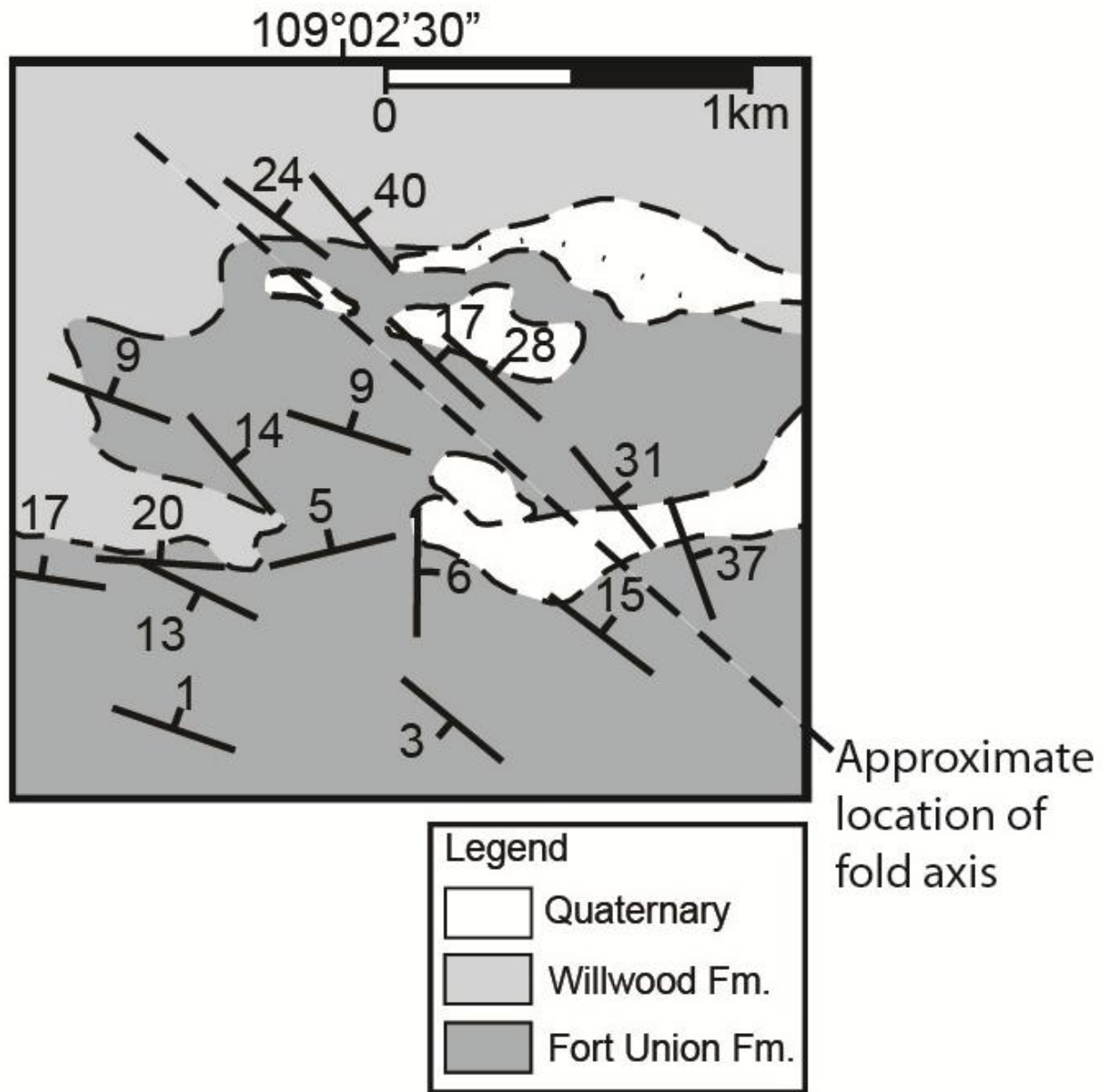
Figure 24. Geologic map of the area southeast of Heart Mountain. The Paleocene Fort Union Formation and late Paleocene-Eocene Willwood Formation are folded in this area where they transition from nearly horizontal to northeast-dipping.
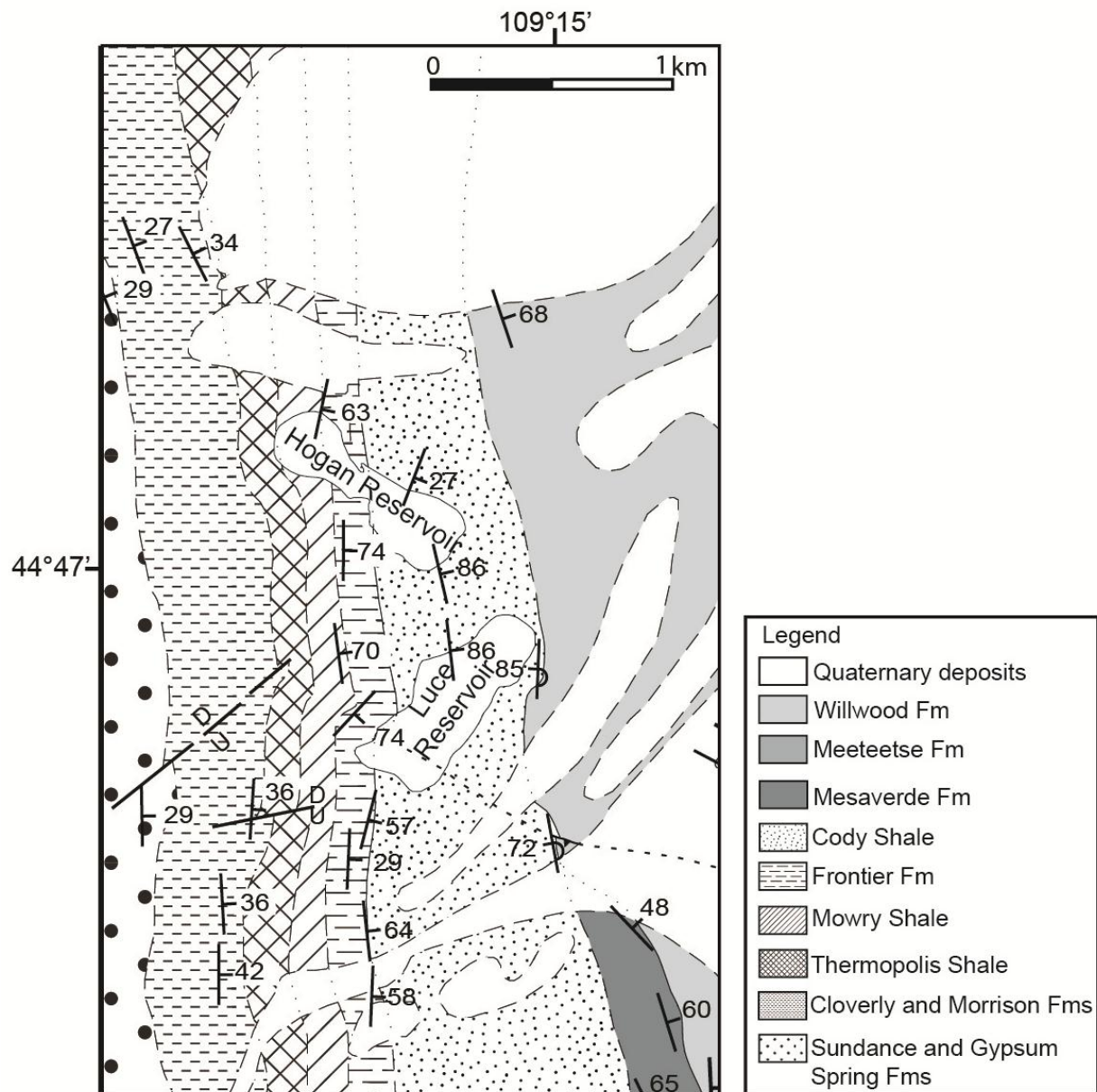
Figure 25. Geologic map of Hogan Reservoir. Cretaceous strata generally strike north-south in this area and contain joint sets used to find shortening directions in this area.

south-southwest-directed shortening (Fig. 26). It is probable that the joints at Hogan Reservoir formed as a result of north-northeast-directed shortening whereas the present-day north-striking Cretaceous strata were tilted as a result of east-directed shortening.

Discussion

Cretaceous-Paleogene Angular Unconformities

Southwest of Heart Mountain, Late Cretaceous rocks generally strike northwest-southeast and lie in angular discordance with the overlying Fort Union and Willwood Formations (Fig. 16). Northward, the Late Cretaceous strata transition to a north-south orientation where they are tilted conformably with the overlying Fort Union Formation (Fig. 27). Recall that northwest of Heart Mountain, the Late Cretaceous-Fort Union strata lie at angular discordance with the overlying gently-dipping Willwood Formation (Fig. 8). Synchronous black chert conglomerate in the upper Fort Union Formation changes orientation from steeply dipping and in conformable contact with Late Cretaceous strata northwest of Heart Mountain to nearly horizontal and at angular discordance with Late Cretaceous strata southwest of Heart Mountain. Equal area projections clearly show differences in orientations below and above angular unconformities northwest and southwest of Heart Mountain (Fig. 28). The differing ages of the unconformities suggest that they formed at different times. South and southeast of Heart Mountain, the Willwood Formation is in conformable depositional contact with the Fort Union Formation and a thin section of upper Fort Union and lower Willwood strata can be seen slightly folded in some places.

Timing of Deformation

Differences in the orientation of Late Cretaceous rocks as well as the differing ages of tilted sediments indicate that northwest and southwest of Heart Mountain, deformation occurred at different times and with different shortening directions. Southwest of Heart Mountain,

80
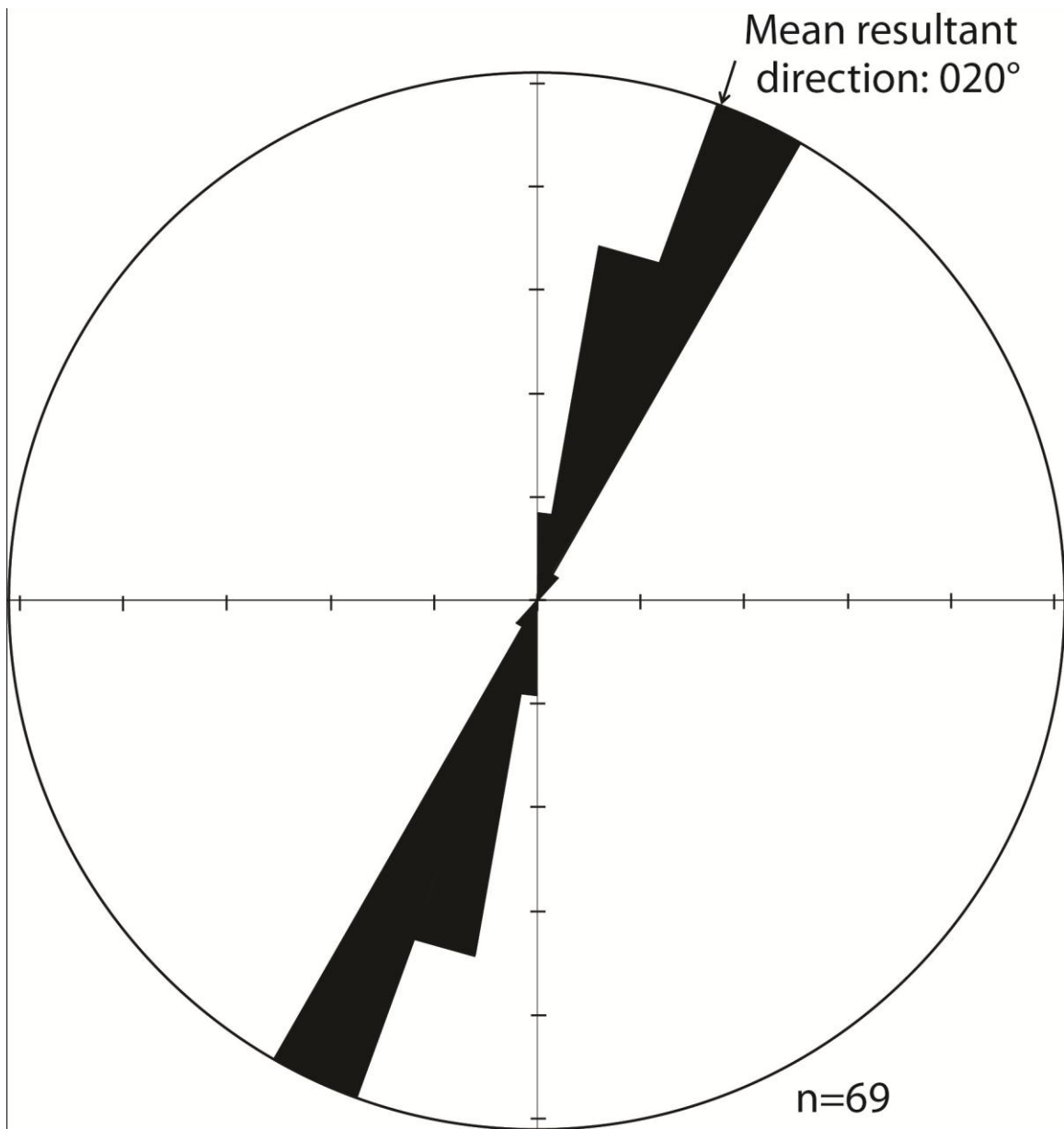
Figure 26. Rose diagram showing orientations of joints found in north-south striking Cretaceous strata near Hogan Reservoir. Bedding is rotated to horizontal. Mean strike of joints is 020°, indicating north-northeast to south-southwest directed shortening.
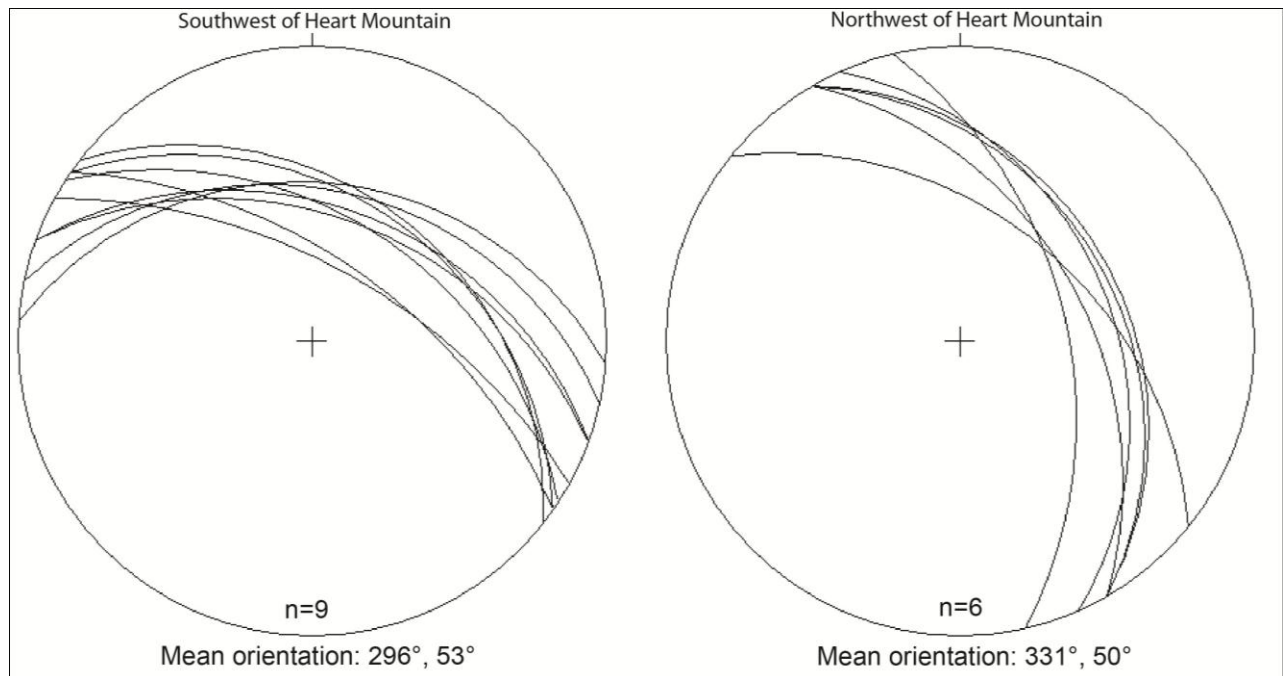
Figure 27. Equal area projections showing differences in mean bedding orientations of Late Cretaceous layers, southwest and northwest of Heart Mountain. Southwest of Heart Mountain, the mean bedding orientation is 296°, 53°N. Northwest of Heart Mountain, the mean bedding orientation is 331°, 50°E. Equal area projections created using GEOrient version 9.5.0.
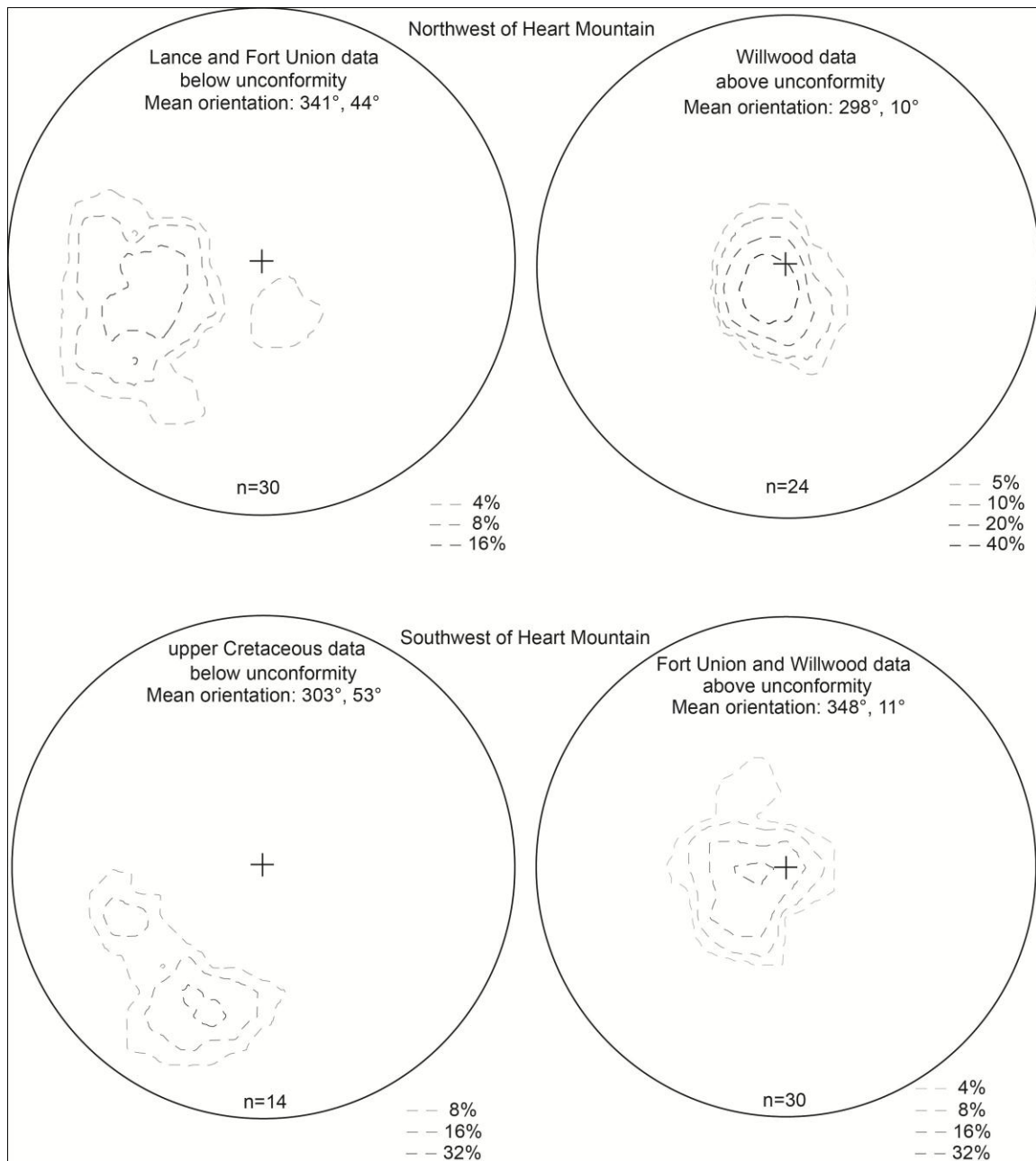
Figure 28. Equal area projections showing density contours of Late Cretaceous layers, Paleocene Fort Union Formation, and late Paleocene-Eocene Willwood Formation above vs. below unconformities northwest and southwest of Heart Mountain. Northwest of Heart Mountain, projections show tilted Lance and Fort Union Formations below gently-dipping Willwood Formation. Southwest of Heart Mountain, projections show tilted Late Cretaceous beds below gently-dipping Fort Union and Willwood Formations. Equal area projections created using GEOrient version 9.5.0.

deformation occurred in the latest Cretaceous-early Paleocene, prior to deposition of the Paleocene Fort Union Formation. After the tilting of Late Cretaceous strata up to and including Lance, Paleocene Fort Union and late Paleocene-Eocene Willwood sediments were deposited unconformably on top of Cretaceous rocks. Northwest of Heart Mountain, deformation occurred in the late Paleocene, resulting in the tilting of Late Cretaceous formations as well as the Paleocene Fort Union Formation. In the latest Paleocene, Willwood sediments were deposited on top of steeply dipping Cretaceous-Paleocene rocks. Southeast of Heart Mountain, a fold is evident within the Fort Union Formation where it can be seen northeast- dipping and in contact with nearly horizontal Fort Union rocks (Fig. 23). The northeast-dipping Fort Union rocks are in similar orientation to tilted basal Willwood strata near the Willwood-Fort Union contact southeast of Heart Mountain. This indicates that some deformation occurred that folded a thin layer of basal Willwood and upper Fort Union strata together, likely synchronous with the deformation that tilted Late Cretaceous-Paleocene Fort Union strata in similar orientation northwest of Heart Mountain. North of the Heart Mountain area, Late Cretaceous-Paleogene rocks are deformed to the east of the Beartooth Mountains and Dead Indian Hill. Previous work by DeCelles et al. (1991) has shown that the Paleocene Fort Union Formation along the northwestern Bighorn Basin margin was deformed in the late Paleocene. Our mapping of deformed late Paleocene-early Eocene Willwood strata east of the Beartooths and Dead Indian Hill suggest that deformation also occurred in the early Eocene.

Our deformation ages are in disagreement with some previous studies focused on the Beartooth uplift: mapping by Pierce (1966) indicated that deformation occurred up to the latest Paleocene; DeCelles et al. (1991) proposed that Beartooth deformation began and ended in the late Paleocene; and Wise (2000) suggested that it occurred throughout the Paleocene, ending in

the late Paleocene. However, our deformation ages are also in agreement with other studies based in the northwestern Bighorn Basin: Dutcher et al. (1986) suggested that synorogenic sediments were late Paleocene in age, but considered that syntectonic deposition may have continued into the Eocene; and Stearns et al. (1974) suggested that the entire region near Rattlesnake Mountain began deforming in the uppermost Cretaceous and lasted into the Eocene. Gries (1990) suggested that the Laramide Orogeny occurred from the Late Cretaceous to late Eocene, specifying that the Beartooth uplift occurred during the Paleocene and the Pat O'Hara uplift occurred in the early to middle Eocene. Our study has indicated that deformation along the western edge of the Bighorn Basin was occurring from the latest Cretaceous into the early Eocene, generally in agreement with the range of ages proposed for the Laramide Orogeny.

<u>Shortening Directions Associated with Deformation</u>

Along the western edge of the Bighorn Basin, differently oriented Late Cretaceous-Paleogene strata reflect a change in shortening directions, from north-northeast- to east-directed. It is likely that a first episode of north-northeast-directed deformation occurred during uplift of the Pat O'Hara mountain block, which strikes roughly WNW and resulted in tilted Late Cretaceous strata that strike WNW southwest of Heart Mountain. This was followed by a second episode of east-northeast-directed deformation during uplift of the Beartooth block, which strikes roughly north and resulted in tilted Late Cretaceous-Paleocene strata that strike nearly due N northwest of Heart Mountain and along the eastern front of the Beartooths. A final stage of east-directed deformation occurred in the early Eocene as a result of the uplift of Dead Indian Hill and continued uplift of the Beartooth Mountains; this episode tilted Late Cretaceous-early Eocene rocks east of Dead Indian Hill and east of the Beartooths, re-deforming the Late

Cretaceous-Paleocene strata along the northwestern Bighorn Basin margin and resulting in their present-day orientations (Fig. 29).

Near Hogan Reservoir northwest of Heart Mountain, north-striking tilted Cretaceous strata formed as a result of east-directed shortening; however, systematic joints within the Late Cretaceous strata indicate a dominant shortening direction of 020° when beds are rotated to horizontal. In a previous study, Wise (2000) proposed that there was a change in shortening directions during Laramide deformation of the Beartooth Mountains, from north-northeast-directed to east-directed. Our study at Hogan Reservoir is in agreement with his hypothesis; it is apparent that the joints formed during the first stage of north-northeast-directed shortening whereas the Late Cretaceous strata were folded to their present orientation as a result of later east-directed shortening during uplift of Dead Indian Hill to the west.

Previous studies have cited a variety of local and large-scale controls to explain variously oriented structures throughout the Rocky Mountains. Proposed controls have included localized pre-orogenic ductile fabrics (Erslev and Koenig, 2009), pre-existing major faults that may have been reactivated depending on their proximity to basement-involved arches (Brown, 1993), large-scale reactivation of pre-existing basement structures (Neely and Erslev, 2009), inversion of Proterozoic extensional fault systems and structures (Marshak et al., 2000; Timmons et al., 2001), the trajectory of Farallon-North American relative plate motions (Saleeby, 2003), a change in movement of the North American plate from west to southwest to south (Gries, 1983, 1990), and unimodal ENE-WSW shortening and compression (Erslev and Koenig, 2009). Studies have shown that there were both internal and external controls on the development of Laramide structures throughout the Rocky Mountains, and the orientations of the Laramide structures are important when determining which control(s) exerted the most influence on their
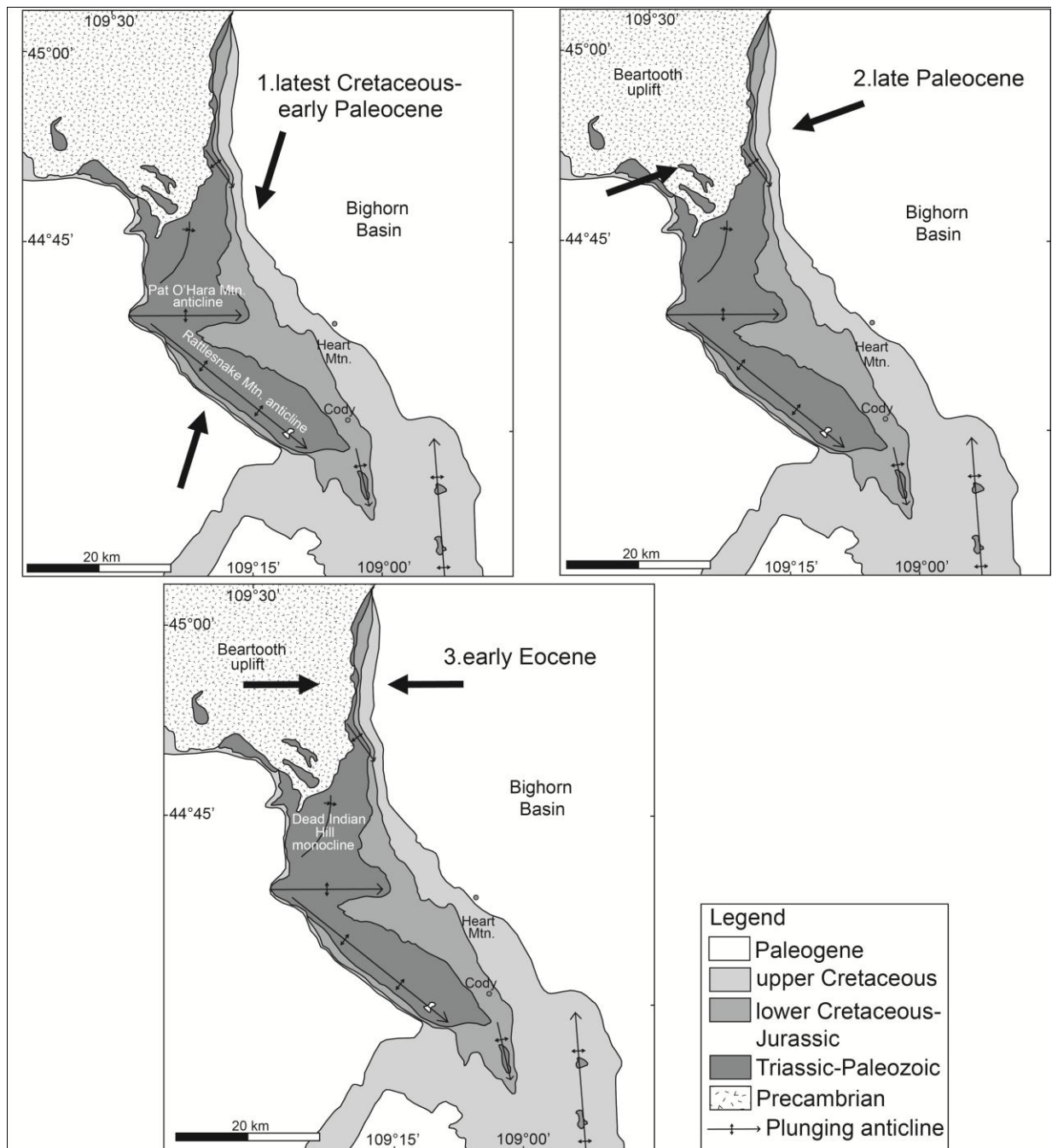
Figure 29. Simplified geologic maps of the western Bighorn Basin and adjacent Laramide structures showing shortening directions during the three stages of deformation. On each map, actively deforming Laramide structures are labeled; arrows show direction of shortening. Three stages of deformation include (1) latest Cretaceous-early Paleocene NNE-SSW shortening as a result of Pat O'Hara and Rattlesnake Mountain uplifts; (2) late Paleocene ENE-WSW shortening as a result of Beartooth uplift; (3) early Eocene E-W shortening as a result of Dead Indian Hill uplift and continued Beartooth uplift.

development (Brown, 1988). Our research has revealed that multiple shortening directions at various intervals of deformation exerted major control on the orientations of Laramide structures along the western edge of the Bighorn Basin. The orientations of structures in our study area suggest that (1) NNE-directed shortening, (2) ENE-directed shortening, and (3) E-directed shortening occurred from the latest Cretaceous to early Eocene. This interpretation is in disagreement with shortening directions from several previous studies of the entire Laramide Orogeny: some studies suggested a single crustal shortening direction, generally ENE or NE (Dickinson and Snyder, 1978; Bird, 1984, 1988; Sales, 1968; Stone, 1969; Lowell, 1983; Blackstone, 1990; Erslev, 1993) while other studies suggested changes in shortening from generally E-directed to more NE- or N-directed (Gries, 1983, 1990; Chapin and Cather, 1981).

A few studies are in agreement with ours, describing a change in shortening directions during the Laramide Orogeny from ENE-directed to E-directed (Bird, 1998; Bergerat et al., 1992). The orientation of their first episode of ENE-directed shortening corresponds with our second episode of ENE-directed shortening, and the orientation of their second episode of E-directed shortening corresponds with our third episode of E-directed shortening. It is evident that NNE-directed shortening during the first stage of Laramide deformation in northwestern Wyoming was a unique event likely resulting from the WNW-striking Pat O'Hara uplift and NW-striking Rattlesnake Mountain uplift. Our proposed shortening directions are in agreement with the change in Beartooth thrust directions from north-northeast to east proposed by Wise (2000); however, Wise cited escape tectonics around the Precambrian Stillwater Complex as the principal control on thrust directions. Our research suggests that changes in shortening directions during multi-stage Laramide deformation were the principal control that resulted in the present-day orientations of the Laramide structures along the western edge of the Bighorn Basin.

Conclusions

Our research has revealed differently oriented Late Cretaceous-Paleogene strata that reflect a change in shortening directions during Laramide deformation. A first episode of north-northeast-directed deformation occurred during the latest Cretaceous-early Paleocene and resulted in tilted Late Cretaceous strata southwest of Heart Mountain. A second episode of east-northeast-directed deformation occurred during the late Paleocene and resulted in tilted Late Cretaceous-Paleocene strata northwest of Heart Mountain and along the eastern front of the Beartooths. A third and final stage of east-directed deformation occurred in the early Eocene and resulted in deformation of Late Cretaceous-early Eocene rocks east of Dead Indian Hill and east of the Beartooths. Near Hogan Reservoir, it is apparent that joints in Cretaceous strata formed during the first stage of shortening during the Pat O'Hara uplift, followed by folding of the Cretaceous strata to their present orientation during the final stage of shortening during the Dead Indian Hill uplift. Shortening directions were a major external control on the development of the Rocky Mountains during the Laramide Orogeny and previous work has shown that many ranges within the Rockies developed as a result of a combination of internal and external controls.

REFERENCES

Bergerat, F., Bouroz-Weil, C., and Angelier, J., 1992, Paleostresses inferred from macrofractures, Colorado Plateau, Western U.S.A.: Tectonophysics, v. 206, p. 219-243.

Bird, P., 1984, Laramide crustal thickening event in the Rocky Mountain foreland and Great Plains: Tectonics, v. 3, p. 741-758.

Bird, P., 1988, Formation of the Rocky Mountains, western United States: A continuum computer model: Science, v. 239, p. 1501-1507.

Bird, P., 1998, Kinematic history of the Laramide orogeny in latitudes 35°-49°, western United States: Tectonics, v. 17, p. 780-801.

Blackstone, D.L., 1986, Structural geology—northwest margin, Bighorn Basin: Park County, Wyoming and Carbon County, Montana: *in* Montana Geological Society and Yellowstone Bighorn Research Association joint field conference and symposium; geology of the Beartooth Uplift and adjacent basins: Yellowstone Bighorn Research Association, p. 125-135.

Blackstone, D.L., 1990, Rocky Mountain foreland structure exemplified by the Owl Creek Mountains, Bridger Range and Casper arch, central Wyoming: Wyoming Geological Association Guidebook, v. 41, p. 151-166.

Bown, T.M., 1979, Geology and mammalian paleontology of the Sand Creek facies, lower Willwood Formation (lower Eocene), Washakie County, Wyoming [Ph.D. thesis]: University of Wyoming, 530 p.

Bown, T.M., 1980, Summary of latest Cretaceous and Cenozoic sedimentary, tectonic, and erosional events, Bighorn Basin, Wyoming: Papers on Paleontology, No. 24, p. 25-32.

Brown, W.G., 1988, Deformational style of Laramide uplift in the Wyoming foreland, *in* Schmidt, C.J., and Perry, W.J., Jr., Interaction of the Rocky Mountain Foreland and the Cordilleran Thrust Belt: Geological Society of America Memoir, v. 171, p. 1-25.

Brown, W.G., 1993, Structural style of Laramide basement-cored uplifts and associated folds, *in* Snoke, A.W., Steidtmann, J.R., and Roberts, S.M., Geology of Wyoming: Geological Survey of Wyoming Memoir, no. 5, p. 312-371.

Bucher, W.H., Chamberlin, R.T., Thom, W.T. Jr., 1933, Results of structural research work in Beartooth-Big Horn region, Montana and Wyoming: AAPG Bulletin, v. 17, issue 6, p. 680-693.

Chapin, C.E., and Cather, S.M., 1981, Eocene tectonics and sedimentation in the Colorado
Plateau-Rocky Mountain area, *in* Dickinson, W.R., and Payne, M.D., Rocky Mountain
Foreland Basins and Uplifts: Denver, Colorado, Rocky Mountain Association of
Geologists, p. 173-198.

Dickinson, W.R., and Snyder, W.S., 1978, Plate tectonics of the Laramide Orogeny, *in*
Matthews, V., ed., Laramide folding associated with basement block faulting in the
western United States: Geological Society of America Memoir 151, p. 355-366.

Dutcher, L.A.F., Jobling, J.L., and Dutcher, R.R., 1986, Stratigraphy, sedimentology and
structural geology of Laramide synorogenic sediments marginal to the Beartooth
Mountains, Montana and Wyoming, *in* Montana Geological Society and Yellowstone
Bighorn Research Association joint field conference and symposium; geology of the
Beartooth Uplift and adjacent basins: Yellowstone Bighorn Research Association, p. 33-
52.

Erslev, E.A., 1993, Thrusts, back-thrusts and detachment of Rocky Mountain foreland arches, *in*
Schmidt, C.J., Chase, R., and Erslev, E.A., Laramide Basement Deformation in the
Rocky Mountain Foreland of the Western United States: Geological Society of America
Special Paper 280, p. 339-358.

Erslev, E. and Koenig, N., 2009, Three-dimensional kinematics of Laramide, basement-involved
Rocky Mountain deformation, USA: Insights from minor faults and GIS-enhanced
structure maps: Geological Society of America Memoirs, v. 204, p. 125-150.

Foose, R.M., Wise, D.U., and Garbarini, G.S., 1961, Structural geology of the Beartooth
Mountains, Montana and Wyoming: Geological Society of America Bulletin, v. 72, p.
1143-1172.

Fossen, Haakon, 2010, Structural Geology: New York, Cambridge University Press, 463 p.

Gingerich, P.D., 1983, Paleocene-Eocene faunal zones and a preliminary analysis of Laramide
structural deformation in the Clark's Fork Basin, Wyoming, *in* Wyoming Geological
Association Guidebook, v. 34, p. 185-195.

Gingerich, P.D., and Clyde, W.C., 2001, Overview of mammalian biostratigraphy in the
Paleocene-Eocene Fort Union and Willwood Formations of the Bighorn and Clarks Fork
Basins: Papers on Paleontology, no. 33, p. 1-14.

Gries, R.R., 1983, North-south compression of Rocky Mountain foreland structures, *in* Lowell,
J.D., Rocky Mountain foreland basins and uplifts: Denver, Colorado, Rocky Mountain
Association of Geologists, p. 9-32.

Gries, R. R., 1990, Rocky Mountain Foreland Structures: Changes in Compression Direction
through Time: Petroleum and Tectonics in Mobile Belts, p. 129-148.

Kraus, M.J., 1979, The petrology and depositional environments of a continental sheet sandstone; the Willwood Formation, Bighorn Basin, Wyoming [Master's thesis]: University of Wyoming, 106 p.

Lillegraven, J.A., 2004, Revisions to upper Cretaceous stratigraphy near Hell's Half Acre, eastern Wind River Basin, central Wyoming: Bulletin of Carnegie Museum of Natural History, v. 36, p. 137-158.

Lillegraven, J.A., 2009, Where was the western margin of northwestern Wyoming's Bighorn Basin late in the Early Eocene?: Papers on Geology, Vertebrate Paleontology, and Biostratigraphy in Honor of Michael O. Woodburne, Museum of Northern Arizona Bulletin, v. 65, p. 37-82.

Lowell, J.D., 1983, Foreland detachment deformation: American Association of Petroleum Geologists Bulletin, v. 67, p. 1349.

Marshak, S., Karlstrom, K., and Timmons, J.M., 2000, Inversion of Proterozoic extensional faults: An explanation for the pattern of Laramide and Ancestral Rockies intracratonic deformation, United States: Geology, v. 28, no. 8, p. 735-738.

Neasham, J.W., and Vondra, C.F., 1972, Stratigraphy and petrology of the lower Eocene Willwood Formation, Bighorn Basin, Wyoming: Geological Society of America Bulletin, v. 83, p. 2167-2180.

Neely, T.G., 2006, Three-dimensional strain at foreland arch transitions: structural modeling of the southern Beartooth Arch transition zone, northwest Wyoming [M.S. thesis]: Colorado State University, 113 p.

Neely, T.G., and Erslev, E.A., 2009, The interplay of fold mechanisms and basement weaknesses at the transition between Laramide basement-involved arches, north-central Wyoming, USA: Journal of Structural Geology, v. 31, p. 1012-1027.

Pierce, W.G., 1965a, Geologic map of the Clark Quadrangle, Park County, Wyoming: U.S. Geological Survey, scale 1:62 500, 1 sheet.

Pierce, W.G., 1965b, Geologic map of the Deep Lake Quadrangle, Park County, Wyoming: U.S. Geological Survey, scale 1:62 500, 1 sheet.

Pierce, W.G., 1966, Geologic map of the Cody Quadrangle, Park County, Wyoming: U.S. Geological Survey, scale 1:62 500, 1 sheet.

Pierce, W.G., 1968, Geologic map of the Pat O'Hara Quadrangle, Park County, Wyoming: U.S. Geological Survey, scale 1:62 500, 1 sheet.

Saleeby, J., 2003, Segmentation of the Laramide slab—Evidence from the southern Sierra Nevada region: Geological Society of America Bulletin, v. 115, no. 6, p. 655-668.

Sales, J.K., 1968, Crustal mechanisms of Cordilleran foreland deformation: A regional and scale-model approach: American Association of Petroleum Geologists Bulletin, v. 52, p. 2016-2044.

Sinclair, W.J., and Granger, W., 1912, Notes on the Tertiary deposits of the Bighorn Basin: Bulletin of the American Museum of Natural History, p. 57-67.

Stearns, D.W., Logan, J.M., and Friedman, M., 1974, Structure of Rattlesnake Mountain and related rock mechanics investigations: Pennsylvania State University, University Park, Pennsylvania, USA, p. 18-25.

Stone, D.S., 1969, Wrench faulting and Rocky Mountain tectonics: The Mountain Geologist, v. 6, p. 67-79.

Timmons, J.M., Karlstrom, K.E., Dehler, C.M., Geissman, J.W., and Heizler, M.T., 2001, Proterozoic multistage (ca. 1.1 and 0.8 Ga) extension recorded in the Grand Canyon Supergroup and establishment of northwest- and north-trending tectonic grains in the southwestern United States: GSA Bulletin, v. 113, no. 2, p. 163-181.

Webb, M.W., and Steel, R.J., 2001, Incised paleovalleys in the Lance Formation, southwestern Bighorn Basin, Wyoming: Annual Meeting Expanded Abstracts-American Association of Petroleum Geologists, v. 2001, p. 212.

Wise, D.U., 2000, Laramide structures in basement and cover of the Beartooth Uplift near Red Lodge, Montana: AAPG Bulletin, v. 84, issue 3, p. 360-375.

CHAPTER 3: SPECTRAL ANALYSIS OF THE LATE PALEOCENE-EARLY EOCENE WILLWOOD FORMATION AND THE TIMING OF LARAMIDE DEFORMATION, NORTHWESTERN BIGHORN BASIN, WYOMING

Introduction

In the latest Cretaceous-Paleocene, deformation of the Beartooth Mountains led to the development of the Clarks Fork and Bighorn Basins in northwestern Wyoming (Johnson and Middleton, 1990; Fig. 1). Associated with this uplift, in the late Paleocene, a thick alluvial sequence of sandstone and conglomerate was deposited adjacent to and sourced from the eastern flank of the rising Beartooth Mountains (Johnson and Middleton, 1990). In the Clarks Fork and Bighorn Basins, the Paleocene Fort Union and late Paleocene-early Eocene Willwood Formations are the only two Paleogene formations exposed, both of which contain rocks deposited synkinematically during the unroofing of the Beartooth Mountains and adjacent Laramide mountain ranges (Gingerich, 1983; Johnson and Middleton, 1990). Lithologic, stratigraphic and structural features of the uppermost member of the Fort Union Formation have been used to constrain the timing of unroofing of the Beartooth Mountains (DeCelles et al., 1991). Previous studies have also used provenance modeling and palynologic analyses of syntectonic Fort Union deposits to constrain the timing and kinematics of Paleocene uplift along the western edge of the Bighorn and Clarks Fork Basins (Jobling, 1974; Dutcher et al., 1986; DeCelles et al., 1991). There has been a range of ages proposed for the onset and end of deformation along the western edge of the Clarks Fork and Bighorn Basins (Pierce, 1965; Dutcher et al., 1986; DeCelles et al., 1991; Wise, 2000; Neely, 2006), and this study aims to
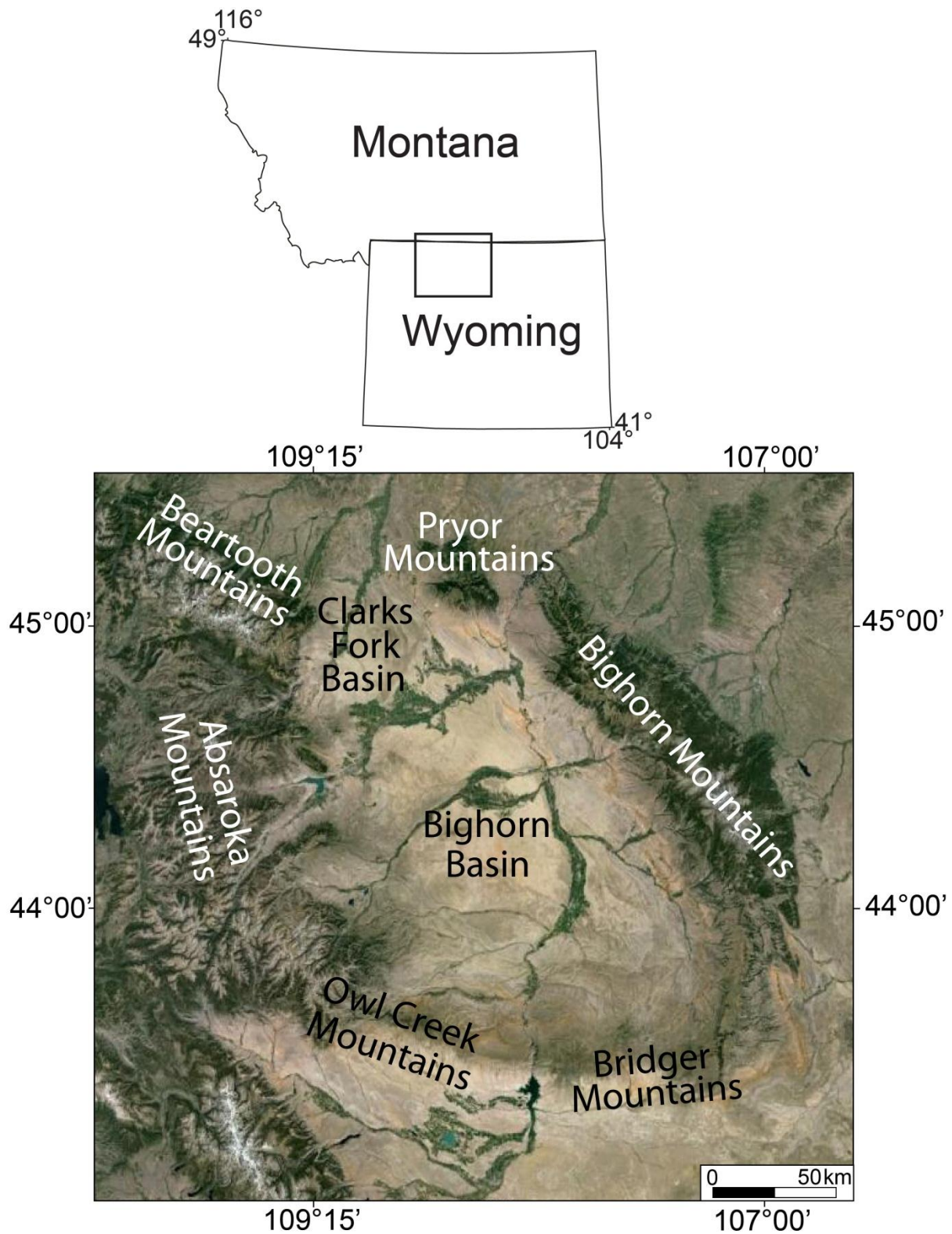
Figure 1. Location map of the Clarks Fork and Bighorn Basins and bounding Laramide ranges. Satellite image from Google Earth.

further constrain the kinematic history of Laramide deformation using sediment accumulation rate calculations and spectral analyses.

The Willwood Formation locally contains abundant vertebrate fossils that have yielded a high-resolution biostratigraphy in mostly undeformed sediments in the central Bighorn Basin (Rose, 1981; Gingerich, 1989). The formation also contains mammalian fossils that are characteristic of the Paleocene-Eocene boundary (Gingerich, 1989) as well as the carbon isotope excursion, or CIE (Koch et al., 1992) that is associated with the Paleocene-Eocene Thermal Maximum (PETM). Along the western edge of the Bighorn Basin, a sparse number of fossil localities have been discovered in deformed Paleogene strata. Near the Beartooth Mountain front, there have been no studies that attempt to correlate deformed Willwood beds with undeformed strata farther basinward. In order to constrain the timing of deformation in Paleogene sediments near the mountain front, absent high-resolution biostratigraphy, other methods are necessary.

The Willwood Formation contains paleosols that alternate rhythmically on various scales. The stacking patterns in the Willwood have been attributed to various mechanisms including autocyclic floodplain development (Clyde and Christensen, 2003; Abels et al., 2013), tectonics (Bown and Kraus, 1993), and climate (Kraus and Aslan, 1993; Aziz et al., 2008; Abels et al., 2013). The 55.8 Ma PETM is recorded in both marine and terrestrial sections around the world (Kennett and Stott, 1991; Koch et al., 1992; Bralower et al., 1997; Zachos et al., 2005; Röhl et al., 2007; Schouten et al., 2007). It occurred during deposition of the Willwood Formation in the Bighorn Basin, resulting in the development of thick, well-developed, densely spaced red-to-purple paleosols (Kraus and Riggins, 2002; Kraus and Davies-Vollum, 2004).

We used sparse fossil data in the Kimball Bench area to calculate possible sediment accumulation rates during basal Willwood deposition. The range of accumulation rates was used to calculate a range of possible absolute ages of the youngest deformed Willwood beds and therefore the age of onset of deformation in this area. We then performed spectral analyses of deformed basal Willwood strata in the Kimball Bench area which we used to confirm the location of Willwood strata that match the description of beds deposited during the 55.8 Ma PETM and therefore assign a specific absolute age to the deformed sediments. Spectral peaks from our analyses correspond with orbital climatic cycles, indicating that precessional cyclicity influenced paleosol development during Paleogene Willwood deposition. Similar studies have used spectral analyses of Willwood strata in the Bighorn Basin with the goal of correlating spectral peaks with orbital climate cycles and also to locate the 55.8 Ma PETM (Aziz et al., 2008; Abels et al., 2013); in these studies, a portable photospectrometer was used to take color measurements. For our spectral analyses, we used a digital camera and ENVI software to take color measurements of basal Willwood sediments in lieu of a portable photospectrometer (method by Levin et al., 2005). In this study, we use a novel approach to determine the absolute age of deformed basal Willwood strata in the Kimball Bench area and therefore the timing of deformation along the western edge of the Bighorn Basin.

Geological Setting

The late Paleocene-early Eocene Willwood Formation rests conformably above the Paleocene Fort Union Formation in the central Bighorn Basin (Neasham and Vondra, 1972). In the central-northern Bighorn Basin, both the Fort Union and Willwood Formations consist of thick fluvial and lacustrine deposits (Fricke et al., 1998). Along the southwestern margin of the

basin, the Willwood Formation rests on top of the Cretaceous Lance and Paleocene Fort Union Formations in angular discordance (Van Houten, 1944; Gingerich, 1983).

In the Clarks Fork and Bighorn Basins, the Fort Union Formation consists of fluvial and alluvial conglomerate, sandstone, siltstone, and mudstone deposits which are lithologically heterogeneous and divided into members (Gingerich, 1983; Johnson and Middleton, 1990). Near the western edge of the Clarks Fork Basin, the Fort Union also contains lacustrine, paludal, and conglomeratic layers along with the more fluvial facies (Hickey, 1980). Along the western edge of the Bighorn Basin, the Fort Union attains its maximum thickness of 3500 meters (Gingerich, 1983). The formation is lithologically heterogeneous and has been divided into separate members/units (Jobling, 1974; Dutcher et al., 1986; Johnson and Middleton, 1990). Proximal to the mountain front, the uppermost member of the Fort Union Formation consists of a sequence of Laramide synorogenic interbedded conglomerate, coarse-grained sandstone, and siltstone deposits. The synorogenic uppermost member of the Fort Union Formation has previously been referred to as the Beartooth Conglomerate (DeCelles et al., 1991), Linley Conglomerate (Flueckinger, 1970), and Proximal facies of the Fort Union Formation (Jobling, 1974). Along the western edge of the basins, this uppermost member of the Fort Union Formation was deposited in response to major uplift of the Beartooth Mountains in the Paleocene. Previous workers have used provenance modeling, palynologic analyses of carbonaceous sediments, and lithologic, stratigraphic and structural relations of syntectonic Fort Union deposits to constrain the timing and kinematics of Paleocene uplift (Jobling, 1974; Dutcher et al., 1986; DeCelles et al., 1991). Palynomorphs and megaflora in the Fort Union Formation indicate a Paleocene age of deposition, although the age range of the species present does not rule out an Eocene age for the stratigraphically highest intervals (Jobling, 1974; Dutcher et al., 1986).

A 1300-meter thick sequence of late Paleocene synorogenic sediments is exposed along the eastern front of the Beartooth Mountains (Flueckinger, 1970). Previous studies provide conflicting interpretations of the ages of these rocks. Pierce (1965) mapped the sequence as the basal Willwood Formation and Johnson and Middleton (1990) retained the basal Willwood designation; Flueckinger (1970) considered the deposits late Paleocene in age; Hickey (1980) considered the sequence Clarkforkian in age (56.8-55.4 Ma) and referred to it as the "conglomeratic member of the Fort Union Formation"; and Gingerich (1983) suggested that the sequence may be as old as Tiffanian (60.2-56.8 Ma). In the central and southern Clarks Fork Basin, the sequence contains red paleosols which are indicative of deposits in the Willwood Formation (Hickey, 1980). Therefore, we consider the synorogenic deposits as part of the basal Willwood Formation.

The late Paleocene-Eocene Willwood Formation is a thick sedimentary unit that overlies the Paleocene Fort Union Formation. The Willwood is traditionally distinguished from the Fort Union Formation by the presence of variegated paleosols (Van Houten, 1944). The Willwood Formation consists of alluvial fan conglomerates along the margins of the basin that grade into predominantly fluvial deposits basinward (Neasham and Vondra, 1972). Van Houten (1944) described four mammalian faunas in the Willwood Formation. The oldest mammal fossils found in the Willwood are latest Paleocene in age and the youngest are from the early Eocene (Van Houten, 1944). Throughout the Bighorn Basin and Clarks Fork Basin, the Willwood Formation consists of a thick sequence of fluvial and alluvial sandstones, siltstones, and mudstones (Gingerich, 1983; Kraus and Davies-Vollum, 2004). The thickness of the formation varies throughout the basin, although an average thickness of 760 meters is generally accepted (Van Houten, 1944; Neasham and Vondra, 1972). The Willwood Formation also contains variegated

paleosols and shales interbedded with sandstones and conglomerates (Van Houten, 1944). The paleosols contain a variety of colors including red, orange, purple, gray, tan, and brown (Bown and Kraus, 1981). The Beartooth, Bighorn, and Owl Creek ranges were the main source of sediments (Kraus and Davies-Vollum, 2004), although it is generally accepted that most orogenic uplift had ended prior to Willwood deposition (Omar et al., 1994).

Along the western edge of the Bighorn Basin, Willwood strata are steeply tilted to overturned where they are in similar orientation to underlying tilted Cretaceous rocks. Basinward, Willwood beds transition to nearly horizontal. North of the Kimball Bench area near the Wyoming-Montana border, a cross section from Pierce (1965) shows a strong angular unconformity between tilted Cretaceous rocks and the overlying gently dipping Paleogene Willwood Formation. The cross section by Pierce (1965) has been used to support the idea that the Willwood Formation is a post-orogenic deposit. However, our mapping has shown that the Willwood Formation transitions from gently dipping to steeply tilted where it is in conformable contact with underlying tilted Cretaceous formations along the western edge of the Bighorn Basin. The goal of this study is to constrain the timing of deformation along the western edge of the Bighorn Basin during Paleogene deposition. The Kimball Bench area is ideal for this study because it contains a continuous exposure of steeply tilted Paleogene Willwood strata that progressively decrease dip to nearly horizontal basinward (Fig. 3). Because there are no internal angular unconformities visible within the sequence of progressively tilted beds, the youngest deformed Willwood strata correspond with the timing of the earliest possible onset of deformation in this area.

Astronomical Cycles in the Willwood Formation

      Previous studies have shown that the Willwood Formation contains cyclic deposits with periods that correlate with precession-scale climate cycles and sub-Milankovitch millennial-scale cycles (Aziz et al., 2008; Abels et al., 2013). Variegated paleosols in the Willwood Formation display rhythmic stacking patterns, which have been explained by a variety of mechanisms: autocyclic floodplain development (Clyde and Christensen, 2003; Abels et al., 2013), tectonics (Bown and Kraus, 1993), and climate (Kraus and Aslan, 1993; Aziz et al., 2008; Abels et al., 2013). Overbank deposits generally have slower accumulation rates which allow for mature paleosol development, whereas the rapid emplacement of channel-avulsion deposits interrupts soil formation processes (Aziz et al., 2008). Precession-scale climatic cycles have been shown to affect the rate of avulsion-belt deposition in the Willwood Formation, where variations in climate induced avulsions that occurred with a regular period close to 21,000 years (Kraus and Aslan, 1993).

      In the north-central Bighorn Basin, the Willwood Formation contains overbank and avulsion deposits that alternate with a cycle thickness of 7.1 meters and a periodicity of 21.6 ky (Abels et al., 2013). This periodicity is within the range of precession-scale climatic cycle periods in the early Eocene which indicates that the alternating deposits were likely influenced by cyclic astronomically forced climate change. Aziz et al. (2008) used spectral analyses of redness in alternating paleosols to constrain astronomical climate control on paleosol stacking patterns in the Willwood Formation. Their sections for analysis were located in the northern Bighorn Basin at Polecat Bench and in the central Bighorn Basin at Red Butte. Their study revealed that there were two significant cycles evident within the stacking patterns in the Willwood: a ~21 ky climatic precession cycle and a 7-8 ky millennial-scale sub-Milankovitch

cycle. At Polecat Bench and Red Butte, astronomical climate variations likely affected paleosol development through cyclic changes in Willwood deposition (Aziz et al., 2008).

<u>Paleocene-Eocene Thermal Maximum</u>

At the end of the Paleocene, there was a short-term rapid warming event known as the Paleocene-Eocene thermal maximum (PETM), previously referred to as the late(st) Paleocene thermal maximum, or LPTM (Fricke et al., 1998, Röhl et al., 2000). The PETM is characterized by a negative carbon isotope excursion (CIE) which occurred on a global scale (Kennett and Stott, 1991; Koch et al., 1992; Bralower et al., 1997, Schouten et al., 2007; Zachos et al., 2007). At this time, there was a sudden decrease in the $\delta^{13}C$ of biogenic marine carbonate by 2.5-4.5 ‰, recorded in benthic and planktonic foraminifera from the latest Paleocene. The drop in carbon isotope ratio was accompanied by mass extinction of benthic foraminifera, changes in ocean chemistry and circulation, and marine warming (Koch et al., 1992; Röhl et al., 2000). A continental carbon isotope excursion was also recorded in the $\delta^{13}C$ of paleosol carbonate and enamel apatite which was similar to the marine carbon isotope excursion in magnitude and duration (Koch et al., 1992).

The geologic age of the Paleocene-Eocene (P-E) boundary is defined as the base of the PETM CIE (Dupuis et al., 2003). The P-E boundary was recently constrained using an astronomically calibrated timescale (Charles et al., 2011). In their study in Spitsbergen, Charles et al. (2011) used U/Pb isotopic dating of zircons from a bentonite layer within the PETM and cyclostratigraphic analysis of the CIE to determine the age of the P-E boundary. Their study presented an age range between 55.728 and 55.964 Ma for the P-E boundary, coeval with the base of the PETM CIE. Röhl et al. (2007) used orbital chronology from cycle stratigraphic

records and analysis of extraterrestrial helium isotopes to find the total duration of the PETM, estimated to be ~170 ky.

Constraining the Timing of Deformation

In the Kimball Bench area of the northwestern Bighorn Basin (Fig. 2), deformed late Paleocene-early Eocene Willwood layers are well exposed. Willwood strata are nearly horizontal in the northeast part of the Kimball Bench area, gradually increasing dip to nearly vertical in the southwest part. Within the progressively tilted beds, there are no visible internal angular unconformities, suggesting that deformation occurred no earlier than after deposition of the youngest tilted bed (Fig. 3). The goal of this study is to find the age of the youngest deformed Willwood strata in this area, representing the oldest possible age of deformation. In order to do this, we used available fossil localities from Rose (1981) and Gingerich and Clyde (2001) and the orientations of Willwood strata in the Kimball Bench area to calculate the true stratigraphic thicknesses between each fossil. We then used the age ranges associated with each fossil locality (known from Gingerich, 1976; Rose, 1981; Gingerich, 1983, 2001) and the stratigraphic distances between them to calculate a minimum and maximum sediment accumulation rate for Willwood deposition in the Kimball Bench area.

Certain beds in the Kimball Bench area contain thick, well-developed, densely spaced red to purple paleosols that match the description of beds deposited during the 55.8 Ma PETM. We chose two sections in the Kimball Bench area for spectral analysis based on the presence of beds that matched this description: the 7RP section and the Kimball Bench section (Fig. 4). Locating beds that were deposited during the PETM allowed us to anchor deformed Willwood strata in the Kimball Bench area to an absolute age. After constraining the absolute ages of deformed Willwood strata using fossil data and the location of the 55.8 Ma PETM, we were able to use our
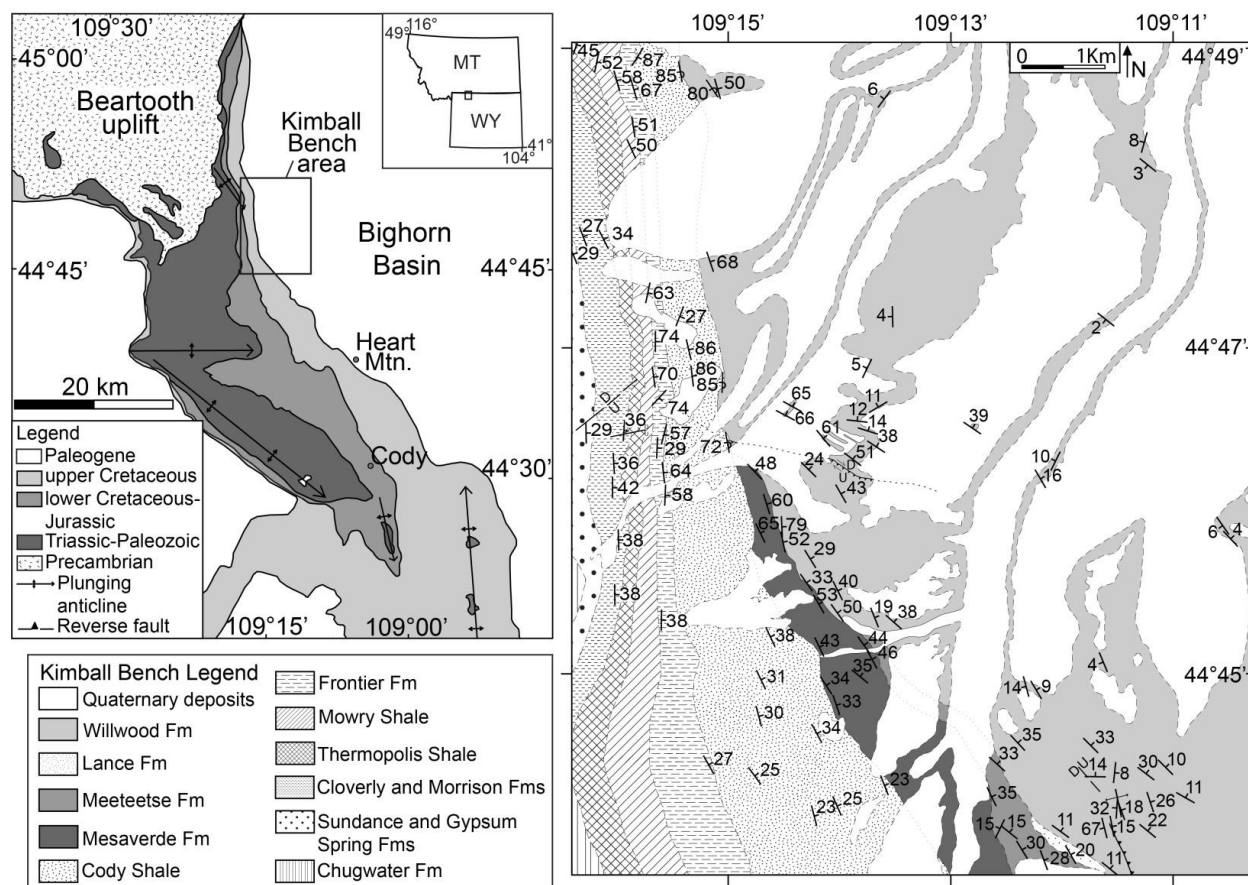
Figure 2. Left: geologic map of the northwestern Bighorn Basin and adjacent Laramide structures, modified from Neely and Erslev, 2009. Right: geologic map of the Kimball Bench study area.
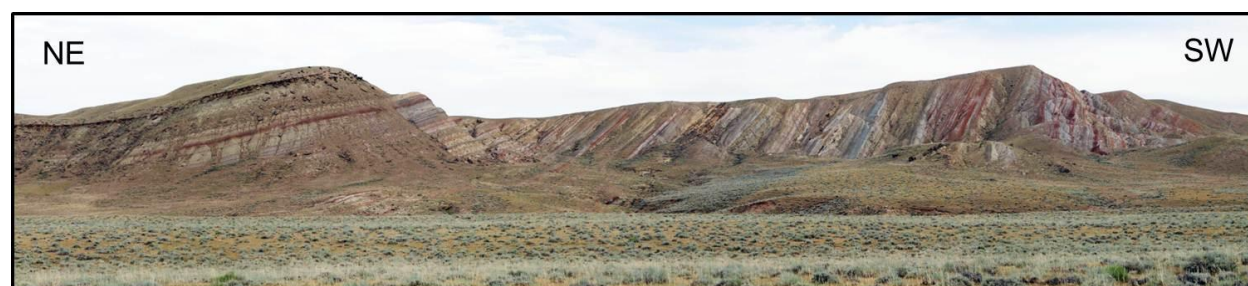
Figure 3. Photograph of progressively tilted late Paleocene-early Eocene Willwood strata at Kimball Bench. Within the progressively tilted beds, there are no visible internal angular unconformities, suggesting that deformation occurred after deposition of the youngest tilted bed.
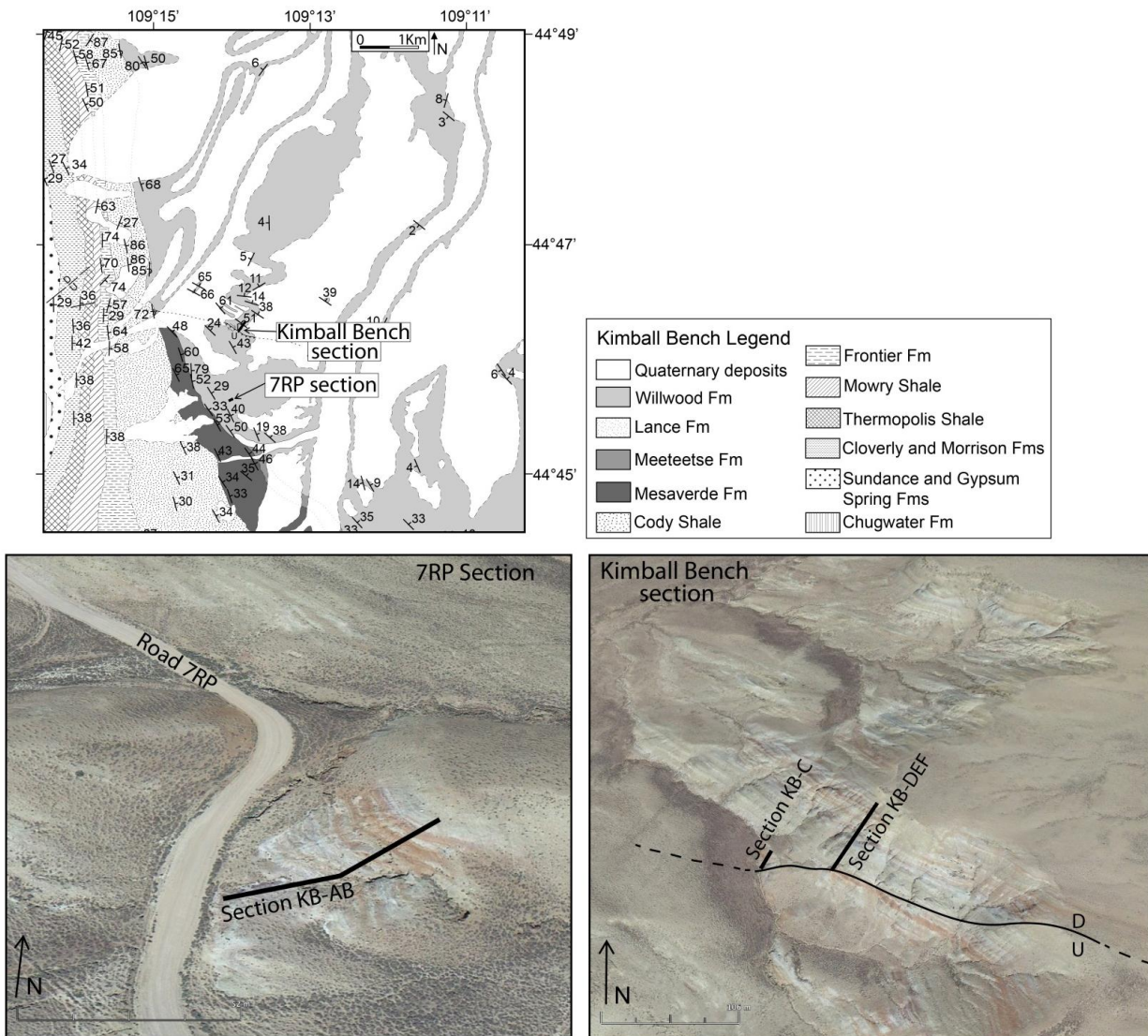
Figure 4. Top: geologic map of the Kimball Bench area showing the locations of the two stratigraphic sections (7RP and Kimball Bench) used for spectral analysis. Bottom: aerial photos of 7RP and Kimball Bench sections used for spectral analysis. Aerial photos from GoogleEarth.

sediment accumulation rate to calculate the age of the youngest deformed Willwood beds in the

Kimball Bench area. These strata correspond with the timing of the earliest possible onset of

Paleogene deformation in this area.

Previous Spectral Analyses, Willwood Formation

Aziz et al. (2008) performed spectral analyses on flat-lying Willwood strata in two

locations in the Bighorn Basin: (1) Polecat Bench (PCB), located in the northern Bighorn Basin

approximately 30 km northeast of Cody; and (2) Red Butte (RB), located in the central Bighorn

Basin approximately 90 km southeast of Cody. In their study, Aziz et al. (2008) took color

measurements using a portable photospectrometer (Minolta CM 508i), which gives a value at

each level after automatically calculating an average of three measurements. They took

measurements at average sampling intervals of 14.5 cm in the PCB section and 21 cm in the RB

section. The redness (a* value) color record of each section was used for spectral analysis.

Redness (a* value) is a coordinate in the CIE L*a*b* (CIELAB) color space, which describes all

the colors visible to the human eye. The three coordinates of CIELAB include lightness (L*), the

position between red and green (a*), and the position between yellow and blue (b*). Negative

values for a* indicate greener colors, while positive a* values indicate more red (Fig. 8). Aziz et

al. (2008) performed time-series analyses of their a* vs. stratigraphic level records of the PCB

and RB sections using the Blackman-Tukey and MC-CLEAN methods. Their time-series

analyses revealed multiple spectral peaks within each section, which they used to evaluate

paleosol cyclicity in the Willwood Formation. The goal of their study was to attribute a

mechanism to the rhythmic stacking patterns seen in Willwood paleosols. To do this, they first

needed to match up the spectral peaks from their time-series analyses with absolute-age data.

They used absolute-age data based on carbon isotope records, paleomagnetic data, and sparse fossil data from previous studies. After they matched their stratigraphic sections to absolute-age records, Aziz et al. (2008) calculated a sediment accumulation rate of 391 m/my for this part of the Bighorn Basin. Using this sediment accumulation rate, they calculated the minimum and maximum cycle thicknesses that corresponded to the 19-23 ky orbital precession cycle. A 7.4 meter cycle thickness was calculated for the 19 ky Milankovitch precession cycle and a 9 meter cycle thickness for the 21 ky Milankovitch precession cycle. Their time-series analysis of the Polecat Bench data showed a peak at 7.7 meters which corresponds with the 20 ky orbital precession cycle. The time-series analysis of the Polecat Bench data also revealed a peak at ~3.3 meters which correlates with a period of ~8 ky, similar to millennial-scale sub-Milankovitch cycles found in successions of lacustrine and marine sediments of Pliocene-Pleistocene age. There were other spectral peaks in their time-series analyses, but Aziz et al. (2008) determined that they were "weakly resolved…due to the dominance of the 3.3 m and 7.7 m spectral components" and therefore were not of use to correlate with Willwood cyclicity. Their study suggested that precession and millennial-scale climate variations affected paleosol development in the Willwood Formation through cyclic changes from predominately overbank deposition with extensive paleosol development to predominately channel-avulsion deposition with periodic halts in soil formation (paleosols) because of high sediment accumulation rates (Aziz et al., 2008).

Abels et al. (2013) did a similar study in which they estimated a cyclicity of 21.6 ky within Willwood strata in the Deer Creek Amphitheater section in the McCullough Peaks area, located in the northern Bighorn Basin approximately 25 km northeast of Cody. In their study, they measured stratigraphic sections by digging ~1 m wide trenches down to fresh rock and

designated field units based on lithologies. They measured color reflectance in the field at 10 cm

vertical resolution using a portable photospectrometer (Minolta CM 508i) and performed time-

series analyses of their color records using the Redfit program (Schulz and Mudelsee, 2002) and

the Analyseries 1-1 program (Paillard et al., 1996). The power spectra of their color records

showed peaks that corresponded to cycle thicknesses between 4.5 and 8.5 meters with a

dominant cycle thickness of 7.1 meters. They compared three previously calculated sediment

accumulation rates to find an average sediment accumulation rate of ~329 m/my for their study.

Using this rate, their dominant cycle thickness of 7.1 meters corresponds with average cycle

duration of 21.6 ky, within the duration of the orbital precession period. The study by Abels et al.

(2013) is in agreement with that of Aziz et al. (2008), suggesting that astronomically forced

climate change directly contributed to the development of alternating intervals of red paleosols

that formed on overbank mudstones and intervening heterolithic intervals that display weak

paleosol development.

Spectral Analysis and Absolute Age Calculations

For this study, we performed a similar analysis to that of Aziz et al. (2008) and Abels et

al. (2013). They utilized a photospectrometer to measure redness values of Willwood sediments

in each of their studies; however, we used a digital camera and ENVI software to measure

redness values using the method described in Levin et al. (2005). Spectrophotometers have a

high cost associated with them and field spectrometers are difficult to travel with over rugged

terrain (Levin et al., 2007). When we began this project, we were able to obtain a portable

photospectrometer (ASD Fieldspec3) to measure color records in the field. We found that it was

difficult and time-consuming to carry the photospectrometer over long distances and up the steep

slopes of deformed strata in our study area. Levin et al. (2007) outlined a method of measuring

color records using a digital camera and ENVI software, which we utilized for this study due to the low cost and simplicity. We collected samples from two stratigraphic sections: the first section, KB-AB, is 111 m thick. The second section, KB-C and KB-DEF, is 320 m thick, located one kilometer northeast of the lower section (Fig. 4). We excavated each section, digging ~1 m wide trenches. We dug down to fresh surfaces and took samples at 30 cm intervals in the 7RP and Kimball Bench sections for analysis (Fig. 5). We crushed each sample and air-dried them for a minimum of seven days before sieving them to remove larger pieces of rock. Each sample was carefully flattened using a textbook that was set on top of the sample in order to eliminate shadows from larger pieces of rock. We originally placed color strips around each sample which we had planned to use to calibrate the camera RGB values as outlined in Levin et al. (2007); however, when we measured the RGB values in the color strips for the first ten samples, we did not see any discrepancies among RGB values from each color strip and therefore concluded that it was not necessary to measure the RGB values of the color strips for every sample. The redness values we obtained were also very similar to those from Aziz et al. (2008) and Abels et al. (2013), indicating that the values we obtained using this method are accurate and reproducible. A 10 megapixel digital camera (Nikon D40x) was positioned on a tripod with the lens facing downward toward the sample. Images were taken in natural light with no flash and no artificial lighting system (Fig. 6). The camera used JPEG standard compression for photographs, which Levin et al. (2007) demonstrated "did not hamper the accurate identification of the samples' color." JPEG images have a high compression ratio which allows for a greater number of photographs to be taken and stored, which is important for field-based projects such as this one (Levin et al., 2007). To measure redness values, we processed the digital images using ENVI 5.0 software. For each image, we defined a region of interest (ROI) over the central part of the

109
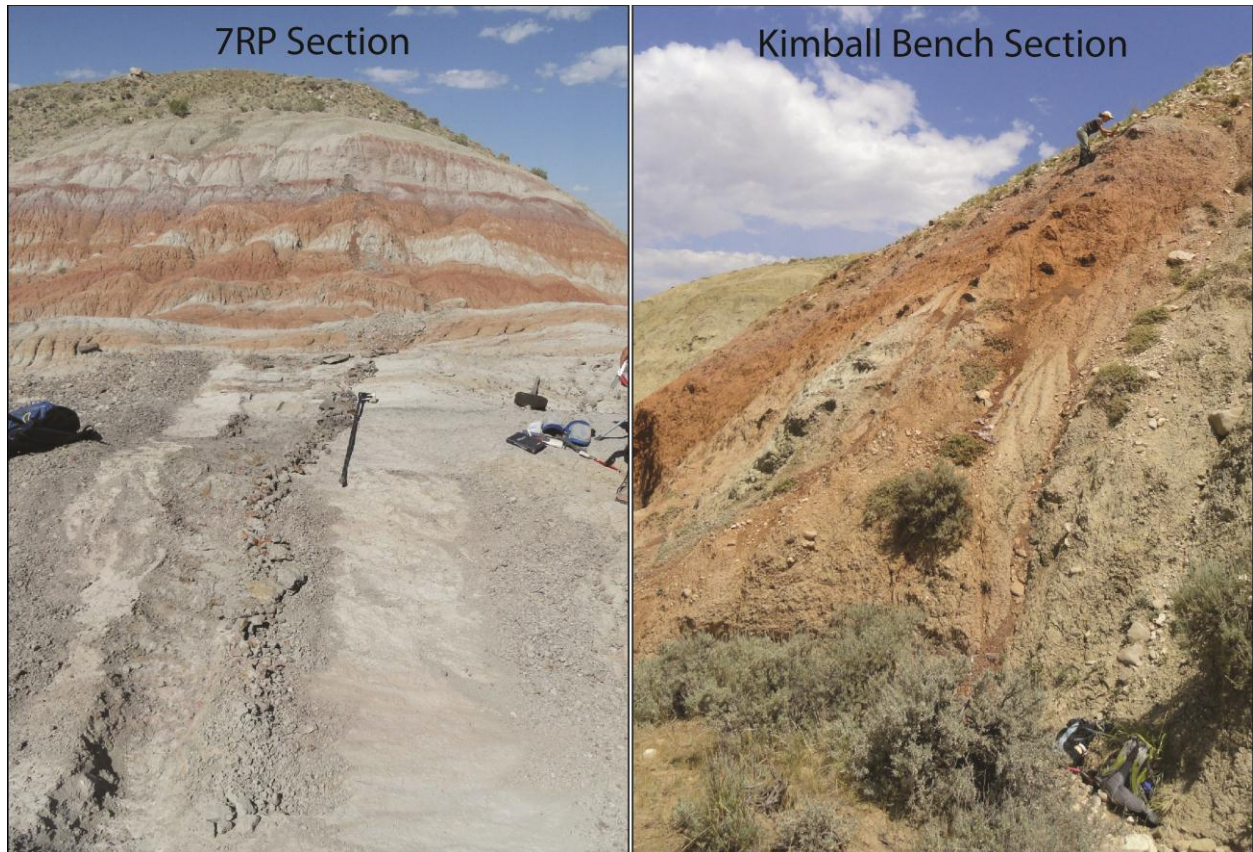
Figure 5. Excavation sites where we collected samples for spectral analysis. Samples were taken perpendicular to the strike of bedding at 30 cm increments at each section.

Figure 6. Examples of prepared samples photographed for spectral analysis. Samples were crushed, dried, and photographed. Before photographing each sample, we used a sieve to remove larger chunks of rock and then flattened the fine sediments using a textbook. Width of sample area is approximately 15 cm.

sample. ENVI was used calculate the RGB values within each ROI. Using the OpenRGB

program, we converted the RGB values for each sample to CIELAB color space, in which a* is

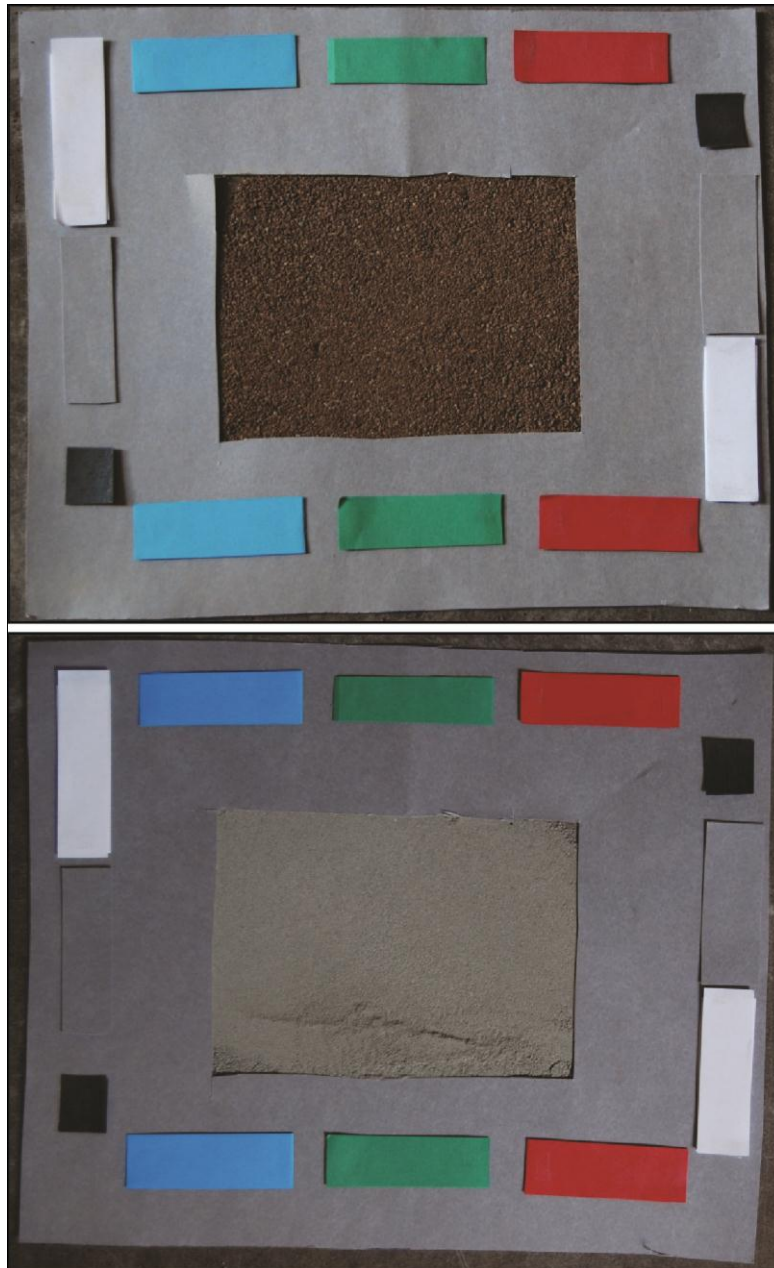the redness value. We used 3-5 photographs per sample and averaged the redness values to

obtain an average a* per sample for our analysis. We then compared our redness values to those

of the studies by Aziz et al. (2008) and Abels et al. (2013). Our maximum redness values are

similar to their maximum values while our minimum redness values have a greater magnitude

than theirs (Fig. 7). The greater magnitude of negative redness values indicates that our samples

contained more green than the samples in the Aziz et al. (2008) and Abels et al. (2013) studies

(Fig. 8).

      We performed a time-series analysis of our a* vs. stratigraphic level record (Fig. 9) using

the fast Fourier transform (FFT) method in Microsoft Excel 2010 (Klingenerg, 2005). Our time-

series analysis revealed multiple spectral peaks within our sections which we used to evaluate

cyclicity in the Willwood Formation (Fig. 10). To determine which (if any) orbital climatic

cycles correspond with spectral peaks in our data, we first needed to match up the spectral peaks

from our time-series analysis with absolute-age data. We used sparse mammalian fossil localities

in the Kimball Bench area to calculate sediment accumulation rates during Willwood deposition.

Spectral peaks from our FFT correspond with cycle thicknesses and in order to test whether the

cycle thicknesses from the FFT can be correlated with specific orbital climatic cycles such as the

19-23 ky precession cycle, the sedimentation rate was multiplied by the period of the cycle in

question. In the study by Aziz et al. (2008), they calculated a sediment accumulation rate of 391

m/my in the northern Bighorn Basin, which indicated that a cycle thickness between 7.4 and 9

meters corresponded with a 19-23 ky precession cycle (391 m/my * 0.019 my = 7.4 m) in that

part of the basin. There are numerous spectral peaks in our FFT, most of which do not
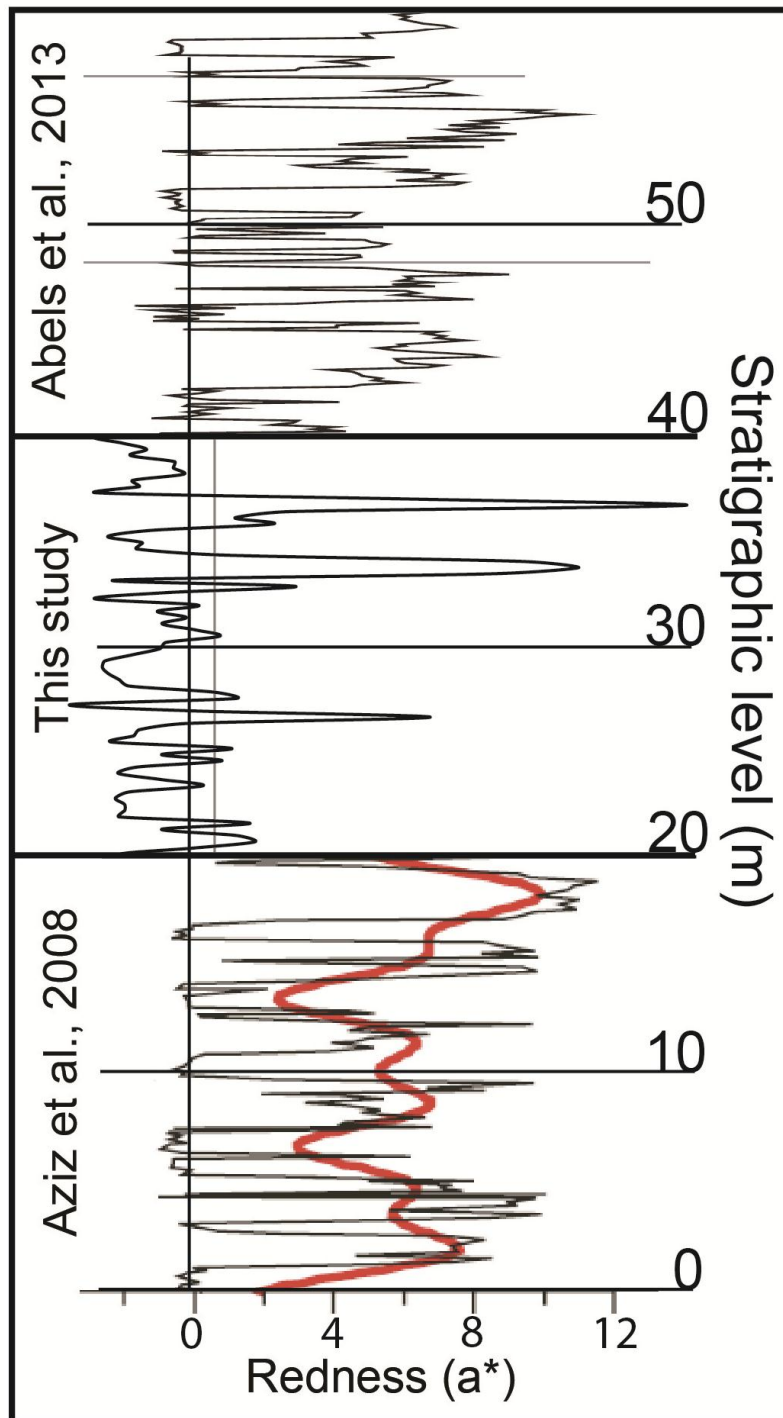
Figure 7. Comparison of redness values from Abels et al., 2013 (upper portion), this study (middle portion), and Aziz et al., 2008 (lower portion). Our maximum redness values are similar to those of the other studies while our minimum redness values have a greater magnitude than those of the other studies (indicates that our samples contain more green than other studies).

113
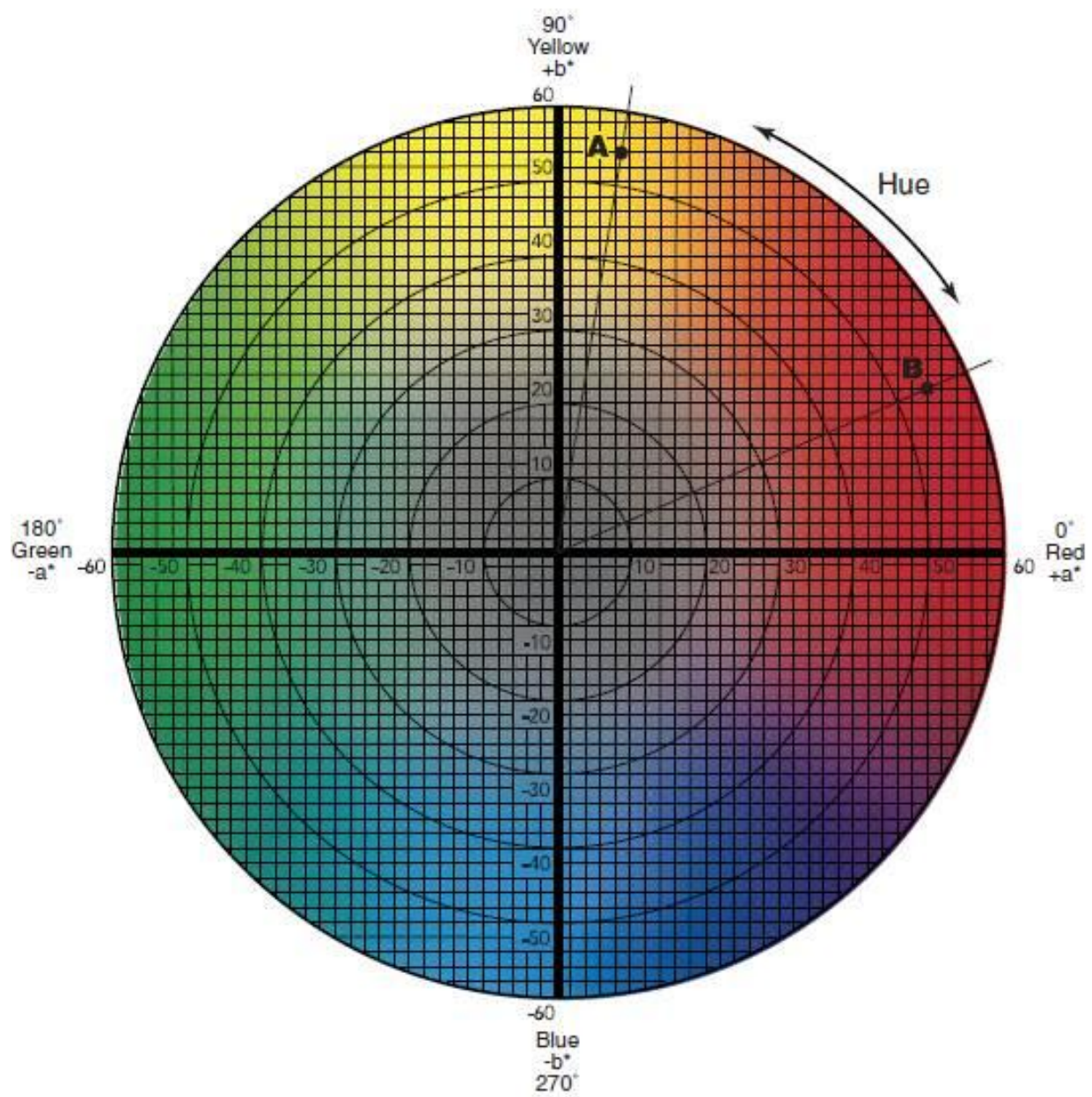
Figure 8. CIELAB color chart. Redness value (a*) is along the horizontal axis.

114
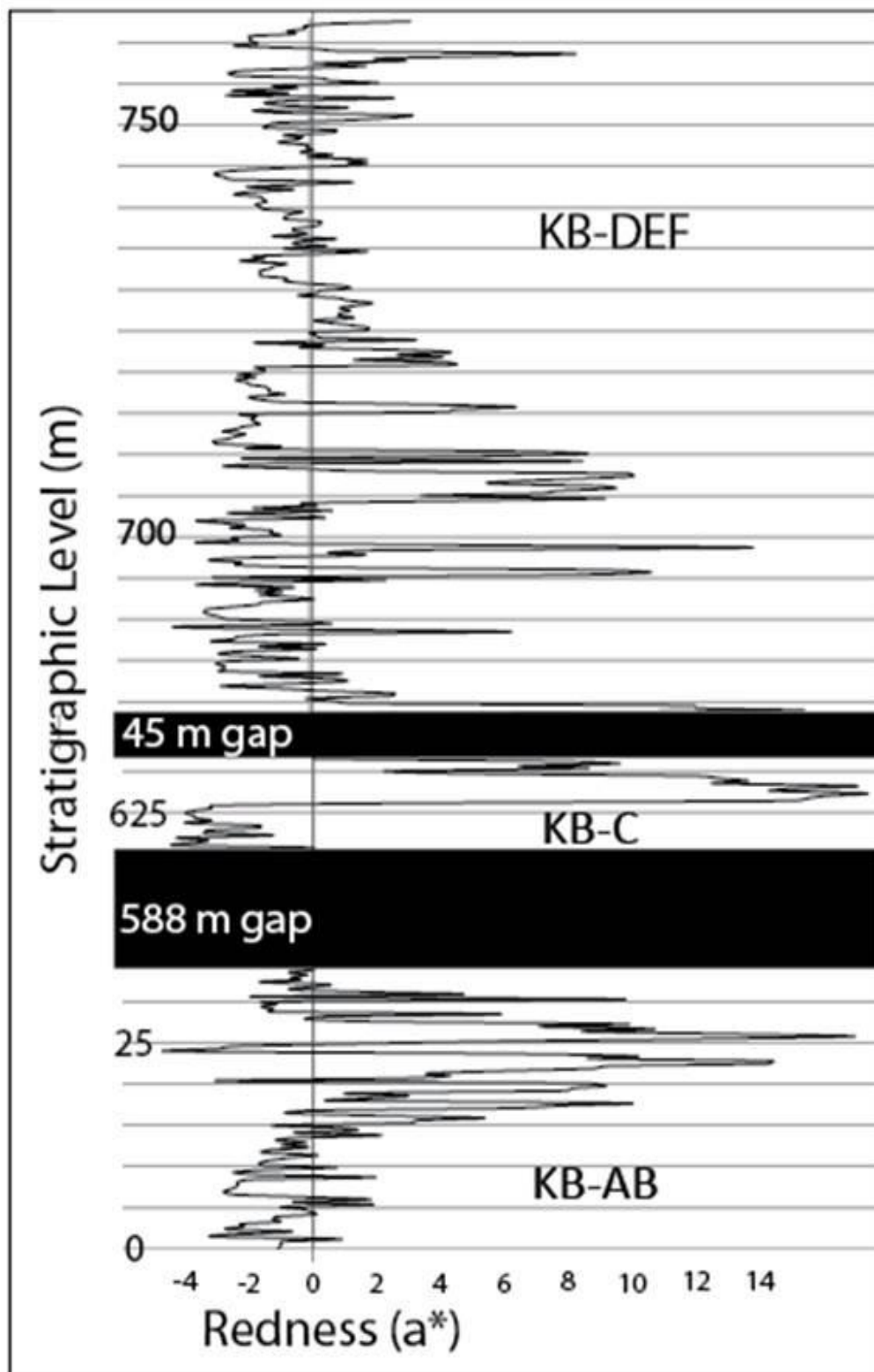
Figure 9. Stratigraphic level (m) vs. redness (a*) plot. KB-AB is from the 7RP section, KB-C and KB-DEF are from the Kimball Bench section. Black bars represent missing sections in data.
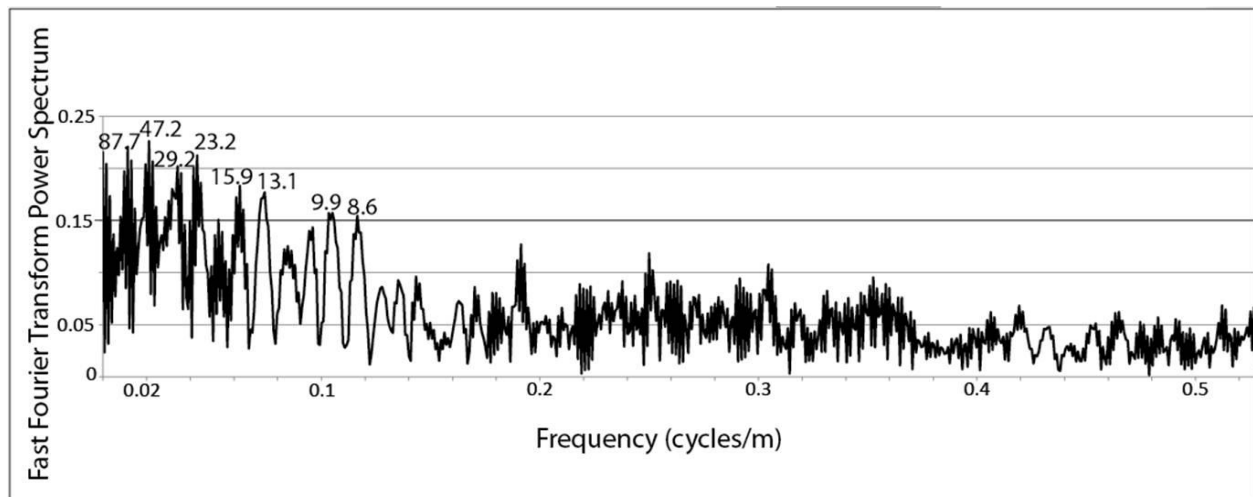
Figure 10. Fast Fourier transform power spectra for a* records. Spectral peaks were used to find correlation with cycle thicknesses; dominant peaks are labeled with cycle thickness in meters.

correspond with orbital climatic cycles (Fig. 10). These peaks likely reflect autogenic or allogenic variations that are not forced by the precession cycle, such as autocyclic floodplain development (Clyde and Christensen, 2003; Abels et al., 2013) or tectonics (Bown and Kraus, 1993). If a spectral peak from our FFT corresponds with a precession-scale climate cycle, it would suggest that the development of paleosols in the Willwood Formation was likely affected by cyclic changes as a result of climate variations.

In the vicinity of Kimball Bench, there are three mammalian fossil localities with established age ranges from studies by Rose (1981) and Gingerich and Clyde (2001). Each fossil locality has a small map area less than 240 square meters in which it was found and for our calculations, we chose a location in the mid-point of each area. Each fossil locality also has a minimum and maximum possible age associated with it and these age ranges were used to calculate the minimum and maximum possible sediment accumulation rates in this area. The true stratigraphic thicknesses among the fossil localities are required to calculate the possible sediment accumulation rates. In order to measure the true thicknesses, we created a cross section through their locations (Fig. 11). Using the true thicknesses between the fossil localities, we calculated the minimum and maximum sediment accumulation rates.

Fossils were described in localities SC-143 and SC-168 (Fig. 11) in a study by Rose (1981). Rose placed both fossil localities in the *Plesiadapis cookei* Zone, which ranges in age from 55.68 to 55.36 Ma (Gingerich, 1976; Rose, 1981; Gingerich, 1983, 2001). Using our cross section through the fossil locations, we were able to calculate the minimum sediment accumulation rate in this area. Using an age of 55.68 Ma for fossils in locality SC-143 and 55.36 Ma for fossils in locality SC-168, we calculated a minimum sediment accumulation rate of 396 m/my. We calculated a maximum sediment accumulation rate using the ages of 55.68 Ma and
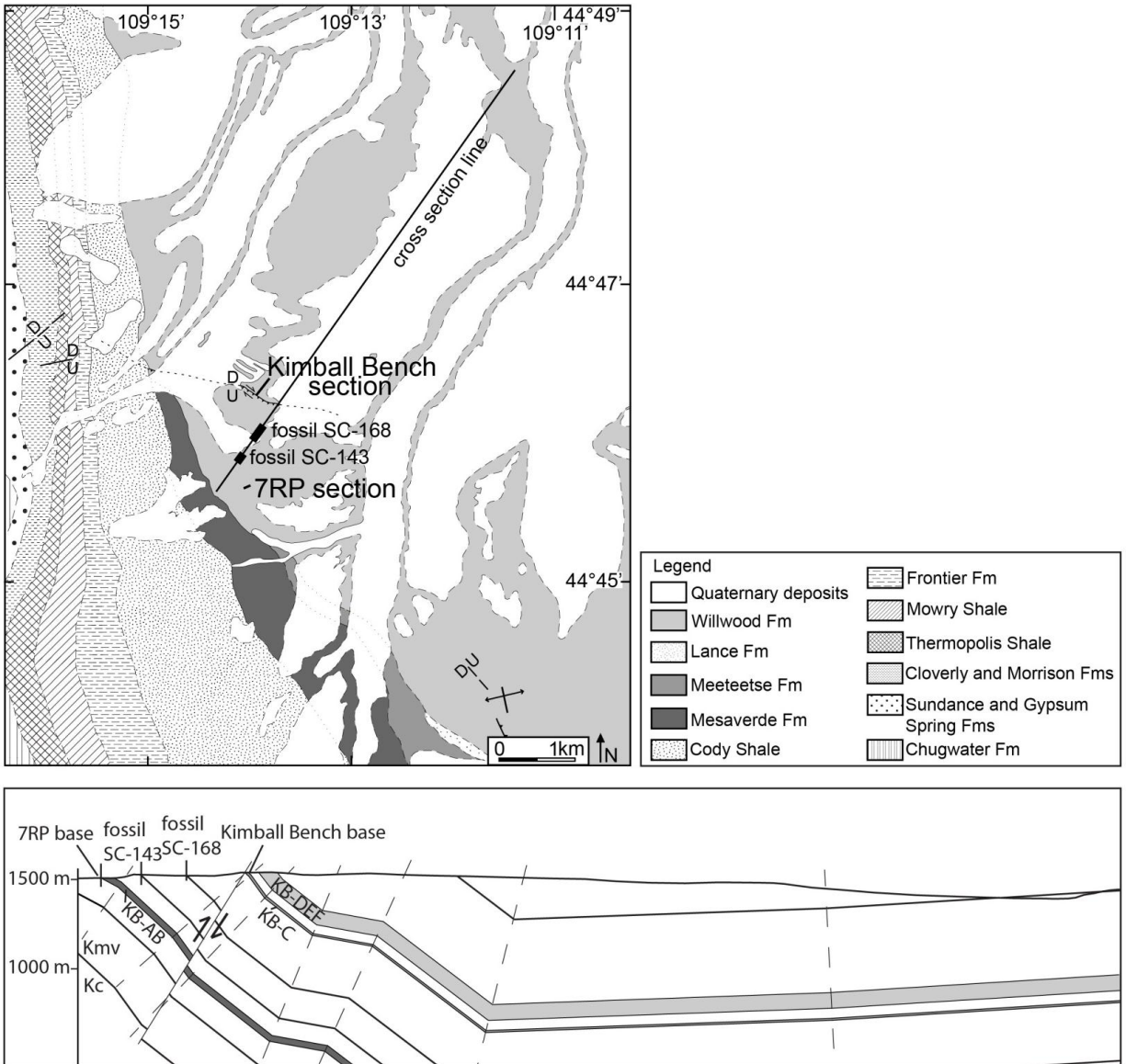
117

Figure 11. Top: generalized geologic map of the Kimball Bench area with line of section, spectral sections, and fossil locations labeled. Bottom: cross section used to find true stratigraphic thicknesses among fossils which were used to calculate the minimum and maximum sediment accumulation rates.

118

55.60 Ma for SC-143 and SC-168, respectively. This resulted in a calculated sediment accumulation rate of 1584 m/my A few kilometers east of the Kimball Bench area, Gingerich (2003) estimated a sediment accumulation rate of 467 m/my and Aziz et al. (2008) estimated a rate of 391 m/my. Given the proximity of their study areas to our study location, we can use a more reasonable range of possible sediment accumulation rates in the Kimball Bench area, between 396 (our calculated minimum) and 700 m/my.

In order to estimate the most probable sediment accumulation rate in the Kimball Bench area, we tested various possible rates by superimposing the projected location of the PETM onto high-resolution aerial photos based on each sediment accumulation rate. In the Willwood Formation, the PETM is marked by the development of densely spaced, well developed, red to purple paleosols. After superimposing possible projected locations of the PETM onto aerial photos, we looked for beds that matched the description of PETM beds. With most sediment accumulation rates, the projected locations of the PETM lie on drab gray and tan beds or sometimes grass-covered beds (Fig. 12). With a sediment accumulation rate of 610 m/my, we found that the projected PETM lies on the base of our KB-AB section, which is comprised of densely spaced, well developed, red to purple paleosols that match the description of beds deposited during the PETM (Fig. 13). Therefore, we used a sediment accumulation rate of 610 m/my for Willwood deposition in the Kimball Bench area and concluded that the PETM is reflected in Willwood sediments of the 7RP section. Using this sediment accumulation rate, we are able to calculate cycle thicknesses that correlate with precession-scale orbital cycles with durations between 19 and 23 ky: for the 19 ky cycle, 610 m/my * .019 my = 11.6 meter cycle thickness; for the 23 ky cycle, 610 m/my * .023 my = 14.0 meter cycle thickness. In our Fourier analysis, there is one spectral peak that corresponds to a 13.1 meter cycle thickness, within the
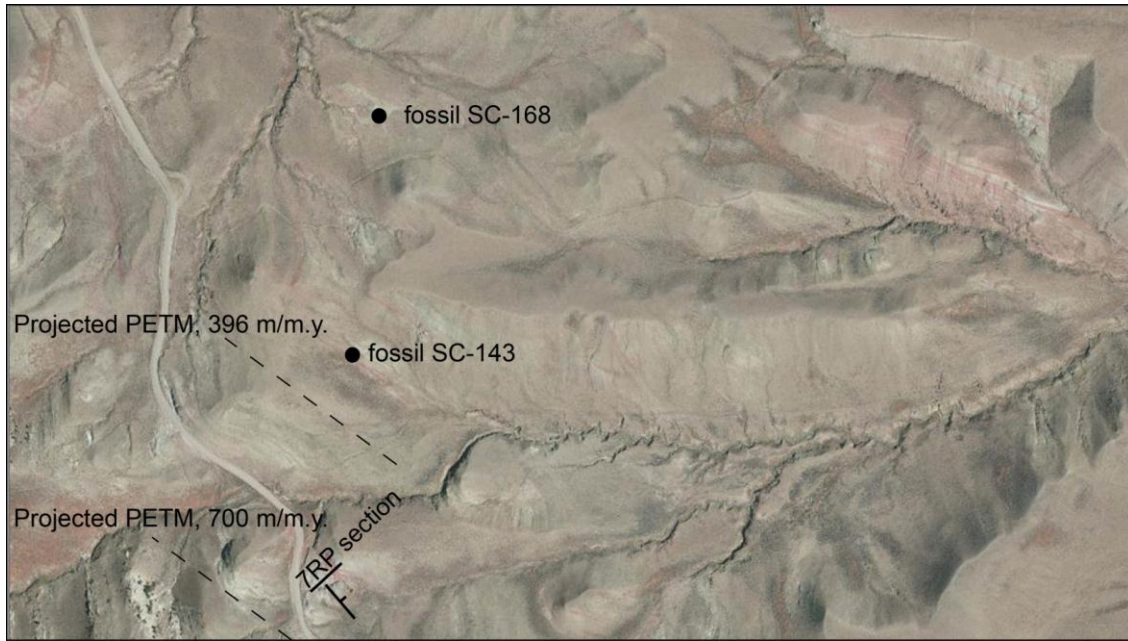
Figure 12. Aerial photo showing fossil locations, spectral section 7RP location, and projected locations of the PETM based on varying sediment accumulation rates including 396 m/m.y. and 700 m/m.y. Often, projected locations of the PETM lie on drab gray and tan beds, as seen in this figure. Aerial photo is from ESRI ArcMap Basemap.

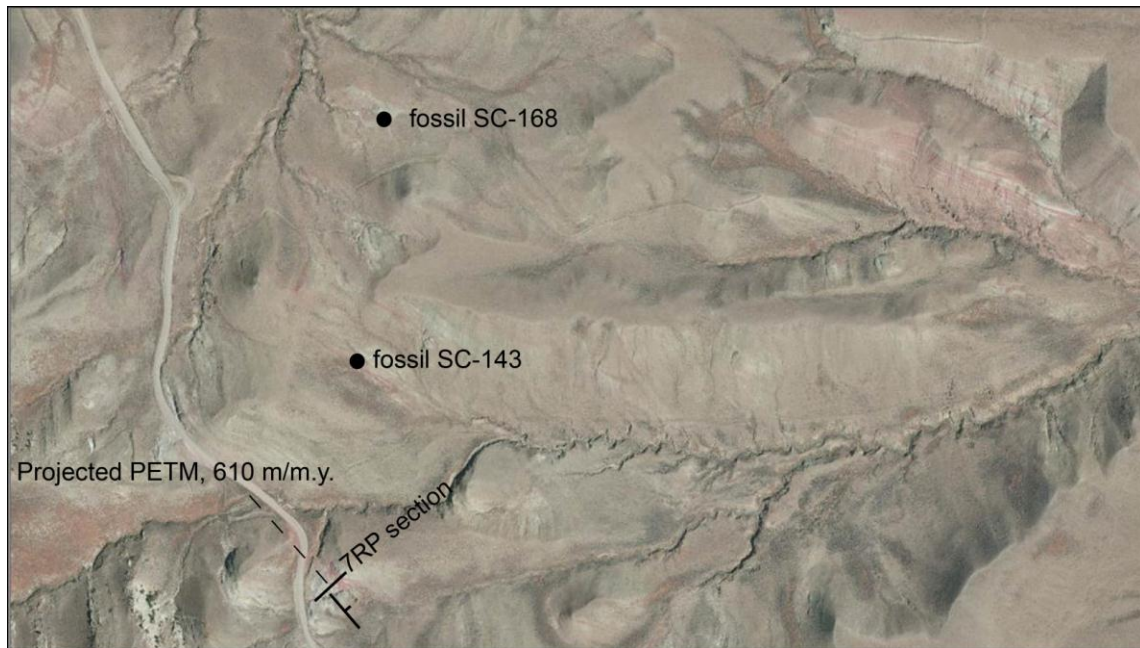Figure 13. Aerial photo showing fossil locations, spectral section 7RP location, and the projected location of the PETM based on a sediment accumulation rate of 610 m/m.y. With a sediment accumulation rate of 610 m/m.y., the projected location of the PETM lies on beds that match the description of beds deposited during the PETM: densely spaced, well developed, red to purple paleosols. Aerial photo is from ESRI ArcMap Basemap.

range of precession-scale cycle thicknesses. The 13.1 meter cycle thickness corresponds to an

astronomical cycle duration of ~21 ky (13.1 m / 510 m/my = .021 my).

Spectral Analysis Conclusions

The Fourier transform of our redness plots reveal multiple spectral peaks, only one of

which corresponds to a precession-scale astronomical cycles. Other dominant peaks from the

Fourier analysis correspond with various cycle thicknesses, likely reflecting autogenic or

allogenic variations that are not forced by the astronomical precession cycle, such as autocyclic

floodplain development (Clyde and Christensen, 2003; Abels et al., 2013) and/or tectonics

(Bown and Kraus, 1993). The 13.1 meter cycle thickness corresponds with a 21 ky cycle

duration, indicating that precession-scale climate variations likely affected the development of

paleosols within the Willwood Formation through cyclic changes from predominately overbank

mudstone deposition (favorable to development of paleosols) to predominately channel-avulsion

deposition which results in weak to no paleosol development. Paleosol development was

probably also affected by autocyclic and allogenic variations, indicated by multiple spectral

peaks in the Fourier transform that do not correspond with precession-scale cyclicity.

Discussion of Deformation History

Our calculated sediment accumulation rate of 610 m/my is significantly higher than those

from studies by Gingerich (467 m/my; 2003) and Aziz et al. (391 m/my; 2008). Because their

study areas are located basinward from ours, it is reasonable to expect that sediment

accumulation rates were lower in the basin than near the mountain front during Paleogene

deposition. Recall that in the Kimball Bench area, deformed Willwood sediments do not contain

internal angular unconformities; therefore, the earliest age of deformation corresponds to the

youngest age of tilted Willwood strata. Because the top of the Willwood has been eroded away,

121

we calculated a range of possible deformation ages that correspond with a range of Willwood thicknesses. In the Kimball Bench area, the minimum thickness of deformed sediments was determined using our geologic map of the area (Fig. 2). Using a sediment accumulation rate of 610 m/my and a minimum thickness of 1085 meters, the youngest deformed Willwood sediments are estimated at 54.2 Ma. It is possible that faulting in the Willwood thickened the sediments in the Kimball Bench area, which would result in a younger calculated age of deformation; however, the only visible faulting in the Kimball Bench area was found during field work and displays 10's of meters of thrust faulting that we accounted for in our calculations (~ 60 meters of displacement).

Because fossil localities SC-143 and SC-168 have a range of ages associated with them, a range of sediment accumulation rates can be calculated for Paleogene deposition in the Kimball Bench area. The location of the PETM in the Kimball Bench area is not well-constrained; however, after scanning aerial photos for beds matching the description of those deposited during the PETM, it is reasonable to assume that the PETM corresponds to the exposed Willwood beds that are stratigraphically below fossil locality SC-143 and display a prominent exposure of thick, well developed, densely spaced, red to purple paleosols (Fig. 13). Using a sediment accumulation rate of 610 m/my, the projected PETM is located in Willwood sediments in the 7RP section which matches the description of beds deposited during the PETM and contain high redness values measured during spectral analysis (Fig. 14). Northeast of the 7RP section near fossil localities SC-143 and SC-168, aerial photos show a thick section of densely spaced bright red paleosols that also match the description of beds deposited during the PETM (Fig. 14). The strata in this location correspond with a stratigraphic level younger than fossil locality SC-143
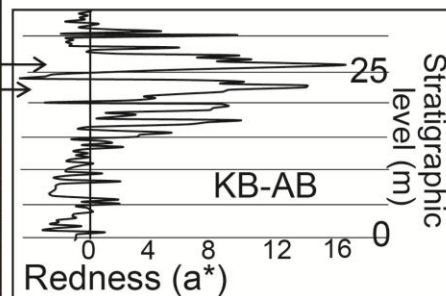
Figure 14. 7RP section in the Kimball Bench area. A sediment accumulation rate of 610 m/my projects the PETM onto this section where paleosols match the description of those deposited during the PETM. Plot of stratigraphic level vs. redness was obtained during spectral analysis and shows high redness values in the 7RP section.

and because the 55.8 Ma PETM is older than fossil locality SC-143, we can reject the possibility that this sequence of paleosols was deposited during the PETM.

Previous studies have suggested a range of ages for the final stages of deformation along the western edge of the Bighorn Basin, from the end of the Paleocene (Pierce, 1965; DeCelles et al., 1991; Wise, 2000) to sometime during the Eocene (Dutcher et al., 1986; Neely, 2006). A study by Neser et al. (Chapter 1) revealed the existence of a deep paleovalley that was carved into Late Cretaceous strata along the western edge of the Bighorn Basin prior to Paleogene Willwood deposition. This paleovalley was the result of slight tilting and differential erosion of Late Cretaceous rocks as tectonism began to the west, prior to the majority of deformation along the western edge of the Bighorn Basin. The deepest section of the paleovalley was in the Kimball Bench area which filled first with fine-grained sediments sourced from the nascent Beartooth Mountains to the west. As the paleovalley filled, there was more widespread deposition of Willwood strata that occurred during the unroofing of the Beartooth Mountains. Lastly, there was the primary phase of deformation which folded both Willwood and Late Cretaceous rocks, resulting in the present-day orientation of Paleogene and Cretaceous rocks along the western edge of the Bighorn Basin. This study indicates that in the Kimball Bench area, the oldest possible age of onset for Paleogene deformation began 54.2 Ma. This resulted in steeply tilted to vertical Late Cretaceous-Paleogene Willwood strata near the basin edge, with the Willwood Formation transitioning to nearly horizontal basinward. Because deformed upper Willwood sediments have been eroded away near the basin edge, it is difficult to constrain the final stages of deformation. However, this study has given insight into the timing of deformation of Willwood sediments in this part of Wyoming, which occurred a few million years later than previously thought.

Conclusions

Along the western edge of the Bighorn Basin in northwestern Wyoming, synkinematic Paleocene Fort Union deposits have previously been used to constrain the timing of Laramide deformation in the northern Rocky Mountains (Jobling, 1974; Dutcher et al., 1986; DeCelles et al., 1991). Our study has revealed steeply tilted late Paleocene-early Eocene Willwood strata in the Kimball Bench area, indicating that deformation occurred after deposition of at least the lower Willwood. This study represents the first to use a digital camera and ENVI software for spectral analyses which we used to constrain the ages of deformed Paleogene sediments along the western edge of the Bighorn Basin. The use of a digital camera as an alternative tool for a photospectrometer allows for a fast, easy, objective method to quantitatively take color measurements in addition to reducing cost and increasing simplicity. We utilized this method of spectral analysis to obtain the absolute age of deformation with precision that previous studies of deformed strata along the western edge of the Bighorn Basin have not achieved before. Our analyses revealed a significant spectral peak corresponding with a 21-ky climatic precession cycle, indicating that precession-scale climate variations likely affected paleosol development within the Willwood Formation by way of cyclic changes from overbank mudstone deposition to channel-avulsion deposition. Our analyses also indicated that deformation in the Kimball Bench area began after the previously accepted Paleocene age of deformation along the western edge of the Bighorn Basin (Jobling, 1974; Dutcher et al., 1986; DeCelles et al., 1991), at least 1.6 Ma into the Eocene. This study has demonstrated that there is a complex multi-stage deformational history in this part of the Rocky Mountains during late Paleocene and early Eocene deposition.

REFERENCES

Abels, H.A., Kraus, M.J., and Gingerich, P.D., 2013, Precession-scale cyclicity in the fluvial lower Eocene Willwood Formation of the Bighorn Basin, Wyoming (USA): Sedimentology, v. 60, issue 6, p. 1467-1483.

Aziz, H.A., Hilgen, F.J., van Luijk, G.M., Sluijs, A., Kraus, M.J., Pares, J.M., and Gingerich, P.D., 2008, Astronomical climate control on paleosol stacking patterns in the upper Paleocene-lower Eocene Willwood Formation, Bighorn Basin, Wyoming: Geology, v. 36, no. 7, p. 531-534.

Bown, T.M., and Kraus, M.J., 1981, Lower Eocene alluvial paleosols (Willwood Formation, northwest Wyoming, U.S.A.) and their significance for paleoecology, paleoclimatology, and basin analysis: Palaeogeography, Palaeoclimatology, Palaeoecology, v. 34, p. 1-30.

Bown, T.M., and Kraus, M.J., 1993, Time-stratigraphic reconstruction and integration of paleopedologic, sedimentologic, and biotic events (Willwood Formation, lower Eocene, northwest Wyoming, U.S.A.): PALAIOS, v. 8, no. 1, p. 68-80.

Bralower, T.J., Thomas, D.J., Zachos, J.C., Hirschmann, M.M., Rohl, U., Sigurdsson, H., Thomas, E., and Whitney, D.L., 1997, High-resolution records of the late Paleocene thermal maximum and circum-Caribbean volcanism: Is there a causal link?: Geology, v. 25, no. 11, p. 963-966.

Charles, A.J., Condon, D.J., Harding, I.C., Palike, H., Marshall, J.E.A., Cui, Y., Kump, L., and Croudace, I.W., 2011, Constraints on the numerical age of the Paleocene-Eocene boundary: Geochemistry, Geophysics, Geosystems, v. 12, no. 6, 19 p.

Clyde, W.C., and Christensen, K.E., 2003, Testing the relationship between pedofacies and avulsion using Markov Analysis: American Journal of Science, v. 303, p. 60-71.

DeCelles, P.G., Gray, M.B., Ridgway, K.D., Cole, R.B., Srivastava, P., Pequera, N., and Pivnik, D.A., 1991, Kinematic history of a foreland uplift from Paleocene synorogenic conglomerate, Beartooth Range, Wyoming and Montana: Geological Society of America Bulletin, v. 103, p. 1458-1475.

Dupuis, C., Aubry, M., Steurbaut, E., Berggren, W.A., Ouda, K., Magioncalda, R., Cramer, B.S., Kent, D.V., Speijer, R.P., and Heilmann-Clausen, C., 2003, The Dababiya Quarry section: lithostratigraphy, clay mineralogy, geochemistry and paleontology: Micropaleontology, v. 49, suppl. 1, p. 41-59.

Dutcher, L.A.F., Jobling, J.L., and Dutcher, R.R., 1986, Stratigraphy, sedimentology and structural geology of Laramide synorogenic sediments marginal to the Beartooth Mountains, Montana and Wyoming, *in* Montana Geological Society and Yellowstone Bighorn Research Association joint field conference and symposium; geology of the Beartooth Uplift and adjacent basins: Yellowstone Bighorn Research Association, p. 33-52.

Flueckinger, L., 1970, Stratigraphy, petrography and origin of Tertiary sediments off the front of the Beartooth Mountain, Montana-Wyoming [Ph.D. thesis]: Pennsylvania State University at University Park, 382 p.

Fricke, H.C., Clyde, W.C., O'Neil, J.R., and Gingerich, P.D., 1998, Evidence for rapid climate change in North America during the latest Paleocene thermal maximum: oxygen isotope compositions of biogenic phosphate from the Bighorn Basin (Wyoming): Earth and Planetary Science Letters, v. 160, p. 193-208.

Gingerich, P.D., 1976, Cranial anatomy and evolution of early Tertiary Plesiadapidae (Mammalia, Primates): Papers on Paleontology, no. 15, p. 1-140.

Gingerich, P.D., 1983, Paleocene-Eocene faunal zones and a preliminary analysis of Laramide structural deformation in the Clark's Fork Basin, Wyoming, *in* Wyoming Geological Association Guidebook, v. 34, p. 185-195.

Gingerich, P.D., 1989, New earliest Wasatchian mammalian fauna from the Eocene of northwestern Wyoming: composition and diversity in a rarely sampled high-floodplain assemblage: Papers on Paleontology, no. 28, 97 p.

Gingerich, P.D., 2001, Biostratigraphy of the continental Paleocene-Eocene boundary interval on Polecat Bench in the northern Bighorn Basin: Papers on Paleontology, no. 33, p. 37-71.

Gingerich, P.D., and Clyde, W.C., 2001, Overview of mammalian biostratigraphy in the Paleocene-Eocene Fort Union and Willwood Formations of the Bighorn and Clarks Fork Basins: Papers on Paleontology, no. 33, p. 1-14.

Gingerich, P.D., 2003, Mammalian responses to climate change at the Paleocene-Eocene boundary: Polecat Bench record in the northern Bighorn Basin, Wyoming: Geological Society of America, Special Paper 369, p. 463-478.

Hickey, L.J., 1980, Paleocene stratigraphy and flora of the Clark's Fork Basin: Papers on Paleontology, v. 24, p. 33-50.

Jobling, J.L., 1974, Stratigraphy, petrography, and structure of the Laramide (Paleocene) sediments marginal to the Beartooth Mountains, Montana [Ph.D. Thesis]: The Pennsylvania State University, 102 p.

Johnson, S.J., and Middleton, L.T., 1990, Tectonic significance of Paleocene alluvial sequence, Clark's Fork Basin, Wyoming-Montana, *in* Specht, R.W., ed., Wyoming sedimentation and tectonics: Wyoming Geological Association 41st Field Conference Guidebook, p. 69-87.

Kennett, J.P., and Stott, L.D., 1991, Abrupt deep-sea warming, palaeoceanographic changes and benthic extinctions at the end of the Palaeocene: Nature, v. 353, issue 6341, p. 225-229.

Klingenberg, L., 2005, Frequency domain using Excel: http://online.sfsu.edu/jtai/downloads/ENGR%20302/Excel.FFT.pdf (accessed May, 2013).

Koch, P.L., Zachos, J.C., and Gingerich. P.D., 1992, Correlation between isotope records in marine and continental carbon reservoirs near the Palaeocene/Eocene boundary: Nature, v. 358, issue 6384, p. 319-322.

Kraus, M.J., and Aslan, A., 1993, Eocene hydromorphic paleosols: significance for interpreting ancient floodplain processes: Journal of Sedimentary Petrology, v. 63, no. 3, p. 453-463.

Kraus, M.J., and Riggins, S., 2002, Effects of the PETM on continental weathering: analysis of alluvial paleosols, Bighorn Basin, Wyoming: Geological Society of America Abstracts with Programs, v. 34, no. 6, p. 535.

Kraus, M.J., and Davies-Vollum, K.S., 2004, Mudrock-dominated fills formed in avulsion splay channels: examples from the Willwood Formation, Wyoming: Sedimentology, v. 51, p. 1127-1144.

Levin, N., Ben-Dor, E., and Singer, A., 2005, A digital camera as a tool to measure colour indices and related properties of sandy soils in semi-arid environments: International Journal of Remote Sensing, v. 26, no. 24, p. 5475-5492.

Neasham, J.W., and Vondra, C.F., 1972, Stratigraphy and petrology of the lower Eocene Willwood Formation, Bighorn Basin, Wyoming: Geological Society of America Bulletin, v. 83, p. 2167-2180.

Neely, T.G., 2006, Three-dimensional strain at foreland arch transitions: structural modeling of the southern Beartooth Arch transition zone, northwest Wyoming [M.S. thesis]: Colorado State University, 113 p.

Omar, G.I., Lutz, T.M., and Giegengack, R., 1994, Apatite fission-track evidence for Laramide and post-Laramide uplift and anomalous thermal regime at the Beartooth overthrust, Montana-Wyoming: Geological Society of America Bulletin, v. 106, p. 74-85.

Paillard, D.L., Labeyrie, L., and Yiou, P., 1996, Macintosh program performs time-series analysis: EOS Transactions American Geophysical Union, v. 77, issue 39, p. 379.

Pierce, W.G., and Andrews, D.A., 1941, Geology and oil and coal resources of the region south of Cody, Park County, Wyoming: U.S. Geological Survey Bulletin, p. 99-180.

Pierce, W.G., 1965, Geologic map of the Clark Quadrangle, Park County, Wyoming: U.S. Geological Survey, scale 1:62 500, 1 sheet.

Rohl, U., Bralower, T.J., Norris, R.D., and Wefer, G., 2000, New chronology for the late Paleocene thermal maximum and its environmental implications: Geology, v. 28, no. 10, p. 927-930.

Rohl, U., Westerhold, T., Bralower, T.J., and Zachos, J.C., 2007, On the duration of the Paleocene-Eocene thermal maximum (PETM): Geochemistry, Geophysics, Geosystems, v. 8, no. 12, 13 p.

Rose, K.D., 1981, The Clarkforkian land-mammal age and mammalian faunal composition across the Paleocene-Eocene boundary: Papers on Paleontology, v. 26, 197 p.

Schouten, S., Woltering, M., Rijpstra, W.I.C., Sluijs, A., Brinkhuis, H., Damste, J.S.S., 2007, The Paleocene-Eocene carbon isotope excursion in higher plant organic matter: Differential fractionation of angiosperms and conifers in the Arctic: Earth and Planetary Science Letters, v. 258, p. 581-592.

Schulz, M., and Mudelsee, M., 2002, REDFIT: estimating rednoise spectra directly from unevenly spaced paleoclimatic time series: Computers & Geosciences., v. 28, no. 3, p. 421-426.

Schulz, M. and Mudelsee, M. (2002) REDFIT: estimating rednoise spectra directly from unevenly spaced paleoclimatic time series: Comput. Geosci., v. 28, p. 421–426.

Van Houten, F.B., 1944, Stratigraphy of the Willwood and Tatman Formations in northwestern Wyoming: Geological Society of America Bulletin, v. 55, no. 2, p. 165-210.

Westerhold, T., Rohl, U., Raffi, I., Fornaciari, E., Monechi, S., Reale, V., Bowles, J., and Evans, H.F., 2008, Astronomical calibration of the Paleocene time: Palaeogeography, Palaeoclimatology, Palaeoecology, v. 257, p. 377-403.

Wise, D.U., 2000, Laramide structures in basement and cover of the Beartooth Uplift near Red Lodge, Montana: AAPG Bulletin, v. 84, issue 3, p. 360-375.

Zachos, J.C., 2005, Rapid acidification of the ocean during the Paleocene-Eocene thermal maximum: Science, v. 308, issue 5728, p. 1611-1615.

Zachos, J.C., Bohaty, S.M., John, C.M., McCarren, H., Kelly, D.C., and Nielsen, T., 2007, The Paleocene-Eocene carbon isotope excursion: constraints from individual shell planktonic foraminifer records: Philosophical Transaction of the Royal Society A, v. 365, p. 1829-1842.